University of Alberta

# Simulation of a Two-Dimensional Bubble Column

by

David Anthony Sharp

A thesis submitted to the Faculty of Graduate Studies and Research in partial fulfillment of the requirements for the degree of Masters of Science

in

Chemical Engineering

Department of Chemical and Materials Engineering

Edmonton, Alberta

Spring, 2000

National Library of Canada
Acquisitions and Bibliographic Services
395 Wellington Street
Ottawa ON K1A 0N4
Canada

Bibliothèque nationale du Canada
Acquisitions et services bibliographiques
395, rue Wellington
Ottawa ON K1A 0N4
Canada

*Your file Votre référence*

*Our file Notre référence*

The author has granted a non-exclusive licence allowing the National Library of Canada to reproduce, loan, distribute or sell copies of this thesis in microform, paper or electronic formats.

L'auteur a accordé une licence non exclusive permettant à la Bibliothèque nationale du Canada de reproduire, prêter, distribuer ou vendre des copies de cette thèse sous la forme de microfiche/film, de reproduction sur papier ou sur format électronique.

The author retains ownership of the copyright in this thesis. Neither the thesis nor substantial extracts from it may be printed or otherwise reproduced without the author's permission.

L'auteur conserve la propriété du droit d'auteur qui protège cette thèse. Ni la thèse ni des extraits substantiels de celle-ci ne doivent être imprimés ou autrement reproduits sans son autorisation.

0-612-60174-9

Canada

University of Alberta

Library Release Form

Name of Author: David Anthony Sharp

Title of Thesis: Simulation of a Two-Dimensional Bubble Column

Degree: Master of Science

Year this Degree Granted: 2000

Permission is hereby granted to the University of Alberta Library to reproduce single copies of this thesis and to lend or sell such copies for private, scholarly or scientific research purposes only.

The author reserves all other publication and other rights in association with the copyright in the thesis, and except as herein before provided, neither the thesis nor any substantial portion thereof may be printed or otherwise reproduced in any material form whatever without the author's prior written permission.

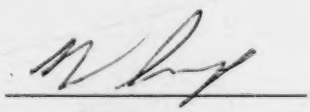

2015 108 Street
Edmonton, Alberta
T6J 5V4

Date: Jan. 28, 2000

University of Alberta

Faculty of Graduate Studies and Research

The undersigned certify that they have read, and recommend to the Faculty of Graduate Studies and Research for acceptance, a thesis entitled Simulation of a Two-Dimensional Bubble Column submitted by David Anthony Sharp in partial fulfillment of the requirements for the degree of Masters of Science in Chemical Engineering.

K. Nandakumar, Supervisor

P. Mees

P. Minev

S. Liu

Date : Jan 28, 2000

## Abstract

The objective of this study is to validated the CFX-F3D code for a two dimensional gas-liquid system by comparing experimental results with simulated results. Experiments were conducted in a two-dimensional bubble column (35 mm wide and a minimum liquid height of 150 mm) to measure the average volume fraction of air in water, methanol, cyclohexane and water/methanol mixtures at different air flow rates. The CFX-F3D code was used to simulate both steady state and dynamic systems. The simulated volume fraction of air agreed well with those measured for all pure liquids under steady state conditions. The dynamics of the bubble column was also investigated by examining the step change from one steady state to another steady state (at a higher air flow rate). It was found that the measured time taken to go from one steady state to another did agree with the simulated ones. However, the micro dynamics of the fluids such as local liquid velocity and local gas holdup need to be compared to experimental values before confidence can be placed in the simulated results.

**Acknowledgements**

There have been many people who have helped me throughout this research project and to whom I am sincerely thankful. I would like to thank Dr. K. Nandakumar for his help, guidance, patients and understanding, Artin Afacan for his help with the experimental work, Dr. P. Mees and Dr. S. Kresta for their valuable suggestions and comments and Bob Barton and Jack Gibeau for their assistance. Lastly, I would also like to thank Amber McQuarrie and Ann Sharp for their support and help.

## TABLE OF CONTENTS


Chapter 1. Introduction 1

Chapter 2. Literature review 4

2.1 Experimental studies 4

2.1.1 Flow regimes in bubble columns 4

2.1.2 Empirical correlations 5

2.1.3 Local gas holdup and flow distributions 8

2.2 Mathematical modeling of bubble columns 9

2.2.1 Euler-Euler method 10

2.2.1.1 Governing equations for Euler-Euler method 11

2.2.1.2 Euler-Euler simulation literature review 16

2.2.2 Euler-Lagrange method 23

2.2.2.1 Solution method for Euler-Lagrange method 23

2.2.2.2 Euler-Lagrange literature review 24

2.2.3 VOF method 28

2.2.3.1 Governing equations for VOF method 28

2.2.3.2 VOF method numerical results 29

2.2.4 Macroscopic models for bubble columns 30

2.3 Review articles 32

Chapter 3. Experimental methods and results 36

3.1 Experimental apparatus and setup 36

3.2 Experimental results 37

3.2.1 Fluid properties 37

3.2.1 Bubble diameter measurements 39

3.2.3 Average gas holdup measurements 40

3.2.4 Experimental step change results (bubble column dynamics 44

Chapter 4. Simulation results 52

4.1 Simulation properties 52

4.1.1 System dimensions and discrete grid 52

4.1.2 Boundary conditions 53

4.1.3 Solution method for Euler-Euler model 54

4.2 Steady state 56

4.3 Dynamic results 59

4.3.1 Step change results 59

4.3.2 Local, instantaneous system parameters 60

4.4 Effects of various discritization schemes 63

4.5 Grid and time tests 65

Chapter 5. Discussion 94

5.1 Steady state 94

5.2 Bubble column dynamics 97

5.2.1 Dynamics of average holdup 97

5.2.2 Spatial variations 99

5.3 Numerical tests 101

Chapter 6. Conclusions and recommendations 104

Nomenclature 106

References 110

Appendix A. Sample CFX-F3D code 116

Appendix B. Fortran user routine USRGRD (grid generation) 119

Appendix C. Fortran user routine USRBCS (boundary conditions) 125

Appendix D. Fortran user routine USRIPT (drag correlation) 135

Appendix E. Fortran user routine USRTRN (dynamic results) 146

## List of Figures


| | | |
|---|---|---|
| Figure 2.1 | Flow regimes in a bubble column for low viscosity fluids. | 34 |
| Figure 2.2 | Structure of numerical control volume. | 35 |
| Figure 3.1 | Experimental bubble column setup. | 46 |
| Figure 3.2 | Images used to get bubble diameters for air-water system. | 47 |
| Figure 3.3 | Images used to get bubble diameters for air-methanol system. | 48 |
| Figure 3.4 | Images used to get bubble diameters for air-cyclohexane system. | 49 |
| Figure 3.5 | Sample image used to get bubble diameters for air-10% methanol in water system for a superficial gas velocity of 1.53 cm/s. | 50 |
| Figure 3.6 | Sample image used to get bubble diameters for air-50% methanol in water system for a superficial gas velocity of 1.53 cm/s. | 50 |
| Figure 3.7 | Sample image used to get bubble diameters for air-90% methanol in water system for a superficial gas velocity of 1.53 cm/s. | 50 |
| Figure 3.8 | Bubble diameters of air-water system. $U_g = 0.815$ cm/s | 51 |
| Figure 3.9 | Bubble diameters of water/methanol mixture system. | 51 |
| Figure 4.1 | Numerical grid for bubble column. | 67 |
| Figure 4.2 | Wall effects on average gas holdup for air-water system. | 68 |
| Figure 4.3 | Wall effects on average gas holdup for air-methanol system. | 69 |
| Figure 4.4 | Wall effects on average gas holdup for air-cyclohexane system. | 70 |
| Figure 4.5 | Average holdup as a function of time for air-water system. | 71 |
| Figure 4.6 | Average holdup as a function of time for air-methanol system. | 72 |

| | | |
|---|---|---|
| Figure 4.7 | Average holdup as a function of time for air-cyclohexane system. | 73 |
| Figure 4.8 | Comparison of numerical, experimental and empirical gas holdups for the air-water system. | 74 |
| Figure 4.9 | Comparison of numerical, experimental and empirical gas holdups for the air-methanol system. | 75 |
| Figure 4.10 | Comparison of numerical, experimental and empirical gas holdups for the air-cyclohexane system. | 76 |
| Figure 4.11 | Average gas holdup at different mass fractions of methanol in water for $U_g = 0.815$ cm/s. | 77 |
| Figure 4.12 | Average holdup for air-water system for step change in air flow rate from $U_g = 0.71$ cm/s to $U_g = 1.78$ cm/s. | 78 |
| Figure 4.13 | Average holdup for air-methanol system for step change in air flow rate from $U_g = 0.38$ cm/s to $U_g = 1.91$ cm/s. | 79 |
| Figure 4.14 | Average holdup for air-cyclohexane system for step change in air flow rate from $U_g = 0.38$ cm/s to $U_g = 1.91$ cm/s. | 80 |
| Figure 4.15 | Local liquid velocity 3.75 cm from the bottom of the column. $U_g = 2.20$ cm/s. | 81 |
| Figure 4.16 | Local liquid velocity 7.5 cm from the bottom of the column. $U_g = 2.20$ cm/s. | 82 |
| Figure 4.17 | Local liquid velocity 11.25 cm from the bottom of the column. $U_g = 2.20$ cm/s. | 83 |
| Figure 4.18 | Local gas holdup in horizontal center of column. $U_g = 2.20$ cm/s. | 84 |
| Figure 4.19 | Local gas holdup in horizontal center of column (Hybrid differencing scheme). $U_g = 2.20$ cm/s. | 85 |
| Figure 4.20 | Local gas holdup in horizontal center of column (Crank-Nicolson time discritization). $U_g = 2.20$ cm/s. | 86 |
| Figure 4.21 | Local gas holdup in horizontal center of column (added mass included in code). $U_g = 2.20$ cm/s. | 87 |

Figure 4.22 Local gas holdup in horizontal center of column (20x60 grid, 0.01 s time step). $U_g$ = 1.53 cm/s. 88

Figure 4.23 Local gas holdup in horizontal center of column (10x30 grid, 0.01 s time step). $U_g$ = 1.53 cm/s. 89

Figure 4.24 Local gas holdup in horizontal center of column (40x120 grid, 0.01 s time step). $U_g$ = 1.53 cm/s. 90

Figure 4.25 Local gas holdup in horizontal center of column (20x60 grid, 0.02 s time step). $U_g$ = 1.53 cm/s. 91

Figure 4.26 Local gas holdup in horizontal center of column (20x60 grid, 0.05 s time step). $U_g$ = 1.53 cm/s. 92

Figure 4.27 Local gas holdup in horizontal center of column (20x60 grid, 0.10 s time step). $U_g$ = 1.53 cm/s. 93

## List of Tables


| | | |
|---|---|---|
| Table 2.1 | Existing empirical correlations for gas holdup. | 6 |
| Table 2.2 | Empirical correlations for gas holdup in pressurized columns. | 7 |
| Table 2.3 | Gas holdup correlations for specific flow regimes. | 7 |
| Table 3.1 | Pure component fluid properties. | 38 |
| Table 3.2 | Water-methanol mixture fluid properties. | 38 |
| Table 3.3 | Average experimental gas holdup values for the pure component systems. | 41 |
| Table 3.4 | Average gas holdup for 0.1 mass fraction of methanol in water. | 41 |
| Table 3.5 | Average gas holdup for 0.3 mass fraction of methanol in water. | 42 |
| Table 3.6 | Average gas holdup for 0.5 mass fraction of methanol in water. | 42 |
| Table 3.7 | Average gas holdup for 0.7 mass fraction of methanol in water. | 43 |
| Table 3.8 | Average gas holdup for 0.9 mass fraction of methanol in water. | 43 |
| Table 3.9 | Experimental step change results for air-water system. | 45 |
| Table 3.10 | Experimental step change results for air-methanol system. | 45 |
| Table 3.11 | Experimental step change results for air-cyclohexane system. | 45 |
| Table 4.1 | Comparison of experimental and numerical gas holdups for pure component systems. | 58 |
| Table 4.2 | Locations of points where dynamic data was taken. | 61 |
| Table 4.3 | Summary of wavelength, minimum and maximum values for the local liquid velocities. | 62 |

Table 4.4 Summary of wavelength, minimum and maximum values for the local gas holdup. 62

Table 4.5 Average gas holdup and range of local gas holdup values for different grids and time steps in numerical bubble column with a gas velocity of 1.53 cm/s. 66

## Chapter 1. Introduction

Computational fluid dynamics (CFD) is emerging as a useful tool for process engineers. It can be used to aid in design, scale-up, trouble shooting, optimization, and detailed flow analysis in many chemical processes. The economic rewards of using CFD are huge since it could replace the need for expensive experimental and pilot plant studies. It can also be used to reduce the shutdown time and aid in finding problem areas in equipment. CFD, however, can only be used with confidence when it has been validated against experimental data. To do this, flow parameters such as velocities, turbulence parameters and pressure fields must be quantitatively compared between the experimental systems and the model predictions. Single phase CFD has already been established as a reliable tool, especially at low Reynolds numbers. Multiphase CFD, however, has not yet reached that stage. The delay in verifying multiphase CFD systems comes from a lack of computational power and lack of detailed experimental data. Multiphase CFD problems are very complex and computationally expensive and as computing power grows, more advanced multiphase systems can be studied. Some work has already been done in all areas of multiphase CFD. This includes work in solid-gas, solid-liquid, liquid droplets in gas and gas bubbles in liquids. In general the work is limited by the availability of detailed experimental data but in many cases a good foundation has been laid. The main problems that arise in multiphase CFD include turbulence modeling and interphase drag correlations. The turbulence equations used for single phase flow are generally extended to multiphase flow, however, it is not known whether or not these models are appropriate. Drag correlations are

usually dependent on the system studied and some models are functions of particle concentrations, system properties and fluid properties. This work, although not answering all of these questions, is an attempt to lay some ground work in the gas-liquid CFD area.

The focus of this work will be on a bubble column. A bubble column is a simple gas-liquid contacter in which gas is introduced at the bottom of a column containing a liquid. The liquid can be of fixed mass in the column or it can have a net flow (either co-current or counter-current to the gas) through the column. For the purpose of validating the CFD model, it is best to consider a simple two dimensional geometry with a fixed mass of liquid. A bubble column can be used for mass transfer, heat transfer, and chemical reactions; so it can be used in many different applications. In this study, the bubble column contains a fixed mass of liquid and is two dimensional. This setup reduces the computational load (compared to a three dimensional setup) when simulating the bubble column while still providing necessary data for multiphase CFD validation. The column is studied both experimentally and numerically and this work focuses not only on steady state macro system properties but also on the dynamic behavior of bubble columns. The dynamic behavior of the local system parameters (such as local liquid velocity and local gas holdup) is also discussed.

In this study, a detailed literature review on both experimental bubble column work and mathematical modeling of bubble columns are presented in Chapter 2. These include a discussion about the flow regimes in bubble columns, experimental techniques used to obtain system data, results of some experimental

studies, numerical modeling of bubble columns and some numerical results. Chapter 3 describes the experimental setup of the bubble column used in this study as well as the experimental results. Presented in Chapter 4 are the numerical results obtained using AEA Technology's CFX-F3D CFD code. Chapter 5 presents a discussion on the comparison of the experimental and numerical results obtained. The conclusions obtained from this study and any recommendations for future work are presented in Chapter 6.

# Chapter 2. Literature Review

Before the 1990's extensive experimental work was done on bubble columns to obtain macroscopic empirical correlations as well as time averaged local parameters. Experimental work has continued since then using more sophisticated instrumentation while at the same time numerical modeling based on CFD has begun. A discussion on bubble column review articles can be found at the end of this chapter.

## 2.1 Experimental studies

This section deals with the experimental work done in bubble columns. It includes discussions on the different flow regimes in bubble columns, empirical models and micro or local system parameters such as the average gas volume fraction.

### 2.1.1 Flow regimes in bubble columns

There are three different flow regimes in bubble columns (Figure 2.1) plus a transition regime (Bisio and Kabel, 1985; Koide, 1996). For low viscosity fluids the homogeneous bubble flow regime occurs in columns with any diameter but only for superficial gas flow rates ($U_g$) less than 3 to 5 cm/s. This flow regime is characterized by no (or very little) bubble coalescence and breakup. The other two regimes are similar in that they both occur at higher gas flow rates, $U_g$ greater than 4 to 7 cm/s, and both involve bubble coalescence and breakup. The slug flow regime occurs in columns with a diameter of less than 10 cm but at superficial gas velocities greater than approximately 5 cm/s. In this regime large groups of bubbles tend towards the center of the column. These larger bubble slugs have a dynamic

horizontal velocity and have also been labeled the vortical-spiral flow regime (Koide, 1996). In this regime pockets or sections of liquid circulate but these eddies are not stationary and move with time. The second regime, known as the heterogeneous churn turbulent regime, occurs in columns with diameters greater than 20 cm and also with superficial gas velocities of greater than 7 cm/s. In this regime the gas tends to flow up the center of the column forcing an overall liquid circulation in the column. This phenomenon is called 'bubble streeting' and has been observed by many researchers (Miyauchi and Shyu, 1970; Rietema and Ottengraf, 1970; Hills, 1974). In the areas between these three flow regimes there is a transition regime in which it is expected that two or more of the above mentioned regimes occurring at once. This can cause strange behaviors in bubble columns such as complete liquid circulation. In this case the liquid flows up one wall and down the other (Koide, 1996).

**2.1.2 Empirical correlations**

Experimentally, bubble columns have been extensively studied from a macro point of view. Many studies deal with the average gas holdup as a function of the superficial gas velocity in bubble columns (Krishna et al., 1994; Chang and Harvel, 1992; Herbrechtsmeier et al., 1985; Salinas-Rodriguez et al., 1998; Hyndman and Guy, 1995; Weiss et al., 1985; Hubertus et al., 1993; Asai and Yoshizawa, 1992; Zhu and Saxena, 1997; Soong et al., 1997). The average gas volume fraction can experimentally be obtained by dividing the difference in the liquid levels with and without gas flows by the liquid level when the gas is flowing (Weiss et al., 1985).

$$\psi_g = \frac{(h_f - h_i)}{h_f} \tag{2.1}$$

Most of the studies mentioned above include empirical correlations that can be used to predict the gas holdup. They are usually functions of the superficial gas flow rate, bubble diameter, and physical properties of the system. Table 2.1 contains some of these types of empirical correlations:

**Table 2.1. Existing empirical correlations for gas holdup.**

| Equation | Reference |
|---|---|
| $\psi_g = 0.672 U_g^{0.578} \rho_l^{0.069} \rho_g^{0.062} \mu_g^{0.107} \sigma^{-0.185} \mu_l^{-0.053} g^{-0.131}$ | Hikita et al. (1980) |
| $\frac{\psi_g}{(1-\psi_g)} = \frac{0.4 \cdot U_g^{0.87} \cdot \rho_l^{0.1} \cdot \rho_g^{0.17}}{\sigma^{0.06} \cdot \mu_l^{0.21} \cdot g^{0.27}}$ | Hammer et al. (1984) |
| $\psi_g = 296 U_g^{0.44} \rho_g^{0.19} \sigma^{-0.16} \rho_l^{-0.98} + 0.009$ | Reilly et al. (1986) |
| $\frac{\psi_g}{(1-\psi_g)^4} = 10.62 \exp(1.49 \mu_l) U_g$ | Weiss et al. (1985) |

Others have studied bubble columns under high pressures and temperatures (Lin et al., 1998, Wilkinson et al, 1992). The empirical correlations that come from these studies have essentially the same form as the previous ones, however, they are also a function of pressure (Table 2.2).

**Table 2.2. Empirical correlations for gas holdup in pressurized columns.**

| Equation | Reference |
|---|---|
| $\frac{\psi_g}{(1-\psi_g)} = 1.44 U_g^{0.58} \cdot \rho_g^{0.12} \cdot \sigma^{-0.16\exp(-P)}$ | Idogawa et al. (1985) |
| $\frac{\psi_g}{(1-\psi_g)} = 0.059 U_g^{0.8} \cdot \rho_g^{0.17} \cdot (\sigma/72)^{-0.22\exp(-P)}$ | Idogawa et al. (1987) |

Since bubble columns can be operated in four different regimes some authors have reported gas holdup correlations for specific flow regions (Table 2.3).

**Table 2.3. Gas holdup correlations for specific flow regimes.**

| Regime | Equation | Reference |
|---|---|---|
| Homogeneous | $\psi = \frac{U_g}{v_\infty (1-\psi)^{2.75\rho_g^{-0.54}}}$ | Krishna et al. (1994) |
| Heterogeneous | $\psi = \psi_{trans} + A(U_g - U_{trans})^{4/5}\ ;\ U_g \geq U_{trans}$ | Krishna et al. (1994) |

### 2.1.3 Local gas holdup and flow distributions

There have been some attempts to acquire local or microscopic quantities in bubble columns (Hills, 1974; Rietema and Ottengraf, 1970; Menzel et al., 1990; Yang et al., 1992; Devanathan et al, 1995; Tzeng et al., 1993; Cheng et al., 1994; Reese and Fan, 1994; Chen et al., 1995; Hyndman and Guy. 1995a, b). This has usually come in the form of either local gas holdup values or local liquid velocities. Hills (1974) used a conductivity probe technique to measure the local void fraction distribution across a column at a specific height. He also used a modified Pitot tube to obtain the liquid velocity distribution across a bubble column at a specific height. Hills (1974) observed that these parameters seemed to be a function of the gas distributor and of the superficial gas velocity. If a gas distributor with large holes (greater than one mm) is used then he found that the liquid rose up the center of the column and fell down at the walls. The volume fraction followed this finding in that it was larger in the center, or upflow, portion of the column and less at the walls. Hills (1974) found this to be the case for all distributor geometries for higher gas flow rates (those in the turbulent flow regime). But for lower gas flow rates with smaller holed gas distributors a fairly constant velocity and volume fraction profile was observed. Rietema and Ottengraf (1970) used a visual technique in which they followed very small dispersed air bubbles to get the local liquid velocity. They found similar results to Hills (1974) in that the liquid was found to be rising in the center of the column and going downwards at the wall of the column. Menzel et al. (1990) found the same thing when they measured the local liquid velocity in a bubble column. Instantaneous values of the continuous phase velocity have recently

been acquired through the use of new techniques. These include Computer Automated Radioactive Particle Tracking (CARPT) (Yang et al., 1992; Devanathan et al, 1995), Particle Image Velocimetry (PIV) (Tzeng et al., 1993; Cheng et al., 1994; Reese and Fan, 1994; Chen et al., 1995), and radioactive tracer gas (Hyndman and Guy. 1995a, b). CARPT is a method in which a set of detectors is used to track the motion of a radioactive particle in time. This technique can be used to obtain local instantaneous velocities, time averaged velocity profiles and time averaged turbulence parameters. For the PIV method neutrally buoyant tracer particles are suspended in the fluid. A laser is used to illuminate the tracer particles and the section can be video recorded and/or a digital signal can be obtained to gather instantaneous flow structures. Another property that has been dealt with by Chang and Harvel (1992) is bubble diameter. They found that bubble diameters increased with increasing superficial gas velocity and with vertical height from the base of the column in an air-water system.

**2.2 Mathematical modeling of bubble columns**

There are several approaches to simulate the bubble column dynamics. There is the Euler-Euler method, the Euler-Lagrange method, the volume of fluid (VOF) method and other methods that only predict macro quantities in bubble columns. For the first three mentioned, the liquid phase is treated as a continuum, but the dispersed phase is handled differently for each method. For the Euler-Euler method the gas phase is handled the same way as the liquid phase, also as a continuum, and the two phases are linked by an interphase transfer term. The frame of reference is taken as a stationary observer for both phases. The main contribution

to the interphase transfer term is the drag force between the two phases. For the Euler-Lagrange method each bubble, or a group of bubbles, is tracked as it passes through the column. The reference frame for the continuous phase is as a stationary observer, while for the dispersed phase the tagged particles (or bubbles) are tracked. This requires a model for the slip velocity of the bubbles rising through the liquid. Sokolichin et al. (1997) found that the Euler-Euler and Euler-Lagrange methods could both be used to simulate flow in a gas liquid system as long as a higher order discritization is used in the Euler-Euler method. The VOF method tracks the movement of each bubble surface, or the gas-liquid interface. The frames of reference are similar to the Euler-Lagrange method except the bubble surfaces are followed instead of the bubbles themselves. Another type of bubble column simulation produces only macro properties such as average gas holdup and overall flow patterns. These models usually include radial void fraction correlations as well as slip velocity correlations or radial velocity profiles and are based on an overall energy balance. They do not give any local, or micro, information in the bubble column.

### 2.2.1 Euler-Euler method

The Euler-Euler method is a volume averaging method. This implies that tracking a bubble from the bottom of the column to the top cannot be accomplished. Instead a velocity and volume fraction for each of the continuous and dispersed phases are calculated in each geometric cell. It is important to first examine the equations that the Euler-Euler method uses before presenting any results. All mathematics presented in this section come from the CFX 4.1 Flow Solver Guide

(1995) from AEA Technology unless otherwise mentioned since this was the program used for all simulation work. An example code has been included in Appendix A.

**2.2.1.1 Governing equations for the Euler-Euler method**

This section details typical equations, and the methods used to solve them, that describe the flow in a bubble column through an Eularian approach.

A finite volume technique is usually used for multi phase CFD work. A finite volume (FV) method divides the solution domain into a finite number of control volumes. A computational node is located at the center of each control volume (CV) and this is where the variable values are calculated. To get the values of the variable at CV surfaces interpolation is usually used. FV methods are used mainly because they can be used for simple, uniform grids as well as for non-uniform grids and systems with complex geometries. Figure 2.2 shows the structure of a control volume and the labeling that accompanies it.

In a bubble column with no mass or heat transfer, the following equations can be used to describe the system. The equations for the liquid phase are:

$$\frac{\partial}{\partial t}(\psi_a \rho_a) + \nabla \bullet (\psi_a \rho_a \mathbf{U}_a) = 0 \tag{2.2}$$

$$\begin{aligned} &\frac{\partial}{\partial t}(\psi_a \rho_a \mathbf{U}_a) + \nabla \bullet \left(\psi_a \left(\rho_a \mathbf{U}_a \otimes \mathbf{U}_a - \mu_a \left(\nabla \mathbf{U}_a + (\nabla \mathbf{U}_a)^T\right)\right)\right) \\ &\quad = \psi_a (\mathbf{B} - \nabla p_a) + C_{a\beta}(\mathbf{U}_\beta - \mathbf{U}_a) + \mathbf{F}_a \end{aligned} \tag{2.3}$$

and for the gas phase the equations are:

$$\frac{\partial}{\partial t}(\psi_\beta \rho_\beta) + \nabla \bullet (\psi_\beta \rho_\beta \mathbf{U}_\beta) = 0 \tag{2.4}$$

$$\begin{aligned} &\frac{\partial}{\partial t}(\psi_\beta \rho_\beta \mathbf{U}_\beta) + \nabla \bullet \left(\psi_\beta \left(\rho_\beta \mathbf{U}_\beta \otimes \mathbf{U}_\beta - \mu_\beta \left(\nabla \mathbf{U}_\beta + (\nabla \mathbf{U}_\beta)^T\right)\right)\right) \\ &= \psi_\beta (\mathbf{B} - \nabla p_\beta) + C_{\beta\alpha}(\mathbf{U}_\alpha - \mathbf{U}_\beta) + \mathbf{F}_\beta \end{aligned} \tag{2.5}$$

Equation 2.2 and 2.4 are known as the continuity equations while Equations 2.3 and 2.5 are the momentum equations for multiphase flow. The buoyancy force, **B**, is given by:

$$\mathbf{B} = \sum_{i=\alpha,\beta} \rho_i g \tag{2.6}$$

The $C_{\alpha\beta}$ (and $C_{\beta\alpha}$) term represents the interphase transfer between each phase. The momentum transfer between the two phases is equal and opposite to each other while the momentum transfer between the same phase must be equal to zero.

$$\begin{aligned} C_{\alpha\beta} &= C_{\beta\alpha} \\ C_{\alpha\alpha} &= C_{\beta\beta} = 0 \end{aligned} \tag{2.7}$$

The interphase non-drag forces, $\mathbf{F}_\alpha$, can include the following parameters: 1) lift force, 2) wall lubrication force, 3) virtual mass force and 4) turbulent dispersion

force. The user of the code can also specify any other relevant forces. If only the drag force is considered then $C_{\alpha\beta}$ can be modeled as:

$$C_{\alpha\beta} = \frac{3}{4}\frac{C_D}{D_p}\psi_\alpha \rho_\alpha \left|\mathbf{U}_\beta - \mathbf{U}_\alpha\right| \tag{2.8}$$

Thus, $C_{\alpha\beta}$ is a function of the slip velocity, bubble diameter, density, volume fraction and the drag coefficient, $C_D$. The drag coefficient and bubble diameters are the only parameters that the CFD code user needs to include. There are many available models for $C_D$. These can range from the simple correlation for drag on a sphere, which does not incorporate any particle-particle or particle-wall interactions, to more sophisticated models. Three models that include particle-particle interactions are those found by Richardson and Zaki (1954), Ishii and Zuber (1979) and Schwarz and Turner (1988). The model proposed by Richardson and Zaki (1954) was meant for systems of solid particles in a liquid media. The drag was said to depend on the particle Reynolds number and the particle concentration. If gas bubbles behaved as rigid particles then this formulation would work fine, however, gas bubbles, unlike solid particles, tend not to have a rigid structure. They also coaless and breakup, and the slip conditions on the walls of bubbles are different from that of solid particles. Thus the Richardson-Zaki model is probably not an adequate model to describe gas-liquid systems. Both the Ishii-Zuber and Schwarz-Turner models were developed for gas-liquid systems and both include bubble-bubble interactions. The Schwarz-Turner model is only a function of the local gas

holdup. The bubble slip velocity is assumed to be constant at 20 cm/s which is in agreement with the experimentally determined terminal velocity of air bubbles with diameters between 1 cm and 10 cm in water (Schwarz and Turner, 1988). The Ishii-Zuber correlation is a function of the fluid properties as well as the gas holdup.

$$C_D = \frac{2}{3} D_p \sqrt{\frac{g\Delta\rho}{\sigma}} X \begin{cases} (1-\psi_d)^{-0.5}; \mu_c >> \mu_d \\ (1-\psi_d)^{-1.0}; \mu_c \approx \mu_d \\ (1-\psi_d)^{-1.5}; \mu_c << \mu_d \end{cases} \tag{2.9}$$

This equation is valid only if the bubbles are in the distorted particle regime. This can be determined if:

$$N_\mu \geq 0.11 + \frac{1+\gamma}{\gamma^{8/3}} \tag{2.10}$$

where

$$N_\mu = \frac{\mu_c}{(\rho_c \sigma \sqrt{\sigma / g\Delta\rho})^{0.5}} \tag{2.11}$$

$$\gamma = 0.5[(1 + 0.08 r_d^{*3})^{4/7} - 1]^{0.75} \tag{2.12}$$

where

$$r_d^* = r_d (\rho_c g \Delta\rho / \mu_c^2)^{1/3} \tag{2.13}$$

This more complicated model for drag seems to be valid for most pure component systems and not for only one system as is the case for the Schwarz-Turner correlation.

Turbulence is usually modeled for the continuous phase in a bubble column. Schwarz and Turner (1988) found that the $k$-$\varepsilon$ model was adequate to use providing separate momentum equations are solved for both phases and no assumptions are made about the void fraction distribution. For the work presented in this study the RNG $k$-$\varepsilon$, was used exclusively. The RNG $k$-$\varepsilon$ model differs from the standard $k$-$\varepsilon$ model only in the equation relating to $\varepsilon$. The following are the equations used for the RNG $k$-$\varepsilon$ turbulence model. The momentum equation is changed to:

$$\frac{\partial}{\partial t}(\psi_a \rho_a \mathbf{U}_a) + \nabla \bullet \left(\psi_a \left(\rho_a \mathbf{U}_a \otimes \mathbf{U}_a - \mu_{a,eff}\left(\nabla \mathbf{U}_a + (\nabla \mathbf{U}_a)^T\right)\right)\right) = \psi_a(\mathbf{B} - \nabla p_a) + \sum_{\beta=1}^{N_p} c_{a\beta}(\mathbf{U}_\beta - \mathbf{U}_a) \tag{2.14}$$

where

$$\mu_{eff} = \mu_a + \mu_{turb} \tag{2.15}$$

$$\mu_{turb} = C_\mu \rho \frac{k^2}{\varepsilon} \tag{2.16}$$

The transport equations for $k$ and $\varepsilon$ are:

$$\frac{\partial \rho k}{\partial t} + \nabla \cdot (\rho \mathbf{U} k) - \nabla \cdot \left((\mu + \frac{\mu_{turb}}{\sigma_k})\nabla k\right) = P^* + G - \rho\varepsilon \tag{2.17}$$

$$\frac{\partial k\varepsilon}{\partial t}+\nabla\cdot(\rho\mathbf{U}\varepsilon)-\nabla\cdot((\mu+\frac{\mu_T}{\sigma_\varepsilon})\nabla\varepsilon)= (C_1-C_{1RNG})\frac{\varepsilon}{k}(P^*+C_3\max(G,0))-C_2\rho\frac{\varepsilon^2}{k} \quad (2.18)$$

where

$$P^*=u_{eff}\nabla\mathbf{U}\cdot(\nabla\mathbf{U}+(\nabla\mathbf{U})^T) \quad \text{for incompressible flows} \quad (2.19)$$

$$G=G_{buoy}=\frac{\mu_{eff}}{\rho\sigma_\rho}\mathbf{g}\cdot\nabla\rho \quad (2.20)$$

$$C_1=1.42 \quad (2.21)$$

$$C_2=1.68 \quad (2.22)$$

$$C_3=0.0 \quad (2.23)$$

$$C_{1RNG}=\frac{\eta(1-\eta/\eta_0)}{(1+\beta\eta^3)} \quad (2.24)$$

$$\eta=(\frac{P}{\mu_T})^{0.5}\frac{k}{\varepsilon} \quad (2.25)$$

$$\eta_0=4.38 \quad (2.26)$$

and

$$\beta=0.015 \quad (2.27)$$

#### 2.2.1.2 Euler-Euler simulation literature review

When the Euler-Euler method is used to simulate a bubble column there are two approaches that can be taken. Either steady state or dynamic (time dependent) simulations can be performed. Most of the work done has focused on the steady state bubble column simulations (Ranade, 1992; Svendsen et al., 1992; Torvik and

Svendsen, 1990; Schwarz and Turner, 1988). However, Becker et al. (1994) and Sokolichin and Eigenberger (1994) have performed dynamic simulations of bubble columns. For all numerical studies mentioned the systems studied are isothermal systems and both phases are considered incompressible.

Schwarz and Turner (1988) were among the first to use the form described above (two sets of continuity and momentum equations) to solve for the flow parameters in a bubble column. They tested the $k$-$\varepsilon$ turbulence model for flows in gas-liquid systems and found that it was an adequate model if two momentum equations were used to model the system, and no assumptions were made about the void fraction distribution. For their numerical experiment they used an air-water system. The column diameter was 1.12 m and the liquid height was 0.93 m. The gas flow rate was set at $6.8 \times 10^{-4}$ $m^3/s$ and was introduced at the center of the bottom of the column. They assumed the system to be cylindrically symmetric so the equations (solved in cylindrical coordinates) were two dimensional. They used the Schwarz-Turner drag correlation as mentioned above and considered the pressure to be common between the two phases. They solved the equations using the general purpose package PHOENICS. No slip conditions were employed at the walls. The top surface was assumed to be flat and the liquid flow through the surface was set to zero. They found the flow field and volume fractions in the column appeared to be correct, however, they were not compared to any experimental data. They found that the liquid went up the center and down the walls and the volume fraction of the gas phase was larger in the center. The simulation data for the radial vertical velocity agrees fairly well with the experimental data at different heights in the column.

They also observed good agreement between the experimental and simulated turbulent kinetic energy. This was a good stepping stone in bubble column simulations, however, it does not give any information on the dynamics of the bubble column since the equations were solved as time independent. Also, the liquid height to diameter (*H/D*) ratio was less than one so this system is not comparable to most experimental or industrial bubble columns.

The bubble column Torvik and Svendsen (1990) studied had a diameter of 0.145 m and a liquid height of 4.52 m. In the air-water system they assumed the bubble column to have axial symmetry and set the radial velocities to zero at the walls. The turbulence parameters and liquid axial velocity at the wall were set using special wall functions. They specified all the variables at the inlet. At the outlet the gradients were set to zero unless mass transfer was occurring. If there was mass transfer in the column then no liquid or gas was allowed to enter through the top surface. The $k$-$\varepsilon$ turbulence model was used for the liquid phase. They also used the Schwarz-Turner drag model and included a lift force (Magnus force). Upwind differencing was used for the continuity equations while hybrid differencing was used for the momentum and scalar equations. They used the SIMPLEC method to solve the momentum equations as well as the PEA method. Good agreement was observed with experimental data for the axial liquid velocity 1.6 m above the base of the bubble column. However, the radial volume fraction and turbulent kinetic energy simulation results, although qualitatively good, did not match up well with that observed experimentally. Svendsen et al. (1992) used the same method as above except the model was extended to include the interaction between the

pressure and gas fraction fluctuations. They found good agreement again in the axial liquid velocity with the simulated values for the air-water system (a coalescing system). They also tested a non-coalescing system (air-water/propanol) and found good qualitative agreement, but not good quantitative agreement in the center of the column. The radial volume fraction had good agreement with experimental values at the higher gas flow rate (0.08 m/s) but with a gas flow of 0.06 m/s the agreement was not as good. The radial turbulent parameters obtained from the simulation were close to the experimental values but did not fluctuate as much as the experimentally observed ones. This work was a definite improvement over that done in 1990 but still did not predict all of the parameters well. Both works studied the steady state behavior and did not give any information on the dynamics in the column. From available experiments it is not even clear that meaningful steady states exist for bubble columns. Also, because of the low order of accuracy of the differencing scheme used, numerical diffusion would have been present. A higher order discritization scheme needs to be used for accurate results.

Ranade (1992) produced a "numerical simulation approach to investigating bubble columns". The model used was a simplified Euler-Euler model in which the slip velocity between the phases was specified so that the gas phase momentum equation was not required. It was also assumed that the radial component of the slip velocity was zero (e.g. the bubbles go straight up the column with no side-to-side motion). He further assumed that the tangential component of liquid velocity was zero everywhere so that a tangential symmetry was obtained. The boundary conditions include no slip at the walls, no slip at the bottom, axial symmetry, free

slip at the top, in which no liquid can cross the surface, and the inlet of gas was performed by using source terms in the appropriate inlet cells. In conjunction with Schwarz and Turner (1988), Ranade (1992) used the $k$-$\varepsilon$ turbulence model to simulate the turbulence of the liquid phase. He used a two phase flow solver called TPFLOW (details of this can be found in Ranade, 1991) and did not compare any of the numerical results to experimental results, however he performed many numerical experiments. The first of which was a grid test in which the turbulent kinetic energy and the axial liquid velocity were plotted against radial position for two different grids. The axial velocity did not change substantially when the grid was doubled but the turbulent kinetic energy did increase by a large amount. He also looked at the effect on the sparger area at the inlet and found that both the radial gas holdup and the axial liquid velocity did not change considerably with a reduction in the sparging area. He also studied the effect on column diameter and superficial gas velocity effects on the average gas holdup and the maximum axial velocity. The axial velocity was found to increase with increasing column diameter and superficial gas flow rate. The average holdup, however, only increased with increasing superficial gas velocity but remained constant over a large diameter range (0.15 m to 0.6 m). He found that both the average gas holdup and the predicted axial velocity varied largely with a changing slip velocity. Thus, it would seem to be important to specify the correct slip velocity if this method was to be used to simulate bubble columns. He looked at the effect of changing the height to diameter ratio in the bubble column. A significant change (both qualitatively and quantitatively) was found in the axial velocity component from the base of the

column to the top when the height to diameter was doubled and quadrupled. He also observed that changing the turbulence parameters did not significantly affect the axial velocity, but did affect the turbulent kinetic energy when the turbulence constant was changed. Again, by time averaging the momentum and continuity equations this study failed to provide any information on the dynamics of bubble columns and since the results were not compared to experimental results this study does not provide any information on the validity of this multi phase CFD code.

Dynamic simulations of bubble columns have also been performed. Becker et al. (1994) and Sokolichin and Eigenberger (1994) completed a two part study on bubble column simulations. In the first part (Sokolichin and Eigenberger, 1994) they describe the numerical model and gave some liquid velocity profile results. In their model they included groups of bubbles with different masses, a gas density dependent on the local pressure, no bubble coalescence or breakup and assumed laminar viscosity for the liquid phase. Both phases were assumed to have the same pressure. They used the Schwarz-Turner correlation to model the friction force between phases. The liquid phase was modeled as above but the dispersed phase included continuity and momentum balances for each group of bubbles. They also used a finite volume discritization method and a version of the SIMPLER algorithm (Patankar, 1980) which gave an efficient iterative solution for each time step. They used a two dimensional rectangular bubble column with a width of 0.5 m, a depth of 0.08 m and a height of 2 m. Also, in the first study, (Sokolichin and Eigenberger, 1994) they presented the instantaneous and time averaged liquid velocities for a uniformly aerated bubble column. The instantaneous liquid velocity profiles show

the time dependence or dynamic behavior in a bubble column while the time average liquid velocity field is qualitatively correct. The liquid rises in the center and comes down at the walls as observed in many experimental studies (Miyauchi and Shyu, 1970; Rietema and Ottengraf, 1970; Hills, 1974). However, there is no experimental data to compare their findings with. In the second part of their study (Becker et al., 1994) they examined a partially aerated bubble column. The gas was only allowed to enter through the left side of the column, which forces a net liquid circulation in the column. The local gas holdup was plotted across the width of the column at many vertical positions. It was compared visually with a photograph of the bubble column and qualitatively agreed very well. The actual gas holdup values from the experiment were not reported so, quantitatively, it is not known how close the simulated results were to the experimental ones. They measured the liquid velocities in the experimental bubble column using Laser Doppler anemometer (LDA) and compared it to the liquid velocities obtained through their mathematical model. Again, reasonable agreement was observed between the two. Both have the expected liquid circulation profile, but the two were not exact replicates and no numerical values are given so that the errors between the simulation and experimental results are hard to obtain. At higher gas flow rates the liquid circulation patterns change. They found experimentally that the bubble plume stayed at the left wall until it passed the midpoint of the column. At which time it moved towards the center of the column. This is a good test to see if the numerical model could indeed pick up this phenomenon, and it did. Their model seems to capture the dynamics of the bubble column rather well, qualitatively. However, in

order to have confidence in a model it must also be quantitatively accurate and this work lacks the quantitative comparison between experimental and numerical data.

### 2.2.2 Euler-Lagrange method.

The Euler-Lagrange method needs more computing power than the Euler-Euler method does because it is necessary to track hundreds of thousands of bubbles as they make their way through the column. It is important to first discuss the solution method for the Lagrangian approach to bubble column simulations.

#### 2.2.2.1 Solution method for Euler-Lagrange method.

For this method the equations for the continuous phase are the same as in the Euler-Euler method (i.e. the continuity and momentum equations are solved). This method is different, however, in the way the dispersed phase is modeled. A single bubble or a group of bubbles with the same mass have mean relative rise velocities that come from experimental correlations (Lapin and Lubbert, 1994). A group of bubbles of the same mass can be used instead of one single bubble because bubbles of the same mass, and thus size, would all have the same slip velocities. Grouping bubbles together and following the motion of a group of bubbles rather than a single bubble also greatly decreases the computational load to simulate a bubble column. The motion of the bubbles is also determined from the local liquid flow field. The overall or macro system describing the liquid phase is solved first. Then the gas phase or bubble positions and velocities are solved and substituted back into the macro model. The equation of motion for each bubble is:

$$m_i \frac{d\mathbf{v}_i}{dt} = \sum \mathbf{F}_i \tag{2.28}$$

where

$$\sum \mathbf{F}_i = \mathbf{F}_{total} = \mathbf{F}_p + \mathbf{F}_D + \mathbf{F}_{VM} + \mathbf{F}_L + \mathbf{F}_G \tag{2.29}$$

and the bubble positions are calculated using:

$$\frac{d\mathbf{x}_i}{dt} = \mathbf{v}_i \tag{2.30}$$

This repetition of iterations continues until some convergence criterion is met and the simulation can be advanced in time.

**2.2.2.2 Euler-Lagrange literature review**

Since the Euler-Lagrange model tracks the bubbles as they move through the column it is possible to get bubble positions and trajectories. The liquid velocity is calculated from the momentum and continuity equations so detailed information can be gathered from the Euler-Lagrange mathematical model. As mentioned above, there is not enough experimental work done on the dynamics of local parameters in bubble columns so most of the Euler-Lagrange work can only be justified visually. Webb et al. (1992), Lapin and Lubbert (1994) and Delnoij et al. (1997) have all published works on bubble column simulation using the Euler-Lagrange method.

Webb et al. (1992) completed a study in a two dimensional bubble column with a width of 0.3 m, a height of 0.5 m and a depth of 0.01 m. The gas inlet at the bottom of the column consisted of 7 evenly spaced orifices. They used a constant orifice gas flow rate of 2 $cm^3/s$ and assumed the bubbles to have a constant diameter of 6 mm. To model turbulence they used the $k$-$\varepsilon$ turbulence model. The liquid

surface was assumed to be flat and contain no tangential stresses. At the walls they assumed a no slip condition and a 'wall-function method' was used to model the flow between the wall and the fully developed turbulent flow in the column. They solved the differential equations using the SIMPLE method. The Lagrangian model includes the drag, buoyancy and pressure forces acting on the bubbles. It was also assumed that there is a constant slip velocity between the phases in the bubble column. Bubble-bubble interactions (coalescence and breakup) are considered using the model from Que (1991). In their results they looked at non-uniformly as well as uniformly distributed gas inlet and also considered the start up and shut down dynamics of the bubble column. With a non-uniform gas inlet profile they observed (numerically) what would be expected watching an experiment of the same. The bubbles tended to stay in clusters and formed a relatively straight line from the base to the top. The liquid circulation pattern is what would be expected in that the liquid went up with the bubble plume and came down away from the plume (at the walls). When the gas was introduced uniformly across the bottom of the column they observed what would be expected experimentally as well. The bubbles tended towards the middle and the liquid flow went up the center and down at the walls. The dynamic start up of the bubble column captured the essential flow characteristics qualitatively. From time zero (when the bubbles are first introduced into the bottom of the stagnant bubble column) it took approximately two seconds for the system to reach a macro steady state (i.e. the average holdup remained constant). With the large density difference between the phases it would be expected

that this would happen quickly. However, none of these results are compared to experimental results so they can not be taken as more than qualitatively correct.

Lapin and Lubbert (1994) also simulated the flow in a two dimensional bubble column using an Euler-Lagrange method. Instead of following the motion of single bubbles through the bubble column they tracked groups of bubbles with the same mass. This was done to reduce the computational power required to simulate the bubble column. This can be done since they believe that "clustering of bubbles is really happening in bubble columns. At gas holdups encountered in practice, the bubbles do not move altogether independently from each other; adjacent bubble are in the same gross motion". In the model they present they do not include bubble-bubble interactions. To solve the discritized equations they used a method similar to the SIMPLER algorithm and used an adaptive time stepping procedure. The grid they used was not uniform but had smaller elements at the wall than in the center of the column. In a 4.0 m by 1.0 m column they released 20,000 bubble clusters and tracked them as they made their way through the column. They assumed the slip velocity between the phases was 10 cm/s. They observed fingering of the dispersed phase and noticed the chaotic structure of the velocity pattern. They also ran a simulation in a 0.5 m by 1.5 m column in which the gas was introduced into the column only through one 2.5 cm inlet. They continuously injected 2000 bubble clusters per second and assumed a slip velocity of 20 cm/s for this run. The column was run for 45+ seconds and time snap shots of the bubble positions and velocity patterns were taken at various times. This experiment showed the time dependence or dynamic behavior of the bubble column. Another numerical experiment in a 1.0

m by 1.5 m column was performed in which the gas was introduced across the entire bottom of the column. For this numerical experiment they assumed a slip velocity of only 5 cm/s (very small bubbles). This study again showed the chaotic behavior of bubble columns and appears to be qualitatively correct. However, in this study there is no experimental data to compare the numerical results to, so quantitatively the results can not be validated.

Delnoij et al. (1997) did compare their dynamic numerical results to experimental work done by Becker et al. (1995). They found that at a high flow rate, in a non-uniformly aerated bubble column, their numerical results agreed very well with the development of a powerful liquid circulation, which causes the bubble swarm to be pushed against a wall. At lower flow rates Becker et al. (1995) found the flow to be highly dynamical with a vertical liquid velocity oscillation occurring every 41 seconds. They found a similar result and observed the same flow pattern and structure that Becker et al. (1995) obtained. However, the period of oscillation they observed numerically was 30 seconds instead 41 seconds. They predicted the difference was due to the two dimensional nature of their model. The model they used had a no slip condition placed on the column walls and the top surface had a free slip condition and was considered as an impermeable wall for the liquid phase. The bottom of the column was also specified as an impermeable wall but with a no slip condition. No turbulence models were used for the liquid phase.

### 2.2.3 VOF method

This solution method, like the Euler-Lagrange method, is computationally expensive. In this case the movement of the gas-liquid interphase (which separates

the gas in the bubble from the surrounding fluid) is tracked, instead of the movement of the bubble as in the Euler-Lagrange case. This model has an advantage in that the bubble dynamics, such as the motion, shape, volume and pressure, can be obtained from the motion of the bubble surface without making any assumptions.

#### 2.2.3.1 Governing equations for VOF method

As mentioned above the VOF method solves the liquid phase using the continuity and momentum equations. For the gas phase, the positions of the bubbles are determined by tracking the position of the gas-liquid interfaces between the bubbles and the surrounding liquid. Thus no assumptions need to be made about the bubbles being perfectly spherical or having the same pressure as the liquid phase. The movement of the interface is calculated based on the function $\psi$ (the gas phase volume fraction, equals one inside the bubble and zero in the liquid). At the interface $\psi$ is a value between zero and one. The governing equation for $\psi$ is shown in two dimensional form.

$$\frac{\partial \psi}{\partial t} = -u\frac{\partial \psi}{\partial x} - w\frac{\partial \psi}{\partial z} \tag{2.31}$$

#### 2.2.3.2 VOF method numerical results

Lin et al. (1996) completed a numerical study using the VOF method as well as some experimental work using PIV (Particle Image Velocimetry) to obtain instantaneous bubble column results. They looked at two different systems; air-glycerin and air-water. To compare instantaneous results from the PIV experimental

data and the VOF numerical simulation they looked at liquid velocities for the region in front of bubbles and the vortex sizes. For the air-glycerin system they found the liquid velocities to be within 5% of each other and also observed the vortex sizes were equivalent in both the experimental and numerical results. For the air-water system they also found good quantitative agreement. They found that the vortex sizes were very close numerically and experimentally and the liquid velocity at the side walls and in front of the bubbles were also very close. However, they fail to show if these parameters stay bounded in time and if they follow some pattern of oscillation or remain stationary. They give instantaneous results for only one or two time frames when a time dependent figure needs to be shown comparing the numerical and experimental vortex sizes and local liquid velocities.

Delnoij et al. (1997) also completed a numerical study in a bubble column using the VOF method. They used the VOF method to predict the movement and shape of large bubble(s) rising through a liquid. They observed the spherical cap shape of the bubble and also included multi-bubble runs. They produced images showing the bubble positions and shape as well as including the instantaneous liquid velocity throughout the column. They also produced results showing bubble coalescence. These results, although very promising, were not compared to experimental results so it is not known if this VOF method compares well quantitatively with experimental results.

### 2.2.4 Macroscopic models for bubble columns

This section contains information on other bubble column simulations that have been done, namely simulations based on an energy balance. This type of model

does not give information on what is happening in the column but predict macro quantities in the column such as the average gas holdup and the overall flow pattern.

More recently energy balances have been done over the entire bubble column and are used to predict the average gas holdup and the overall flow pattern in the column. Garcia-Calvo and Leton (1994) and Garcia-Calvo et al. (1996) have all performed such energy balances. Garcia-Calvo et al. (1994 and 1996) used the following equations to model the bubble column:

$$E=W+S \tag{2.32}$$

where

$$E = P(10^6)U_g \ln\left(1+\frac{\rho_l g H}{P_{atm}(10^6)}\right) \tag{2.33}$$

$$S = \psi v_s \rho_l g H \tag{2.34}$$

$$W = \frac{0.64(2)^{3N/2} N^3 n^2 \rho H v_{l0}^3}{D}\left(\frac{1}{2(3N-1)}+\frac{1}{(3N-1)}-\frac{\sqrt{2}}{3N}\right) \tag{2.35}$$

where N is a model constant and is dimensionless (will be discussed later) and the velocity of the liquid in the core is calculated from:

$$v_{lc} = \frac{v_{l0}}{1-\psi}\left(\frac{N}{N+2}\right) \tag{2.36}$$

and the gas holdup is calculated from:

$$\psi = \frac{U_g}{v_s + 0.5 v_{lc}} \tag{2.37}$$

The average holdup and core liquid velocity can be found from Equations 2.32, 2.36 and 2.37. They assumed a bubble slip velocity, or terminal rise velocity ($v_s$), to be 25 cm/s for air-water systems and used an empirical formulation for salt solutions and CMC solutions. For their paper in 1994 they used a value of 2.3 for $N$. The numerical data obtained was compared to an extensive amount of experimental data. Most of the experimental data on gas holdup values were within ± 30% of their numerically predicted values. They found the same agreement for the liquid velocity in the center of the columns as well as for axial dispersion coefficient $D_l$. In 1996 they used a model constant of $N = 2.0$ and made $W$ dependent on whether the flow in the column was laminar or turbulent. Equation 2.35 is for turbulent flow and for laminar flow the following equation was used:

$$W = \frac{2HK}{(N-1)(n+1)+2}\left(\frac{2^{(N+2)/2}\,N v_{l0}}{D}\right)^{n+1} \qquad (2.38)$$

With this added feature to their model they were able to reduce their margin of error from ± 30% to ± 20% for the overall gas holdup. Most of their numerical data did fall within ± 20% of the experimental data. As mentioned above, the major shortcoming of this model is that it does not provide the user with any of the dynamics of the bubble column.

## 2.3 Review articles

This section contains references and brief descriptions of bubble column review articles. These articles give information about experimental work, empirical correlations, comparisons of numerical studies and discussions on Euler-Euler and Euler-Lagrange models.

An overview of the experimental work that has been done on bubble columns can be found in the study done by Koide (1996). He looked at such things as flow regimes, empirical correlations for the average gas holdup, mass transfer, bubble sizes, and advanced experimental techniques being used in bubble columns. He also discussed flow models for bubble columns.

An article by Deckwer and Schumpe (1993) gives an overview of the of the design and scale up of bubble columns. They give recommendations as to what to use for scale up and design and give empirical correlations to predict the average gas holdup and mass transfer. This study does not include any simulation work.

Sokolichin and Eigenberger (1994) presented a comprehensive review of the numerical simulations of bubble columns. They provide a solid overview of the different numerical models that can be used (Euler-Euler and Euler-Lagrange). They discuss past numerical studies and pros and cons of the different models. They present and fully explain the different terms that can affect the interphase transfer term. A similar type of paper was produced by Delnoij et al. (1997). They talk about the Euler-Euler, Euler-Lagrange and VOF models. They also give an overview of some advanced experimental techniques that are producing instantaneous velocity results.

An interesting study by Sokolichin et al. (1997) also discussed the Euler-Euler and Euler-Lagrange methods. However, in this paper they tested the two models to see if they would produce the same results. They found that the two models produced identical results if a high order discritizing scheme was used in the Euler-Euler model. If a low order (UPWIND) scheme was used for the Euler-Euler method, numerical diffusion completely blurred the results to the point that they were not even qualitatively correct.

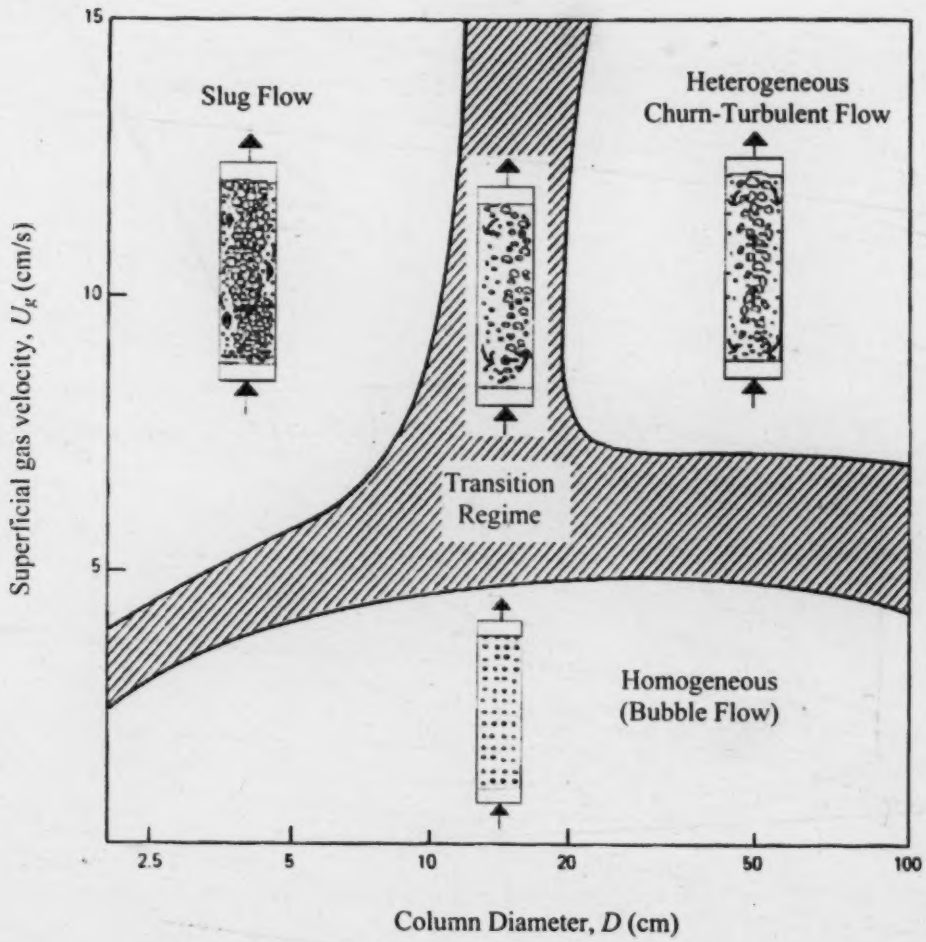


**Figure 2.1. Flow regimes in a bubble column for low viscosity fluids. Figure taken from Bisio and Kabel (1985) and diagrams from Koide (1996).**

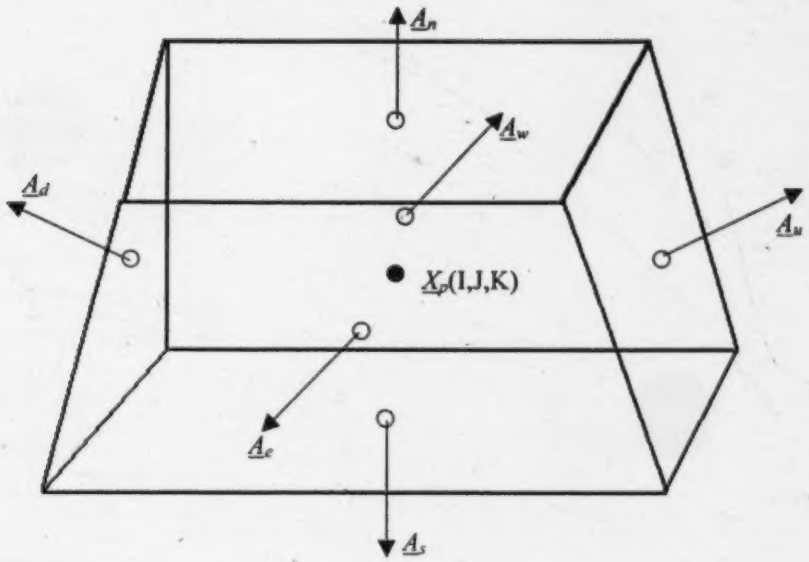


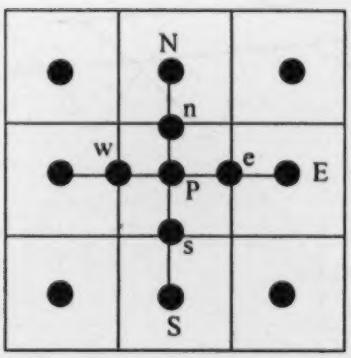


**Figure 2.2. Structure of numerical control volume. Top shows full 3 dimensional case and bottom shows the 2 dimensional case.**

# Chapter 3. Experimental methods and results

In order to verify predictions from a mathematical model of a bubble column it is necessary to have experimental data for comparison. This section describes the bubble column used to obtain the experimental data, how that data was obtained and the results found.

## 3.1 Experimental apparatus and setup

The bubble column setup used in the experimental study is shown in Figure 3.1. The bubble column is constructed of glass so that flow regimes and liquid levels could easily be observed. The gas (air from the buildings main supply) was introduced through the bottom of the column. As the gas entered the column it passed through a sintered glass plate. The sintered glass plate was used to get an even distribution of gas over the bottom of the column. The column was 3.5 cm wide and 1 cm deep. These dimensions were chosen in order to produce two dimensional flow in the bubble column. The liquid level was always kept at a height greater than 15 cm and less than 25 cm. Pressure taps in the form of manometers were placed on the side of the column every 5 cm from the base to the top in order to get sectional gas holdup values. For the steady state case air is supplied from the building's main supply, it passes through a flow control valve (hooked up to a digital flow controller) and enters the bottom of the bubble column. For this case the on/off hand valve is closed. For the step change experiments, the air is split into two separate lines. One line includes an on/off valve before passing through a rotameter and the second line includes a digital flow control valve. Both lines then rejoin before entering the bottom of the column. In order to calibrate the flow rates

through the digital flow valve and the rotameter the same setup was used as above except the outlet to bubble column was moved so the air flow went through a soap meter instead of the bubble column. The flow rate was obtained by averaging the time it took a soap film interface to rise through the soap meter a certain distance.

## 3.2 Experimental results

This section gives the results obtained experimentally from the bubble column. These include the fluid properties, bubble diameter measurements, average gas holdup measurements for various liquids and dynamic results when a step change in flow rate is induced.

### 3.2.1 Fluid properties

For the pure component systems of air-water, air-methanol and air-cyclohexane the properties of the fluids are given in Table 3.1. The surface tension for water is much higher than it is for any of the other liquids. The densities of all three liquids are approximately the same with water being slightly larger than methanol and cyclohexane. Table 3.2 shows the fluid properties for the air-water/methanol mixture systems used in this study. The surface tension of the methanol-water mixture system decreases sharply as methanol is added to pure water. The surface tension gradient is much smaller when considering adding small amounts of water to pure methanol. All fluid properties were obtained at 20 °C and 101.3 kPa pressure (surface tensions measured at 95 kPa).

**Table 3.1. Pure component fluid properties.**

| Fluid | Density*, $\rho$ ($kg/m^3$) | Viscosity*, $\mu$ (kg/m·s) | Surface tension** $\sigma$ (N/m) |
|---|---|---|---|
| Air | 1.222 | 0.000018 | N/A |
| Water | 998.0 | 0.0010 | 0.07275 |
| Methanol | 792.0 | 0.00059 | 0.0196 |
| Cyclohexane | 774.0 | 0.00095 | 0.0238 |

* From Perry et al. (1984)

** Measured

**Table 3.2. Water-methanol mixture fluid properties.**

| Mass fraction of Methanol in water | Density*, $\rho$ ($kg/m^3$) | Viscosity*, $\mu$ (kg/m·s) | Surface tension** $\sigma$ (N/m) |
|---|---|---|---|
| 0.1 | 972.7 | 0.000949 | 0.0517 |
| 0.3 | 925.8 | 0.000854 | 0.0383 |
| 0.5 | 883.1 | 0.000768 | 0.0317 |
| 0.7 | 844.3 | 0.000691 | 0.0274 |
| 0.9 | 808.7 | 0.000622 | 0.0237 |

* From Perry et al. (1984)

** Measured

### 3.2.2 Bubble diameter measurements

Bubble diameters at various flow rates were measured using a visual method. The bubble column was video recorded in sections using a high-resolution 8 mm camcorder. Images were extracted from the 8 mm tape using the Snappy software. Figures 3.2 to 3.4 show images taken from pure component systems at various flow rates. For the methanol/water mixture system Figures 3.5 to 3.7 show images used to obtain the bubble diameters for methanol mass fractions of 0.1, 0.5 and 0.9. As can be seen in these three figures the bubble diameter increases as the concentration of methanol increases. At a mass fraction of 0.1 it is almost impossible to distinguish single bubbles. In comparing the images from the pure component systems to the water/methanol systems, it is evident that the bubble diameters are much smaller in the mixture systems than in the pure component systems. A series of similar images were captured in each section of the bubble column from a height of 3 cm to 15 cm or more. The still images were then used with Sigma Scan Pro to obtain the bubble diameters. The program enables the user to specify the length scale (made possible by having a ruler in the background as seen in Figures 3.2 to 3.7) and select the objects (bubbles) which the user wants to be used to calculate the bubble diameters. Only free bubbles were selected because it was difficult to tell the difference between bubbles that were colliding and when there was one bubble moving behind another. In the homogenous flow regime this technique works very well to get average bubble diameters in each section observed. The program computes the area of the selected objects and calculates the diameter by assuming the objects to be spherical ($A = \pi D^2$). For each section (approximately

3 cm in height) many bubbles and images were used to obtain an average bubble diameter. The bubble diameters for the air-water system for three different flow rates are given in Figure 3.8 as a function of distance from the bottom of the column. This is in agreement with the findings of Chang and Harvel (1992) who found that the bubble diameters increase with superficial gas velocity. For the other systems the bubble diameters were only measured in the center section of the column and used only to make sure the bubbles were in the distorted particle regime. For both the methanol and cyclohexane systems, the bubble diameters were similar to that of the water system. The water/methanol system average bubble diameters are shown in Figure 3.9 for a superficial air velocity of 0.815 cm/s. It was not possible to get the bubble diameters for a methanol mass fraction of 0.1 because there are too many bubbles in the system (see Figure 3.5). The small bubble sizes are due to the surface tension gradients on the gas-liquid interface.

### 3.2.3 Average gas holdup measurements

The gas holdup in the column (calculated using Equation 2.1) was obtained for four systems containing pure liquids and the water/methanol mixture systems. The values of the liquid levels were obtained using a ruler measuring from the bottom of the column to the liquid level. Table 3.3 shows the average gas holdup in the bubble column for various pure liquid systems. The results for the water/methanol systems are presented in Tables 3.4 to 3.8. The average gas holdups in the water/methanol systems are higher than those for either the pure water or pure methanol systems. The largest values of the gas holdup occur at a mass fraction of 0.3. As the concentration of methanol is increased the gas holdup decreases. The

errors in the flow rates and gas holdups where found using the uncertainty analysis method in Holman (1988).

**Table 3.3. Experimental gas holdup values for the pure component systems.**

| | Average gas holdup, $\psi$ | | |
|---|---|---|---|
| Superficial gas velocity (cm/s) | Air-water | Air-methanol | Air-cyclohexane |
| 0.377 ± 0.039 | N/A | 0.026 ± 0.003 | 0.019 ± 0.004 |
| 0.716 ± 0.074 | 0.035 ±0.004 | N/A | N/A |
| 0.815 ± 0.085 | 0.041 ± 0.005 | 0.056 ± 0.005 | 0.053 ± 0.006 |
| 1.53 ± 0.16 | 0.073 ± 0.007 | 0.105 ± 0.008 | 0.099 ± 0.008 |
| 1.78 ± 0.19 | 0.092 ± 0.006 | N/A | N/A |
| 1.91 ± 0.20 | N/A | 0.137 ± 0.006 | 0.125 ± 0.006 |
| 2.20 ± 0.23 | 0.115 ± 0.008 | 0.164 ± 0.009 | 0.151 ± 0.009 |

**Table 3.4. Average gas holdup for 0.1 mass fraction of methanol in water.**

| Superficial gas velocity (cm/s) | Average gas holdup, $\psi$ |
|---|---|
| 0.815 ± 0.085 | 0.084 ± 0.007 |
| 1.53 ± 0.16 | 0.118 ± 0.006 |
| 2.20 ± 0.23 | 0.181 ± 0.008 |
| 2.90 ± 0.30 | 0.240 ± 0.007 |

**Table 3.5. Average gas holdup for 0.3 mass fraction of methanol in water.**

| Superficial gas velocity (cm/s) | Average gas holdup, $\psi$ |
|---|---|
| 0.815 ± 0.85 | 0.088 ± 0.005 |
| 1.53 ± 0.16 | 0.131 ± 0.005 |
| 2.20 ± 0.23 | 0.193 ± 0.006 |
| 2.90 ± 0.30 | 0.253 ± 0.005 |

**Table 3.6. Average gas holdup for 0.5 mass fraction of methanol in water.**

| Superficial gas velocity (cm/s) | Average gas holdup, $\psi$ |
|---|---|
| 0.815 ± 0.85 | 0.075 ± 0.006 |
| 1.53 ± 0.16 | 0.116 ± 0.005 |
| 2.20 ± 0.23 | 0.171 ± 0.007 |
| 2.90 ± 0.30 | 0.241 ± 0.006 |

**Table 3.7. Average gas holdup for 0.7 mass fraction of methanol in water.**

| Superficial gas velocity (cm/s) | Average gas holdup, $\psi$ |
|---|---|
| 0.815 ± 0.85 | 0.065 ± 0.006 |
| 1.53 ± 0.16 | 0.104 ± 0.005 |
| 2.20 ± 0.23 | 0.165 ± 0.007 |
| 2.90 ± 0.30 | 0.229 ± 0.006 |

**Table 3.8. Average gas holdup for 0.9 mass fraction of methanol in water.**

| Superficial gas velocity (cm/s) | Average gas holdup, $\psi$ |
|---|---|
| 0.815 ± 0.85 | 0.056 ± 0.006 |
| 1.53 ± 0.16 | 0.101 ± 0.005 |
| 2.20 ± 0.23 | 0.162 ± 0.007 |
| 2.90 ± 0.30 | 0.218 ± 0.006 |

### 3.2.4 Experimental step change results (bubble column dynamics)

The experimental parameter measured for the step change experiments was the average gas holdup. When the on/off valve (Figure 3.1) is opened the gas flow rate instantaneously increases and the average gas holdup in the column immediately increases too. The holdup keeps increasing until a new steady state is reached. To obtain the dynamics of these step changes the liquid level can be observed. When the level starts to move the step is initiated and when the level stops moving the system is again at steady state. To obtain the time this takes, and to get the time for the holdup to reach values between each steady state value, the liquid level was video taped, again using the high resolution 8 mm camcorder. The videotape of the liquid level was then analyzed frame by frame. The exact frame numbers were recorded and knowing that there are 30 frame per second the time for the step change to go from one steady state to another could be obtained. This was repeated a minimum of 10 times so an accurate, average value of the time it takes to go from one steady state to another was obtained. Table 3.9 illustrates the time taken to get from the initial steady state gas holdup to two intermediate points and the final holdup for the air-water system. The flow rates used for the air-water system were 0.716 ± 0.074 cm/s and 1.78 ± 0.187 cm/s. For the air-methanol and air-cyclohexane systems the flow rates were 0.377 ± 0.040 cm/s and 1.91 ± 0.20 cm/s. Tables 3.10 and 3.11 show the values for the air-methanol and air-cyclohexane systems respectively.

**Table 3.9. Experimental step change results for air-water system.**

| | $\psi = 0.035$ | $\psi = 0.056$ | $\psi = 0.074$ | $\psi = 0.092$ |
|---|---|---|---|---|
| Time (s) | 0.0 | 0.4 | 0.8 | 1.2 |

**Table 3.10. Experimental step change results for air-methanol system.**

| | $\psi = 0.026$ | $\psi = 0.062$ | $\psi = 0.107$ | $\psi = 0.137$ |
|---|---|---|---|---|
| Time (s) | 0.0 | 0.4 | 0.9 | 1.5 |

**Table 3.11. Experimental step change results for air-cyclohexane system.**

| | $\psi = 0.019$ | $\psi = 0.055$ | $\psi = 0.094$ | $\psi = 0.125$ |
|---|---|---|---|---|
| Time (s) | 0.0 | 0.4 | 0.9 | 1.5 |

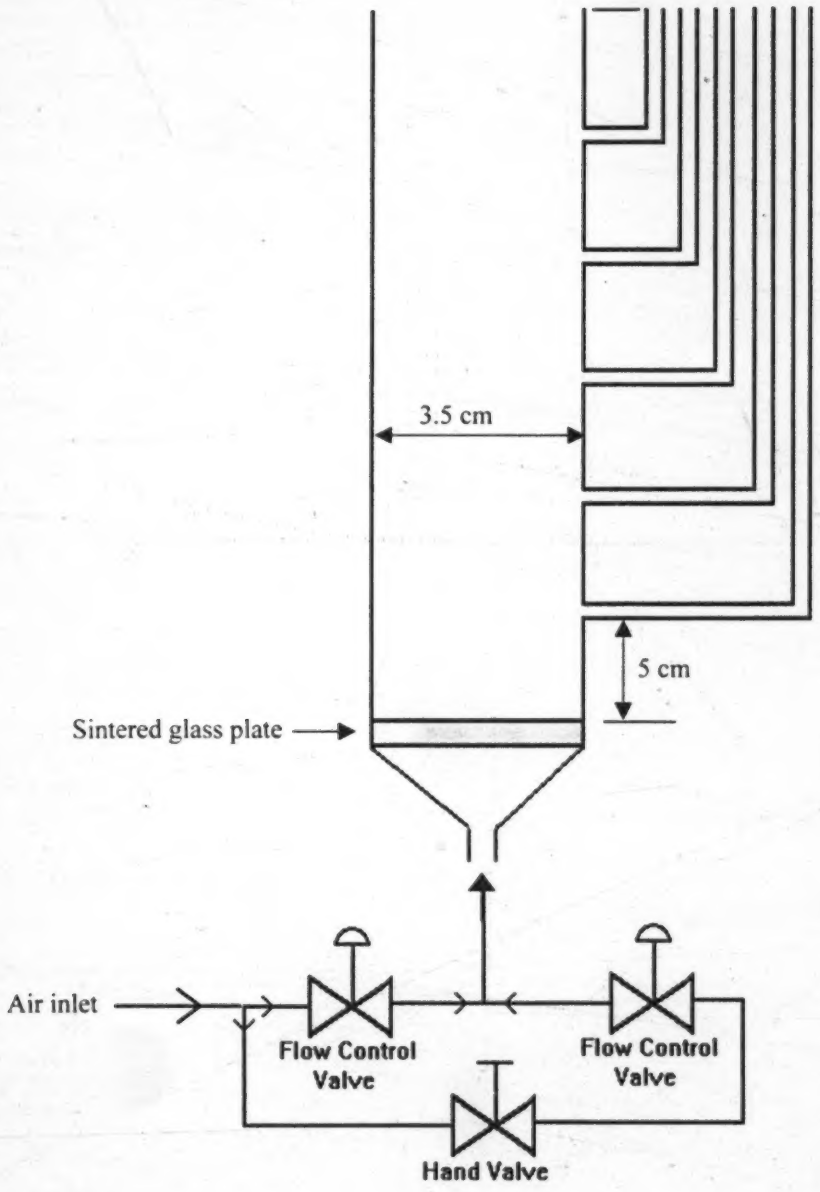


**Figure 3.1. Experimental bubble column setup.**

$U_g$ = 0.815 cm/s

$U_g$ = 1.53 cm/s

$U_g$ = 2.20 cm/s

**Figure 3.2. Images used to get bubble diameters for air-water system.**

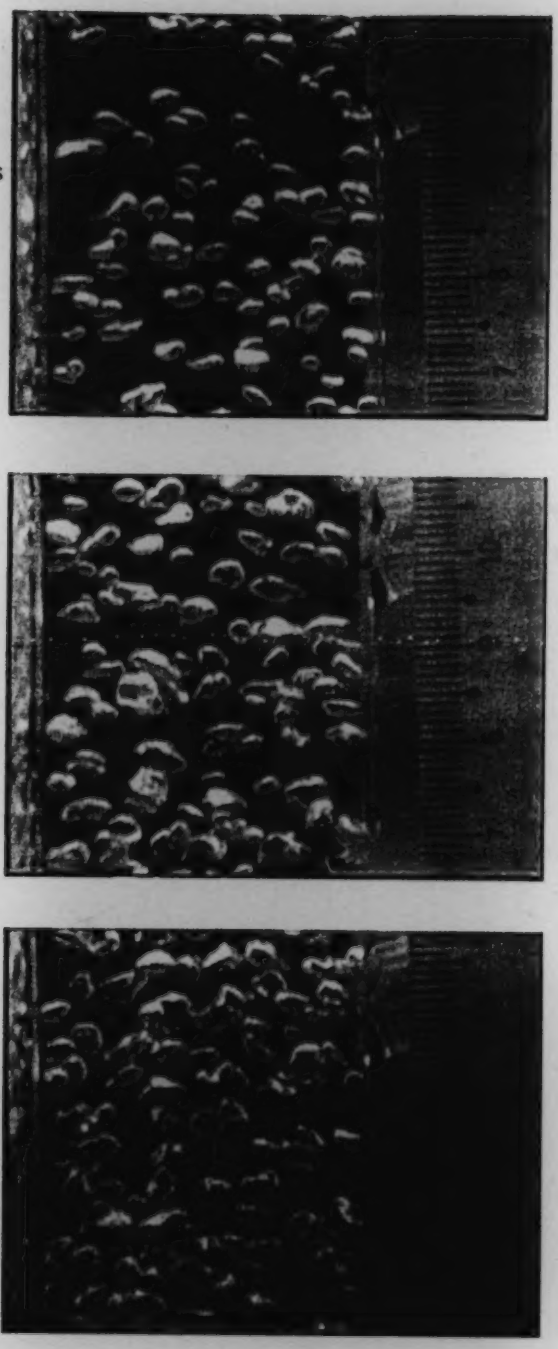


**Figure 3.3. Images used to get bubble diameters for air-methanol system.**

$U_g$ = 0.815 cm/s

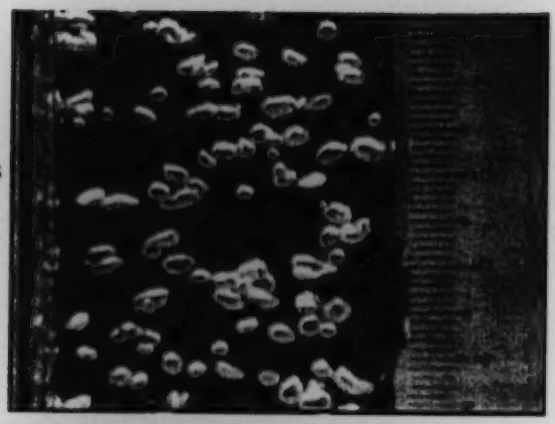

$U_g$ = 1.53 cm/s

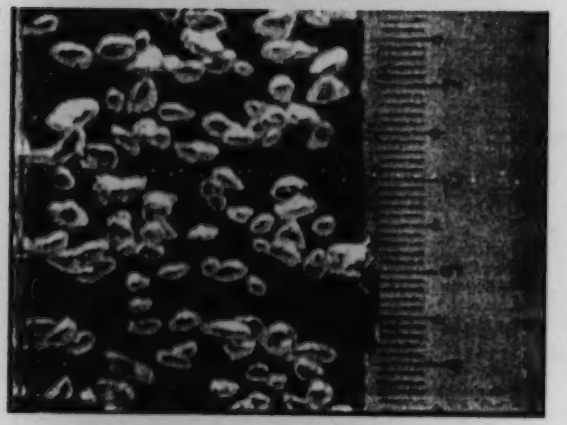

$U_g$ = 2.20 cm/s

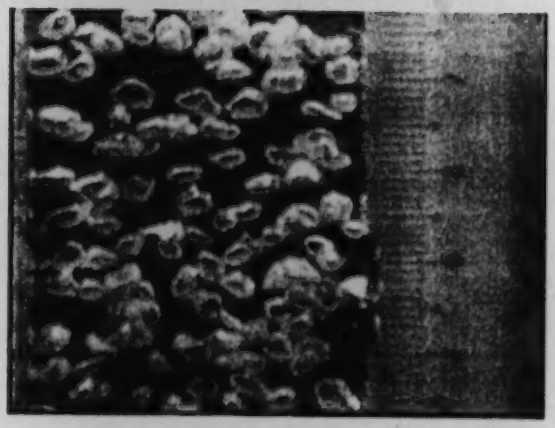

**Figure 3.4. Images used to get bubble diameters for air- cyclohexane system.**

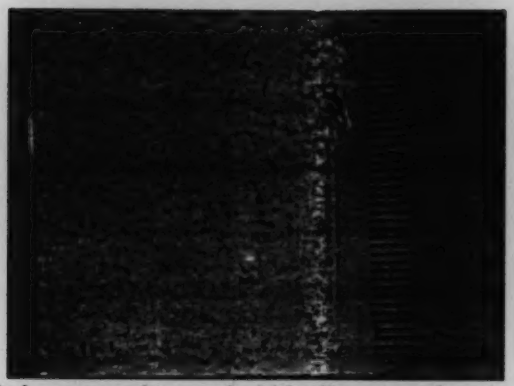

**Figure 3.5. Sample image used to get bubble diameters for air-10% methanol in water system for a superficial gas velocity of 1.53 cm/s.**

**Figure 3.6. Sample image used to get bubble diameters for air-50% methanol in water system for a superficial gas velocity of 1.53 cm/s.**

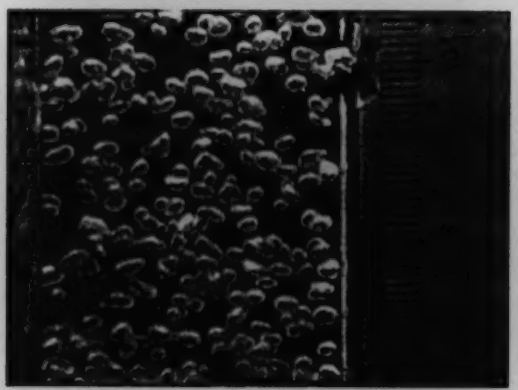

**Figure 3.7. Sample image used to get bubble diameters for air-90% methanol in water system for a superficial gas velocity of 1.53 cm/s.**

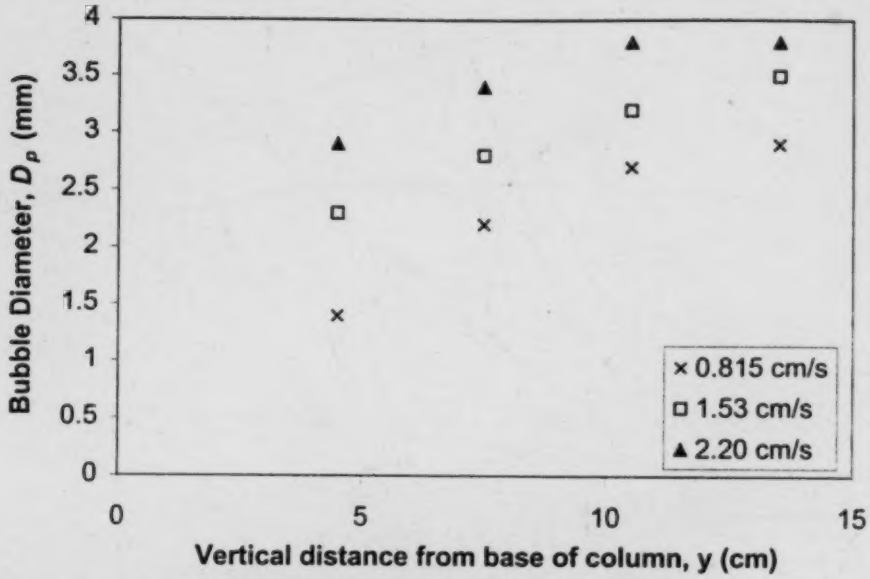


**Figure 3.8. Average bubble diameters of air-water system. $U_g$ = 0.815 cm/s**

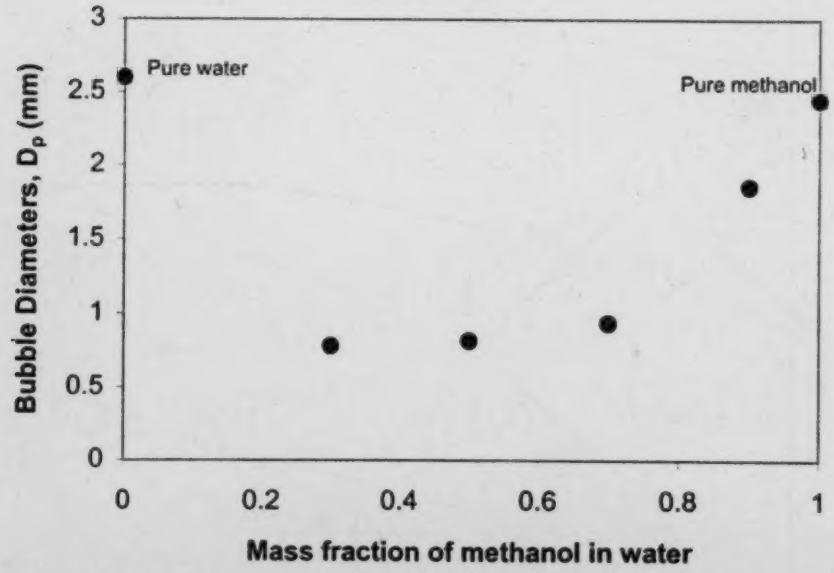


**Figure 3.9. Bubble diameters of water/methanol mixture system.**

# Chapter 4. Simulation results

In this chapter, results of simulations based on a continuum model are presented. The model equations are based on the volume averaged Navier Stokes equations in an Eulerian frame of reference for both the gas and liquid phases. Included are the results for steady state simulations, step change simulations and local velocity and holdup profiles. The simulation results based on different discritization schemes, grid sizes, time steps and the addition of an added mass term are also presented.

## 4.1 Simulation properties

In this section, the simulated bubble column dimensions, discrete grid and boundary conditions are presented. The method used to solve the equations used to model the bubble column is also discussed.

### 4.1.1 System dimensions and the discrete grid

The simulated bubble column was 3.5 cm wide, 15 cm high and 1 cm in depth. This conforms to the dimensions of the experimental bubble column described in the previous chapter. The bubble column was discritized into cells. These dimensions were chosen so that the column could be discritized into a two dimensional system. The grid used for this system was a 20 by 60 grid (1 cell in depth). There were 20 cells across the width of the column and 60 through the height. The 60 cells through the height of the column were evenly spaced while the 20 cells through the width were non-uniformly spaced. The grid spacing was calculated using the following formula (Fletcher, 1988).

$$X(I) = \frac{(2D_x - 1)3.5}{2} \tag{4.1}$$

where

$$D_x = \frac{2.05C_x - 0.05}{2(1 + C_x)} \tag{4.2}$$

and

$$C_x = A_x^{B_x} \tag{4.3}$$

$$A_x = \frac{1.05 + 1}{1.05 - 1} \tag{4.4}$$

$$B_x = \frac{2(i-1)}{n-1} - 1 \tag{4.5}$$

where $i$ is the node number (from 1 to 20), $n$ is the total number of nodes (n=20) and 3.5 is the total width of the column in cm. Figure 4.1 shows the numerical grid used in the simulation. A Fortran user routine was used to make the grid (see Appendix B).

A constant time step of 0.01 s was used for all runs unless otherwise specified. To discritize the equations in time the backward differencing scheme was used.

### 4.1.2 Boundary conditions

The bubble column must have boundary conditions at the system boundaries for the model to be closed. In the model of the bubble column the, boundary conditions must be specified at the side walls, the air inlet (the bottom of the column) and the top of the column. The side walls have a no slip condition for the liquid phase and a slip condition on the dispersed phase. This means that the liquid

velocity is set to zero at the wall while the bubbles can move along the walls. This model was chosen because gas bubbles can rotate at the walls producing a net vertical velocity. At the bottom of the column the liquid phase also has a no slip condition imposed. This is where the gas enters the column and the inlet superficial velocity was specified. Since, experimentally, the air enters through a sintered glass plate of unknown voidage, it was assumed that the voidage was 50% so the superficial velocity specified was the volumetric flow rate divided by the width of the column, the thickness of the column and a factor of ½ (for the assumed sintered glass plate voidage). Periodic boundary conditions were used in the $z$ direction to ensure that all variables have the same value at each end of the computational domain. This ensures that the simulation is two-dimensional. At the top of the column, the liquid-gas interface is modeled using a pressure boundary condition. The velocity of the air through the top boundary is set to be a constant value equal to the rise velocity divided by the gas fraction. A Fortran user routine (USRBCS) was used to set this boundary condition (see Appendix C).

### 4.1.3 Solution method for the Euler-Euler model

To solve the equations used to model the bubble column two iterative steps are taken. This includes an outer iteration and the inner iteration. The inner iteration is done first. All of the variables (velocities, volume fractions, ect.) are held constants except the one being solved for. This is done across the entire domain and for each parameter. The equations are then sent to a linear equation solver and the updated variables are sent to the outer iteration. The outer iteration is a pressure correction step. It is responsible for updating the pressure and correcting the

velocity field so mass is conserved. The semi implicit method for pressure linked equation (SIMPLE) algorithm is one of a few algorithms that are used to model the velocity-pressure coupling. The SIMPLEC algorithm, a slight deviation from the SIMPLE algorithm, was used for this numerical study.

The inner iteration can be solved using different linear equation solvers such as: preconditioned conjugate gradients (ICCG), Stone's method, block Stone's method and the algebraic multi-grid method (AMG). The AMG method was used for the numerical simulations performed for this work and is described below. For the AMG method, the equations are first solved on a coarse grid (in the CFX-F3D code the grids are chosen automatically and algebraically). The coarse grid solution is then interpolated to a finer grid and this continues until the fine grid is the same as the grid chosen by the user.

To solve the differential equations of the inner iteration they must be discritized into a set of linear equations. There are many methods to discritize equations. The simplest, or those of lowest order of accuracy, are the upwind differencing (UDS) and hybrid differencing (HDS) methods. The HDS is the default choice in the CFX-F3D code. For the majority of the simulations performed in this study CCCT method was used to discritize the equations. This scheme is third-order accurate and compensates for the non-physical overshoots of the QUICK scheme. This higher order scheme was used because of the findings in Sokolichin et al. (1997) (see Chapter 2 for discussion). It has the form:

$$\phi_w = (\frac{3}{8} - \alpha)\phi_p + (\frac{3}{4} + 2\alpha)\phi_w - (\frac{1}{8} + \alpha)\phi_{ww} \tag{4.6}$$

where $\alpha$ is a parameter that is dependent on the curvature of the variable $\phi$ (details of this can be found in Alderton and Wilkes (1988)). Fixed time stepping was used with backward differencing being employed as the differencing scheme. Backwards differencing approximates the following differential equation:

$$\frac{\partial \phi}{\partial t} = F(\phi) \tag{4.7}$$

by

$$\frac{\phi^n - \phi^{n-1}}{\Delta t} = F(\phi^n) \tag{4.8}$$

## 4.2 Steady state results

In order to have any confidence in the numerical model the simulation must be able to mirror the macro quantities of the experimental system. For this reason the time averaged gas holdup was computed and compared to those values found experimentally. Since the Ishii-Zuber drag correlation does not take into account wall effects, and the column being used for this study is small (3.5 cm wide and 1.0 cm thick), a series of tests were conducted to adjust the drag correlation to account for the wall effects. This has been done for solid-liquid systems using the Richardson-Zaki drag correlation (Wallis, 1969). For all the systems studied the Ishii-Zuber drag correlation was multiplied by factors ($k^*$) of 1, 1.5 and 2 for all of

the flow rates examined. The bubble column simulation was run with each of these constants and plotted against flow rate. Figure 4.2 shows the results for the air-water system. The results for the air-methanol and air-cyclohexane systems are shown in Figures 4.3 and 4.4. For each system and at each flow rate a linear best fit line was computed. The experimental value of the average gas holdup at that specific flow rate was then put into the linear best fit line equation and the ideal constant was extracted (such that the experimental average gas holdup would equal the numerically predicted gas holdup). This was done nine times (three systems and three flow rates for each system) and an average value of the ideal constant was taken. The average value of $k^*$ was found to be 1.2. This constant of 1.2 was used for the remainder of the simulations. A Fortran user routine (USRIPT) was used to implement this change to the Ishii-Zuber model (see Appendix D)

In order to prove that the average gas holdup was not changing with time (as observed experimentally) Figures 4.5 to 4.7 are used to show the time series of average gas holdup values for the air-water, air-methanol and air-cyclohexane systems respectively. As can be observed in these figures the average gas holdup in the simulated bubble column remains constant, with only minor fluctuations.

Figure 4.8 shows a comparison of the average gas holdup in the bubble column at different flow rates for the air-water system. The average experimental holdup and the holdup predicted from the empirical correlations (Table 2.1) have also been included in this figure. Table 4.1 shows the percent difference between the gas holdups observed experimentally and numerically. The same plots have been presented for the air-methanol and air-cyclohexane systems (Figures 4.9 and 4.10

respectively). Table 4.1 also illustrates the percent differences between the experimental and numerical average holdup results for the air-methanol and air-cyclohexane systems respectively.

**Table 4.1. Comparison of experimental and numerical gas holdups for pure component systems.**

| | % difference between experimental and predicted gas holdup. | | |
|---|---|---|---|
| Superficial gas velocity, $U_g$ (cm/s) | Air-water | Air-methanol | Air-cyclohexane |
| 0.377 | N/A | 3.8 | 21.0 |
| 0.714 | 1.7 | N/A | N/A |
| 0.815 | 5.3 | 0.0 | 0.4 |
| 1.53 | 4.1 | 6.7 | 7.1 |
| 1.78 | 0.8 | N/A | N/A |
| 1.91 | N/A | 5.8 | 5.6 |
| 2.20 | 1.7 | 4.3 | 7.9 |

The water/methanol mixture systems where also simulated. Convergence problems lead to only a limited amount of numerical data. The system was only simulated for a superficial gas velocity of 0.815 cm/s. Figure 4.11 shows the experimental and numerical gas holdups for different amounts of methanol in water. For mass fractions of 0.1, 0.3, 0.5 and 0.7 the predicted holdup is larger than the experimental holdup and for the final point (mass fraction of 0.9) the predicted holdup is below the experimentally measured one. There is good qualitative

agreement, however, in all cases, the predicted value is not within error of the experimental values.

### 4.3 Dynamic results

The dynamics of bubble columns has been studied in two ways. The first was done using a step change in gas flow rate and the second by tracking point liquid velocities and local gas holdup values over time in different sections of the bubble column.

#### 4.3.1 Step change results

The purpose of the step change experiment was to compare the dynamic behavior of the bubble column when simulated numerically to the results obtained experimentally. The experimental results of the step change experiment were discussed in the previous chapter and can be observed in Tables 3.9 to 3.11 for the air-water, air-methanol and air-cyclohexane systems respectively.

The air-water system was studied first. For the air water system the superficial gas velocities used went from the lower flow rate of 0.714 cm/s to the higher rate of 1.78 cm/s. In the numerical simulation the system was run at the lower flow rate for 20 seconds before the step change was done. This was done to ensure the system was at steady state before the step increase in the air flow rate was initiated. After the 20 second period the superficial gas velocity at the inlet of the bubble column was increased to the higher flow rate and the overall holdup was recorded as a function of time. Figure 4.12 illustrates the numerical data obtained from the step change as well as including the experimental data. For the numerical

step change it takes 1.5 s to go from the initial steady state holdup to the final steady state holdup. In Table 3.9 it can be seen that it takes 1.2 s experimentally.

The air-methanol and air-cyclohexane systems were also studied. For these runs the lower flow rate was 0.377 cm/s and the larger flow rate was 1.91 cm/s. As in the air-water system the simulation was run at the lower flow rate for 20 seconds to ensure the system was unchanging and then the superficial gas velocity was increased to the higher flow rate. The overall gas holdup for both systems is plotted against time and the results, along with the experimental data results, are presented in Figures 4.13 and 4.14 . For the air-methanol system it takes 1.5 s to complete the experimental step change and 1.4 s to complete the numerical step change. For the air-cyclohexane system the step change occurs in 1.1 s numerically and 1.5 s experimentally.

### 4.3.2 Local, instantaneous system parameters

The local liquid velocity and the average local gas holdup in the bubble column were recorded at every time step (0.01 seconds) over 30 second spans. This was done using the Fortran user routine USRTRN (see Appendix E). They were recorded at nine points in the column as described in Table 4.2 . The data recorded can be observed in Figures 4.15 to 4.18. Figures 4.15 to 4.17 show the local liquid velocity as a function of time for the air-water system for a flow rate of 2.20 cm/s. Figure 4.18 shows the local gas holdup changes as a function time at the same flow rate (2.20 cm/s). Table 4.3 summarizes the wavelength, minimum and maximum values of the local liquid velocities. The wavelength, minimum and maximum local

gas holdups are summarized in Table 4.4. The average wavelength has been calculated based on the time between maximum peak heights shown in Figures 4.15 to 4.18.

**Table 4.2. Locations of points where dynamic data was taken.**

| Point* | Measured variables** | Horizontal position | Vertical position |
|---|---|---|---|
| bl | llv | 0.875 cm | 3.75 cm |
| bc | llv, lgh | 1.75 cm | 3.75 cm |
| br | llv | 2.625 cm | 3.75 cm |
| cl | llv | 0.875 cm | 7.5 cm |
| cc | llv,lgh | 1.75 cm | 7.5 cm |
| cr | llv | 2.625 cm | 7.5 cm |
| tl | llv | 0.875 cm | 11.25 cm |
| tc | llv,lgh | 1.75 cm | 11.25 cm |
| tr | llv | 2.625 cm | 11.25 cm |

* l = left, c = center, r = right, b = bottom, t = top

** llv = local liquid velocity; lgh = local gas holdup

**Table 4.3. Summary of wavelength, minimum and maximum values for the local liquid velocities.**

| Point (location) | Wavelength (s) | Minimum velocity (cm/s) | Maximum velocity (cm/s) |
|---|---|---|---|
| bl | 3.6 | -0.26 | 0.50 |
| bc | 3.6 | -1.8 | 1.3 |
| br | 3.6 | -0.40 | 0.47 |
| cl | 3.7 | -0.26 | 0.52 |
| cc | 3.7 | -1.8 | 1.3 |
| cr | 3.7 | -0.40 | 0.60 |
| tl | 4.9 | -0.38 | 2.4 |
| tc | 4.9 | -5.4 | 1.5 |
| tr | 4.9 | -0.56 | 2.1 |

**Table 4.4. Summary of wavelength, minimum and maximum values for the local gas holdup.**

| Point (location) | Wavelength (s) | Minimum holdup | Maximum holdup |
|---|---|---|---|
| bc | 3.7 | 0.098 | 0.126 |
| cc | 3.7 | 0.092 | 0.128 |
| tc | 3.7 | 0.081 | 0.124 |

## 4.4 Effects of various discritization schemes

This section shows the results obtained by changing some of the discritization schemes and the way in which the time steps are handled. The effects of including an added mass term to the interphase exchange term are also presented. For all of these tests the system used was the air-water system and the gas flow rate was set to 2.20 cm/s.

The differencing scheme was changed from the higher order CCCT method to a first order Hybrid scheme to see the effects this would have on both the average gas holdup and the local system parameters. The average gas holdup was calculated using the Hybrid method and was found to be 0.113. The average gas holdup as calculated using the CCCT method was 0.115 at this flow rate. The effect that changing the differencing scheme has on the local gas holdup can be observed in Figure 4.19. In this case the average wavelength is 3.7 s as it was using the CCCT discritization scheme. The minimum and maximum values are also similar to those in Table 4.4.

Similar comparisons were again made keeping the original differencing scheme (CCCT) but changing the way in which the time step was handled. Instead of using backwards differencing (first order) as the differencing scheme for time, the Crank Nicolson scheme (second order) was used. The average holdup was found to be 0.112 and ranged from values of 0.111 to 0.113. This is a much larger fluctuation than that observed when using backwards differencing (Figure 4.5). Figure 4.20 illustrates the difference between the local parameters in the bubble column when the Crank Nicolson method is used instead of backwards differencing.

For this method the wavelength of the local holdup of the bottom and center cells are 2.0 s. This is considerably smaller than that observes when backwards differencing was used (3.7 s). At the top of the column the local holdup behaves differently. There is not regular sinusoidal curve but the pattern is repetitive. It repeats every 7.4 s. This is not observed when backwards differencing is used. The minimum values are similar to those when backwards differencing is used (0.09) but the maximum values are quite a bit larger (1.45 for Crank Nicolson compared to 1.25 for backward differencing).

The effect of including an added mass term was also studied. For this test the CCCT and backward differencing methods were used in the numerical model. The average gas holdup including the added mass term was found to be 0.100 (compared to 0.115 without). The effect that using the added mass term has on the local parameters in the bubble column can be observed in Figure 4.21. With the inclusion of added mass to the interphase transfer term the transient effect seem to be dampened out. The wavelength is increased to 9.7 s and the range (minimum and maximum) of the local gas holdup values is reduced to 0.093 to 0.105. This is considerably smaller than that observed for the case where added mass is not included (Figure 4.18).

## 4.5 Grid and time tests

Grid and time step tests were also completed. The grid was both doubled and halved and the time step interval was changed from 0.01 seconds to 0.02 seconds, 0.05 seconds and 0.1 seconds. Similar plots to those above were completed to show the effects these changes have on the results of the simulation. The average gas holdup values are shown in Table 4.5 while the local gas holdups can be observed in Figures 4.22 to 4.27. Figure 4.22 illustrates the local holdup values for a gas superficial velocity of 1.53 cm/s with the 20 X 60 grid and time step of 0.01 s. Figures 4.23 and 4.24 show the same data when the grid is halved (10 X 30) and doubled (40 X 120) respectively. The final three figures (Figures 4.25 to 4.27) show the same data for time steps of 0.02 s, 0.05 s and 0.10 s respectively. Table 4.5 also displays the range of values for the local gas holdup for all six cases. As can be observed in Table 4.5 the average gas holdup does not change for any of the grids and times steps tested. Also, the range of local gas holdup values is larger for the original case (20 X 60 grid and 0.01 s time step) than it is for the other runs. As the time step gets larger the variations become smaller and almost non existent at the large time steps (0.05 s and 0.10 s).

**Table 4.5. Average gas holdup and range of local gas holdup values for different grids and time steps in numerical bubble column with a gas velocity of 1.53 cm/s.**

| Grid time step | Average gas holdup | Minimum local gas holdup | Maximum local gas holdup |
|---|---|---|---|
| 20 X 60 0.01 s | 0.076 | 0.064 | 0.084 |
| 10 X 30 0.01 s | 0.077 | 0.071 | 0.090 |
| 40 X 120 0.01 s | 0.077 | 0.077 | 0.090 |
| 20 X 60 0.02 s | 0.076 | 0.074 | 0.082 |
| 20 X 60 0.05 s | 0.076 | 0.076 | 0.077 |
| 20 X 60 0.10 s | 0.076 | 0.077 | 0.077 |

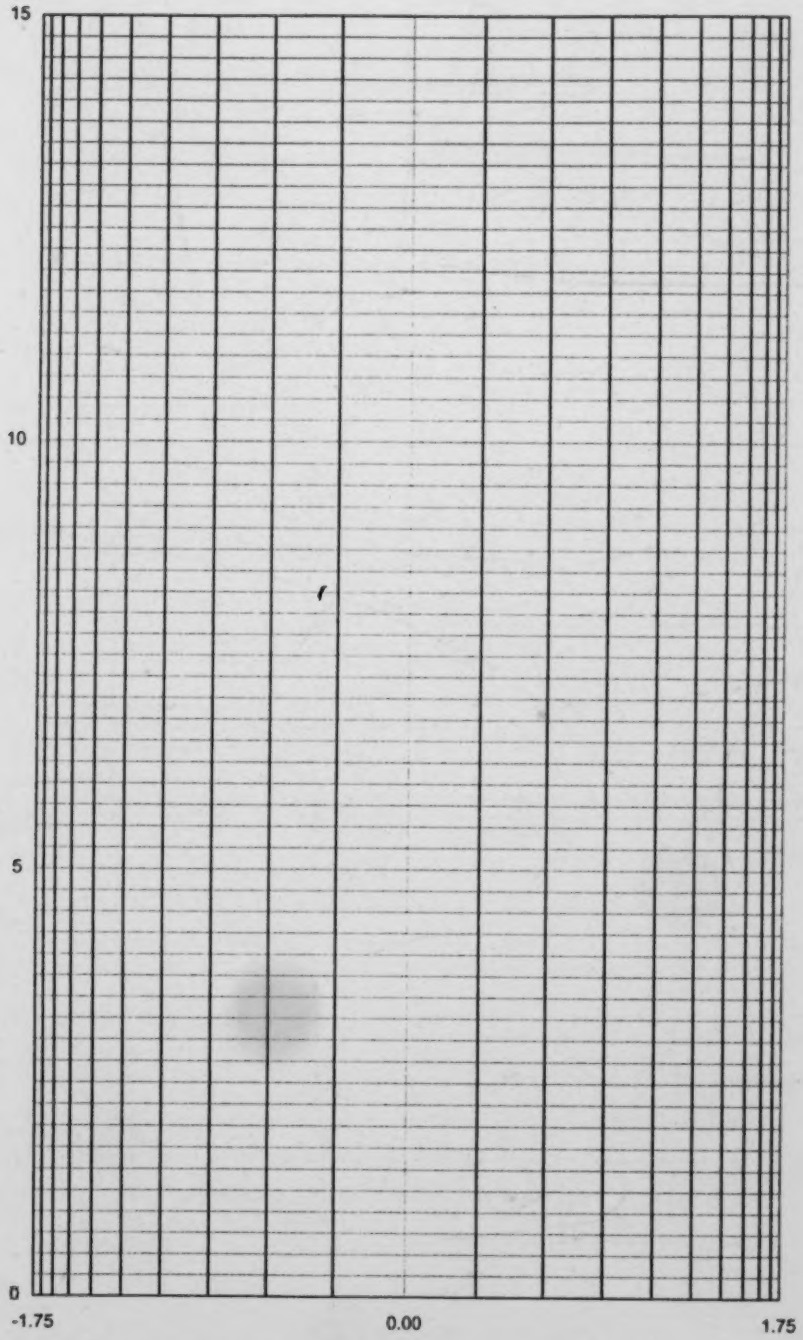


**Figure 4.1. Numerical grid for bubble column (dimensions in cm).**

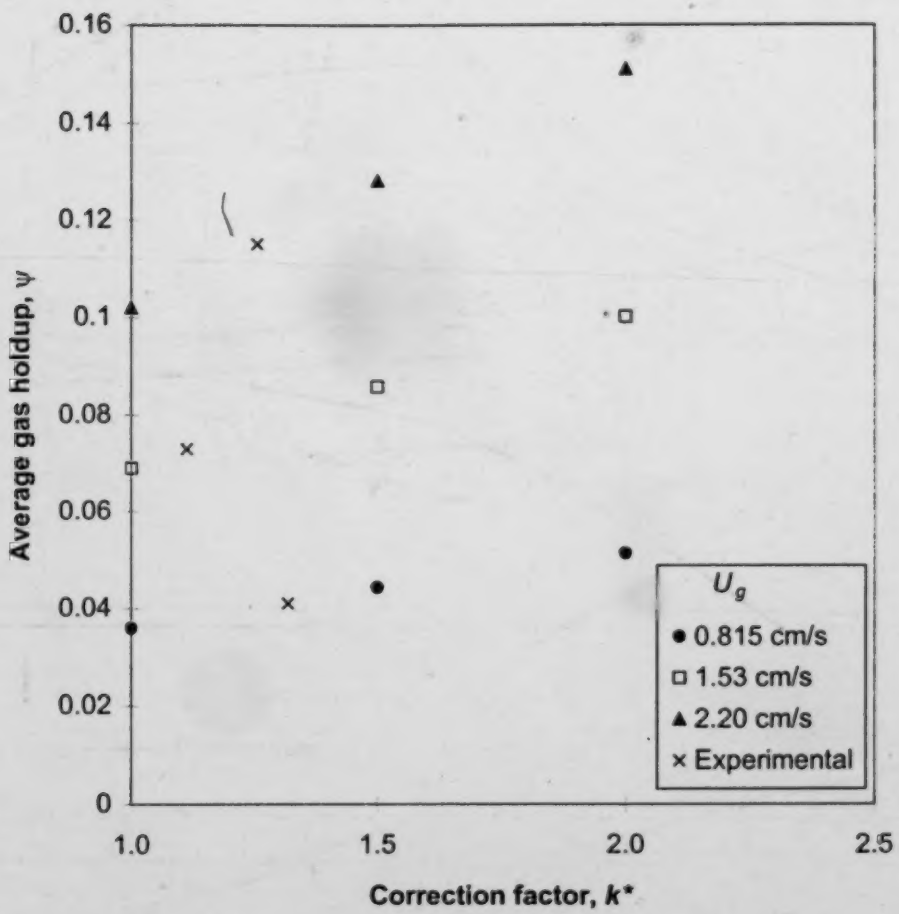


**Figure 4.2. Wall effects on average gas holdup for air-water system.**

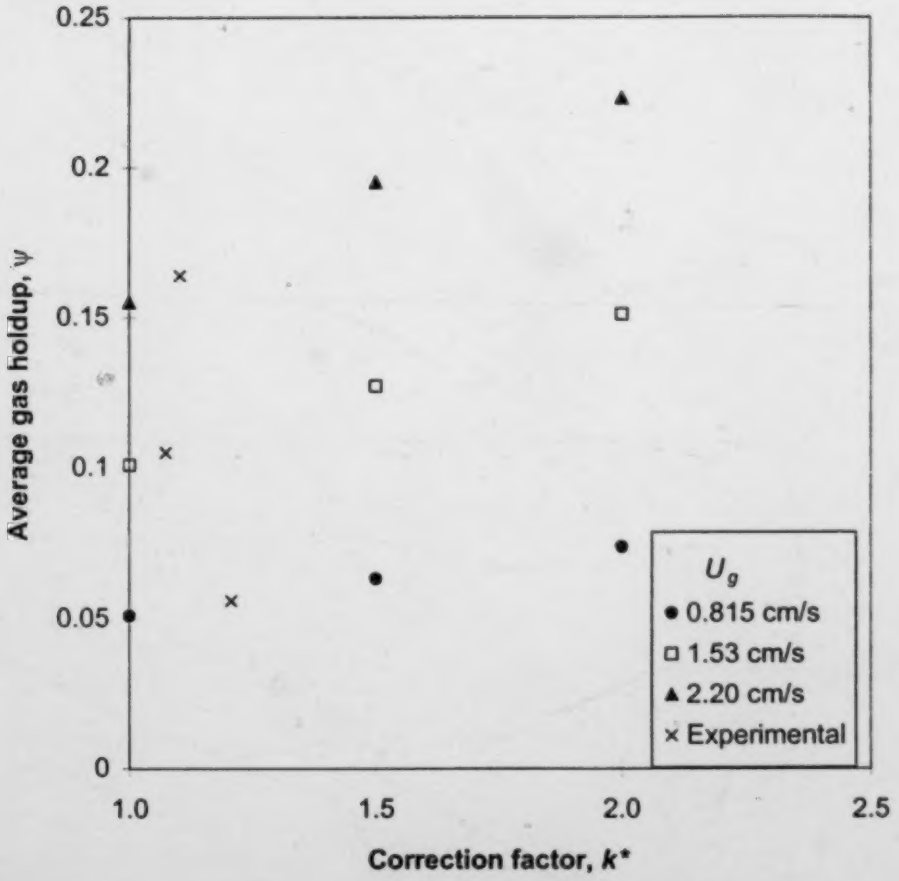


**Figure 4.3. Wall effects on average gas holdup for air-methanol system.**

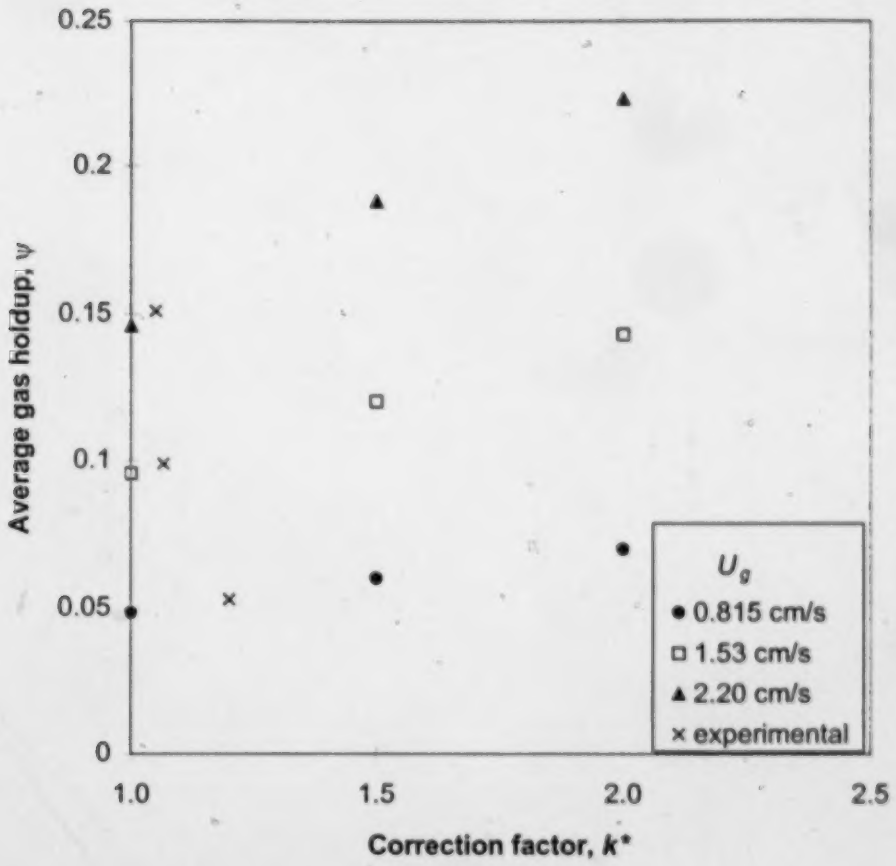


**Figure 4.4. Wall effects on average gas holdup for air-cyclohexane system.**

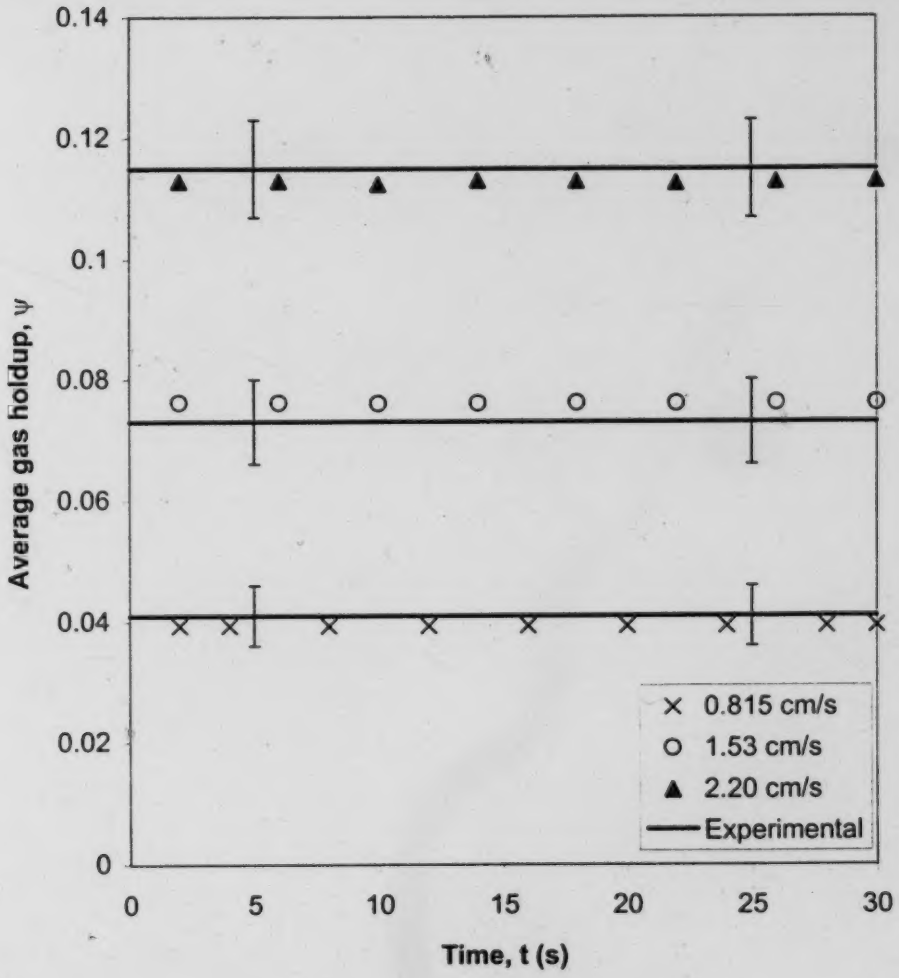


**Figure 4.5. Average holdup as a function of time for air-water system.**

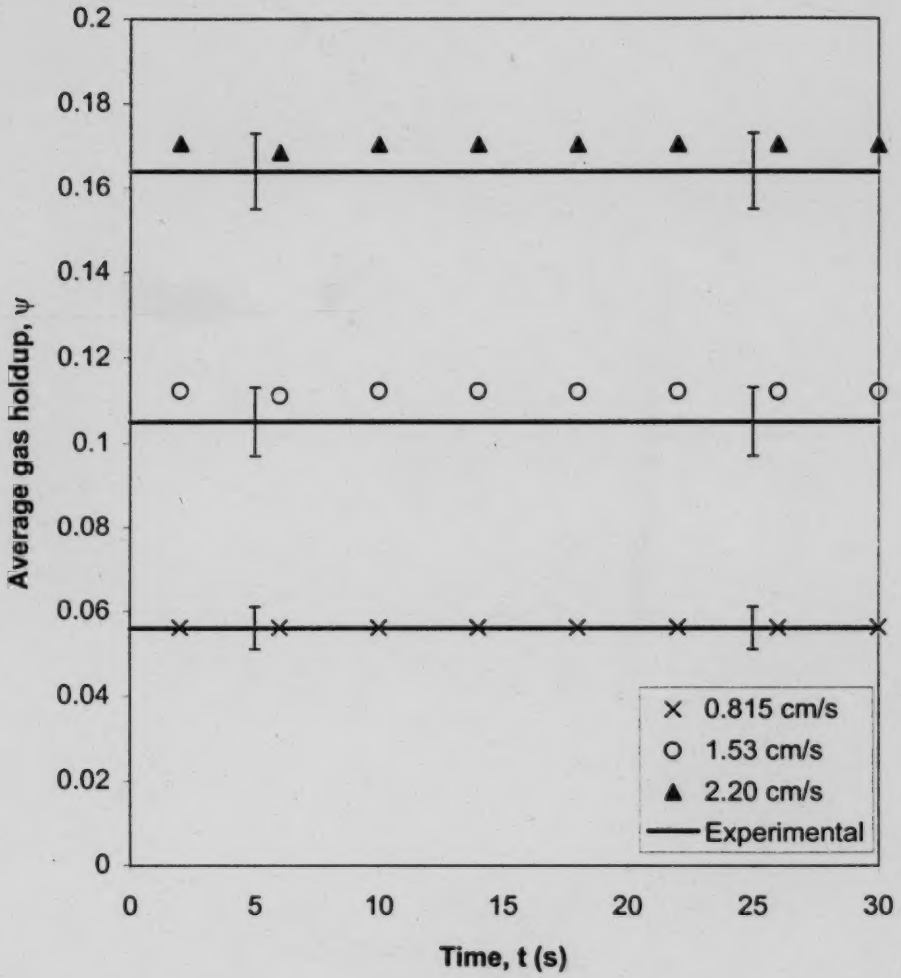


**Figure 4.6. Average holdup as a function of time for air-methanol system.**

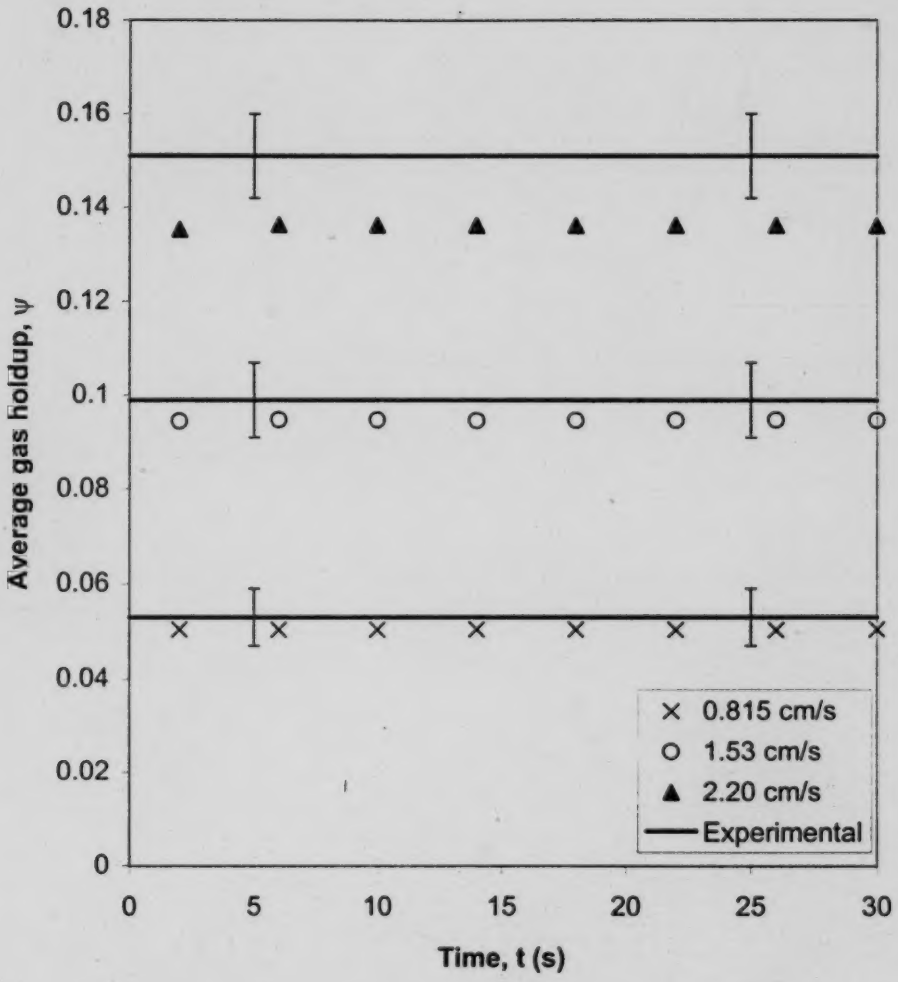


**Figure 4.7. Average holdup as a function of time for air-cyclohexane system.**

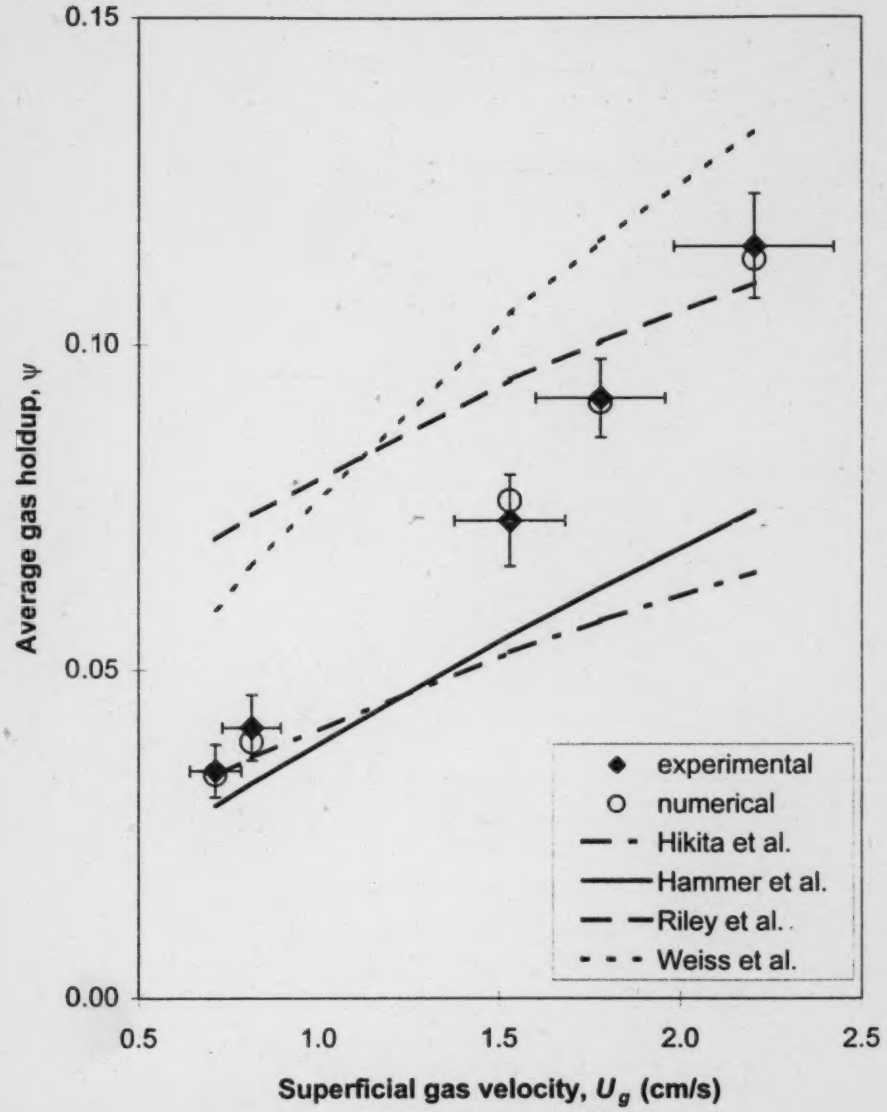


**Figure 4.8. Comparison of numerical, experimental and emperical gas holdups for the air-water system.**

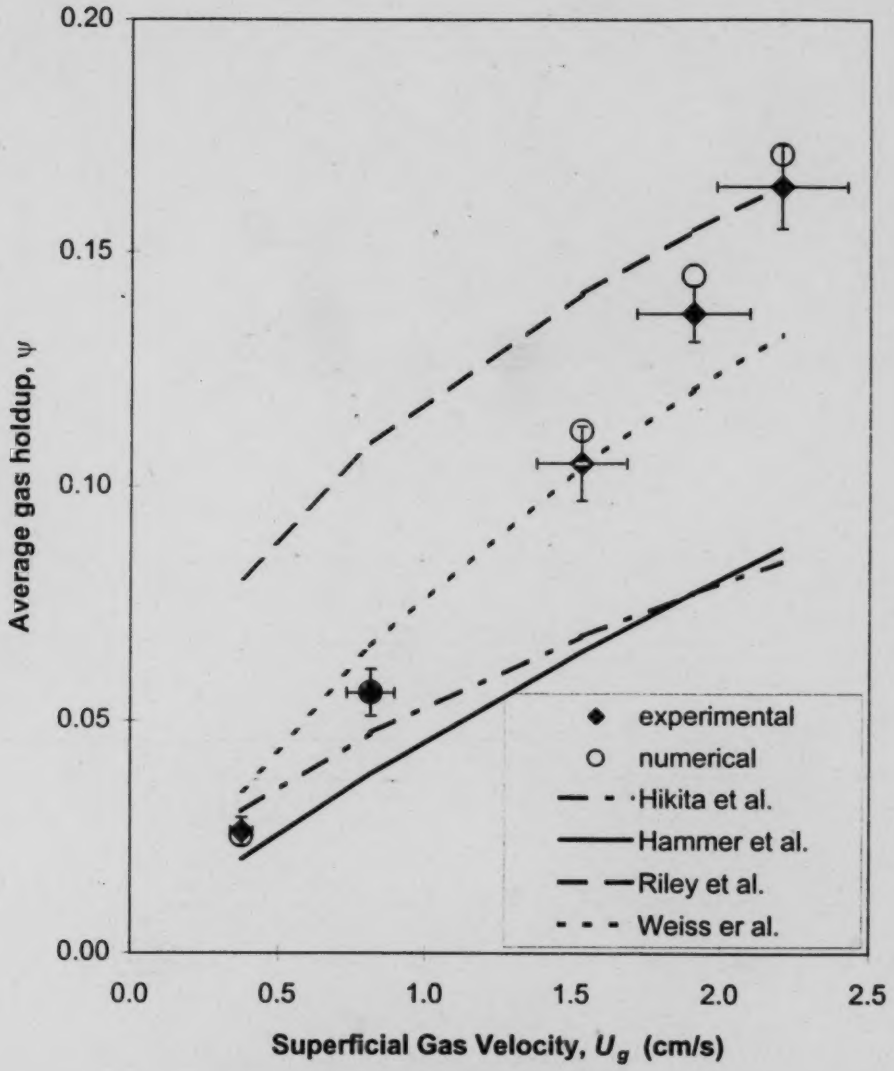


**Figure 4.9. Comparison of numerical, experimental, and emperical ga holdups for the air-methanol system.**

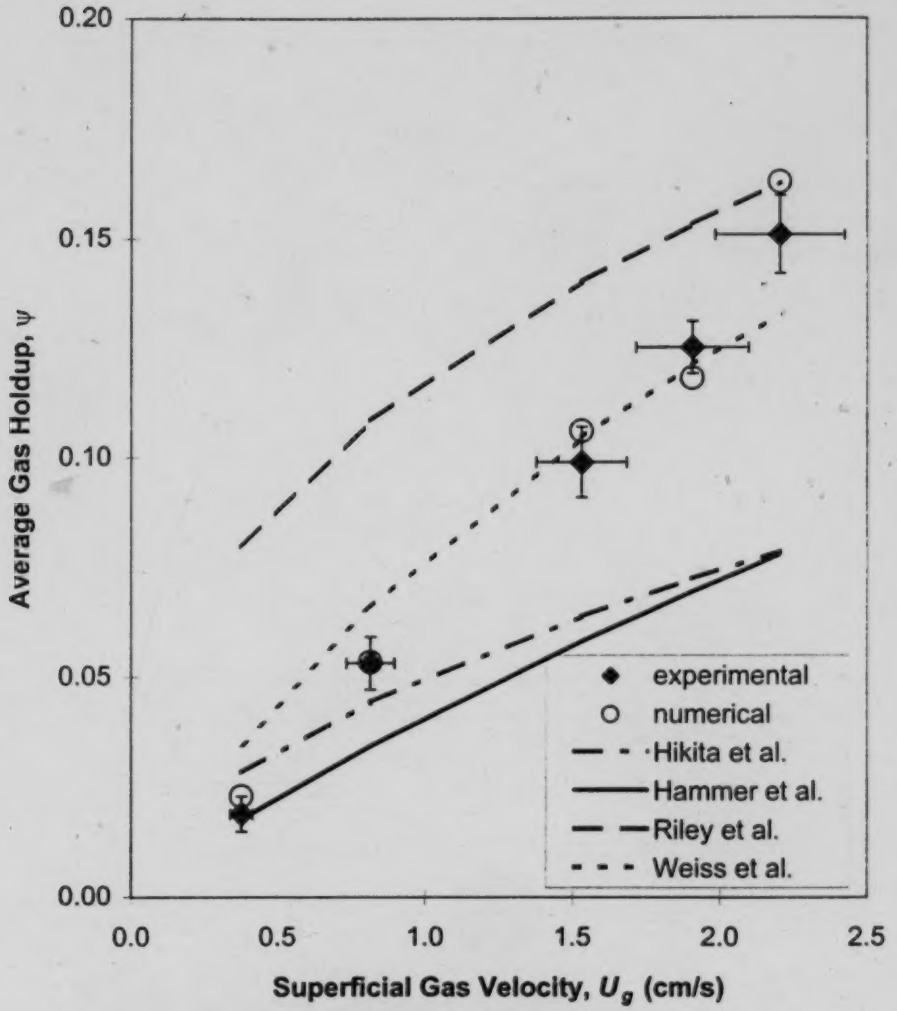


**Figure 4.10. Comparison of numerical, experimental and emperical ga holdups for the air-cyclohexane system.**

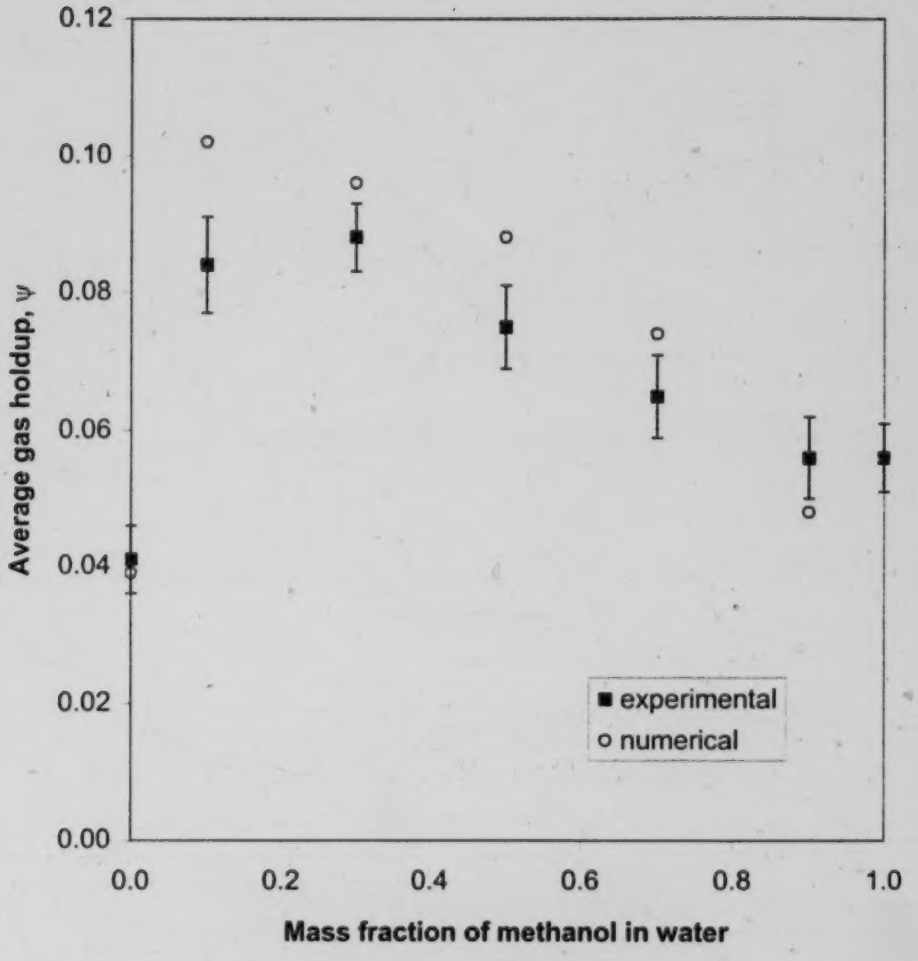


**Figure 4.11. Average gas holdup at different mass fractions of methanol in water for a $U_g$ = 0.815 cm/s.**

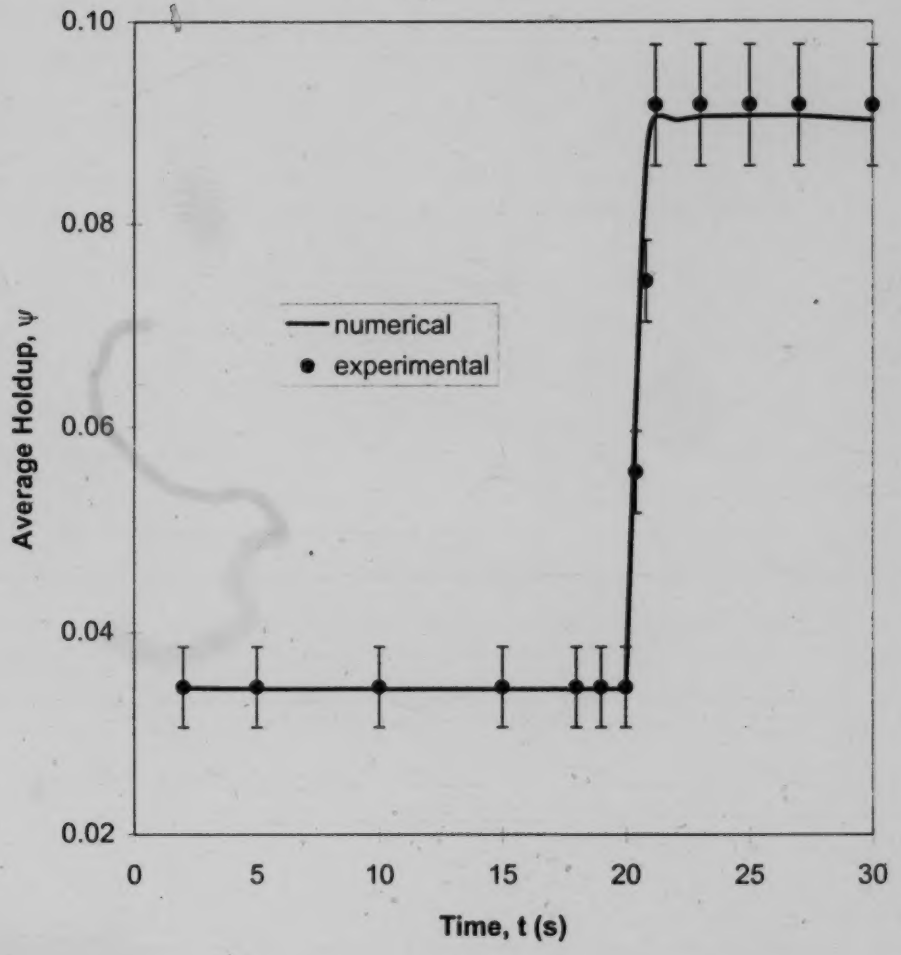


**Figure 4.12. Average holdup for air-water system for step change in air flow rate from $U_g$ = 0.71 cm/s to $U_g$ = 1.78 cm/s.**

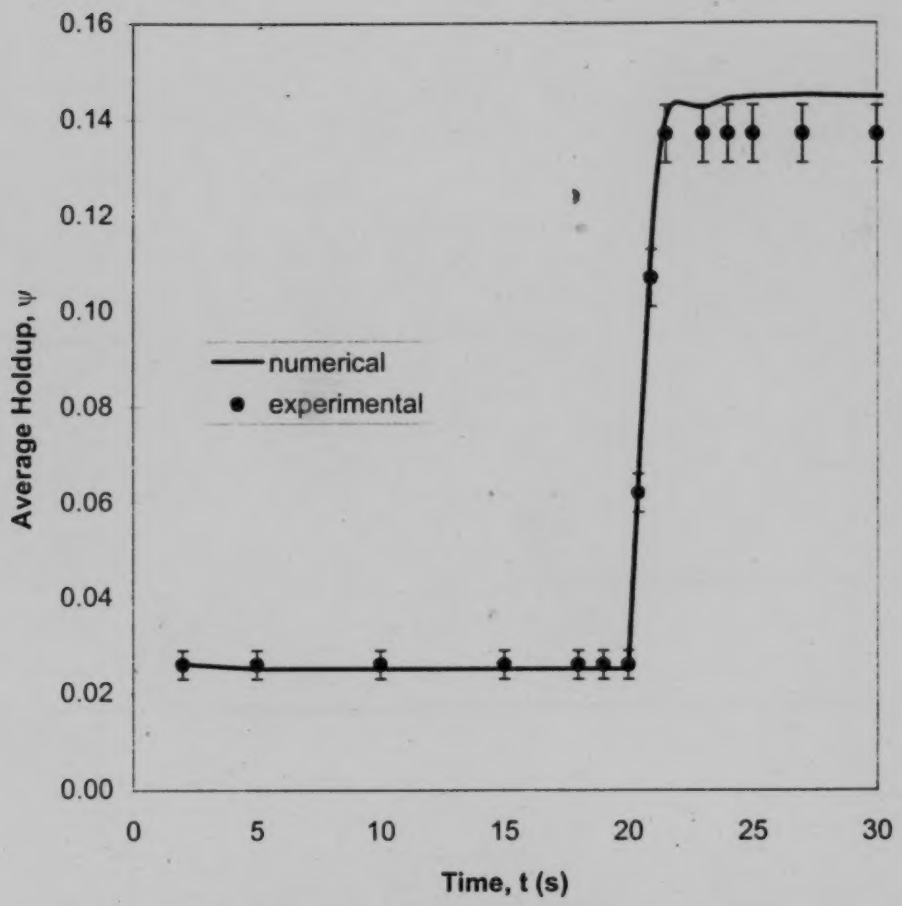


**Figure 4.13. Average holdup for air-methanol system for step change in air flow rate from $U_g$ = 0.38 cm/s to $U_g$ = 1.91 cm/s.**

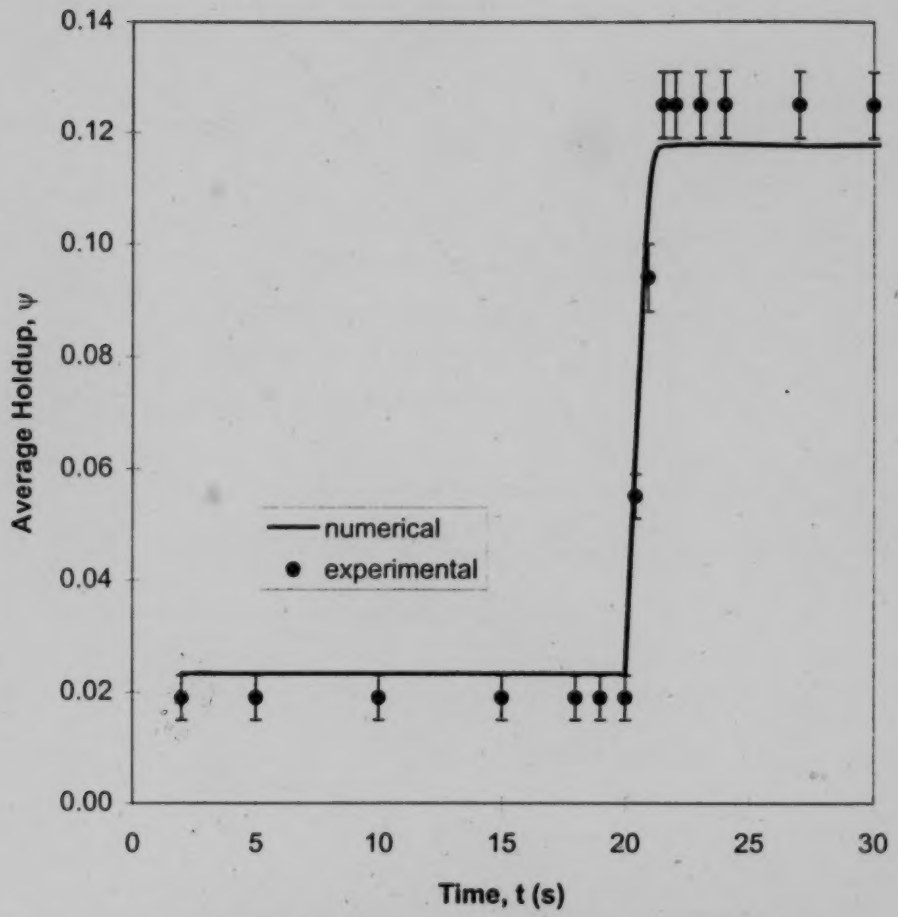


**Figure 4.14. Average holdup for air-cyclohexane system for step change in air flow rate from $U_g$ = 0.38 cm/s to $U_g$ = 1.91 cm/s.**

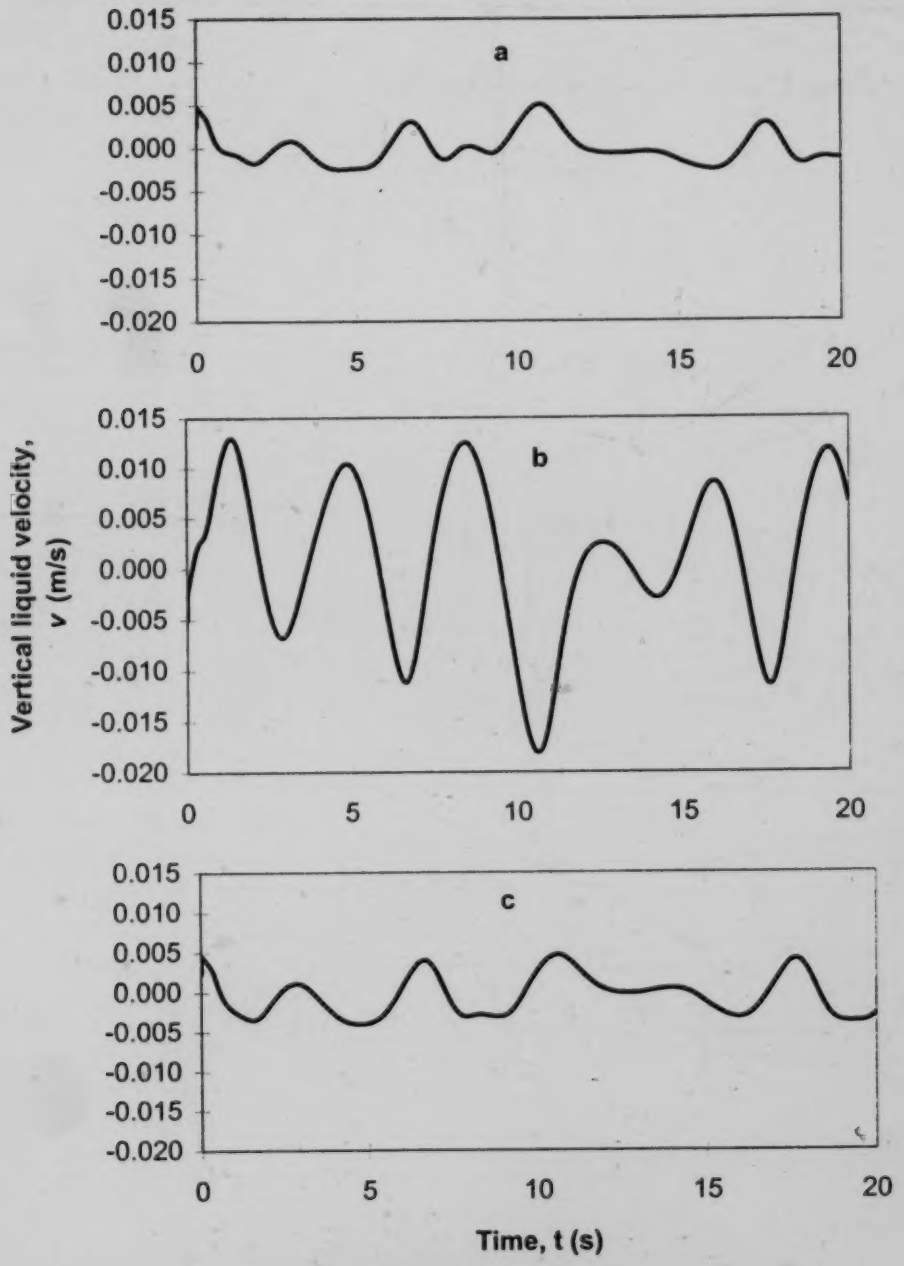


**Figure 4.15. Local liquid velocity 3.75 cm from the bottom of the column. a) bottom-left (bl), b) bottom-center (bc), c) bottom-right (br). $U_g$ = 2.20 cm/s.**

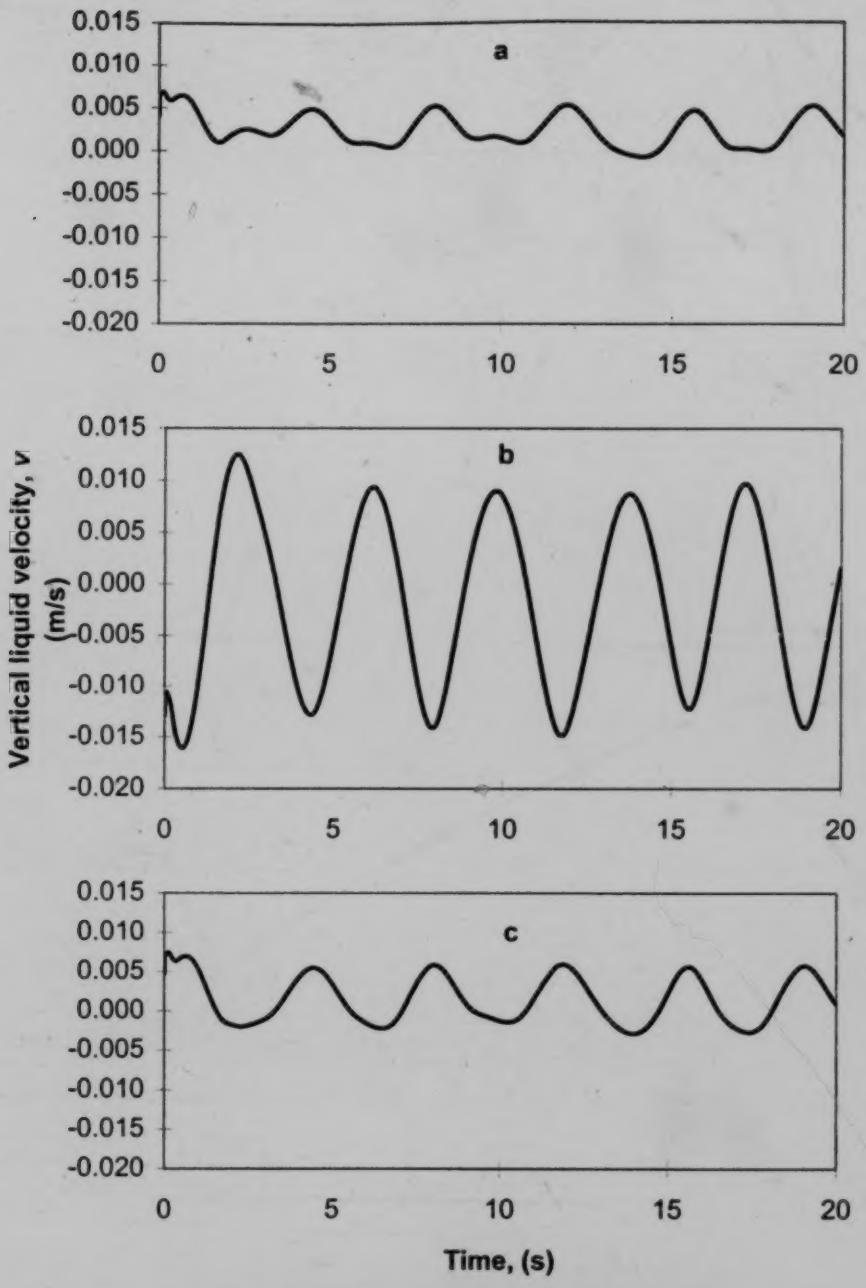


**Figure 4.16. Local liquid velocity 7.5 cm from the bottom of the column. a) center-left (cl), b) center-center (cc), c) center-right (cr). $U_g$ = 2.20 cm/s.**

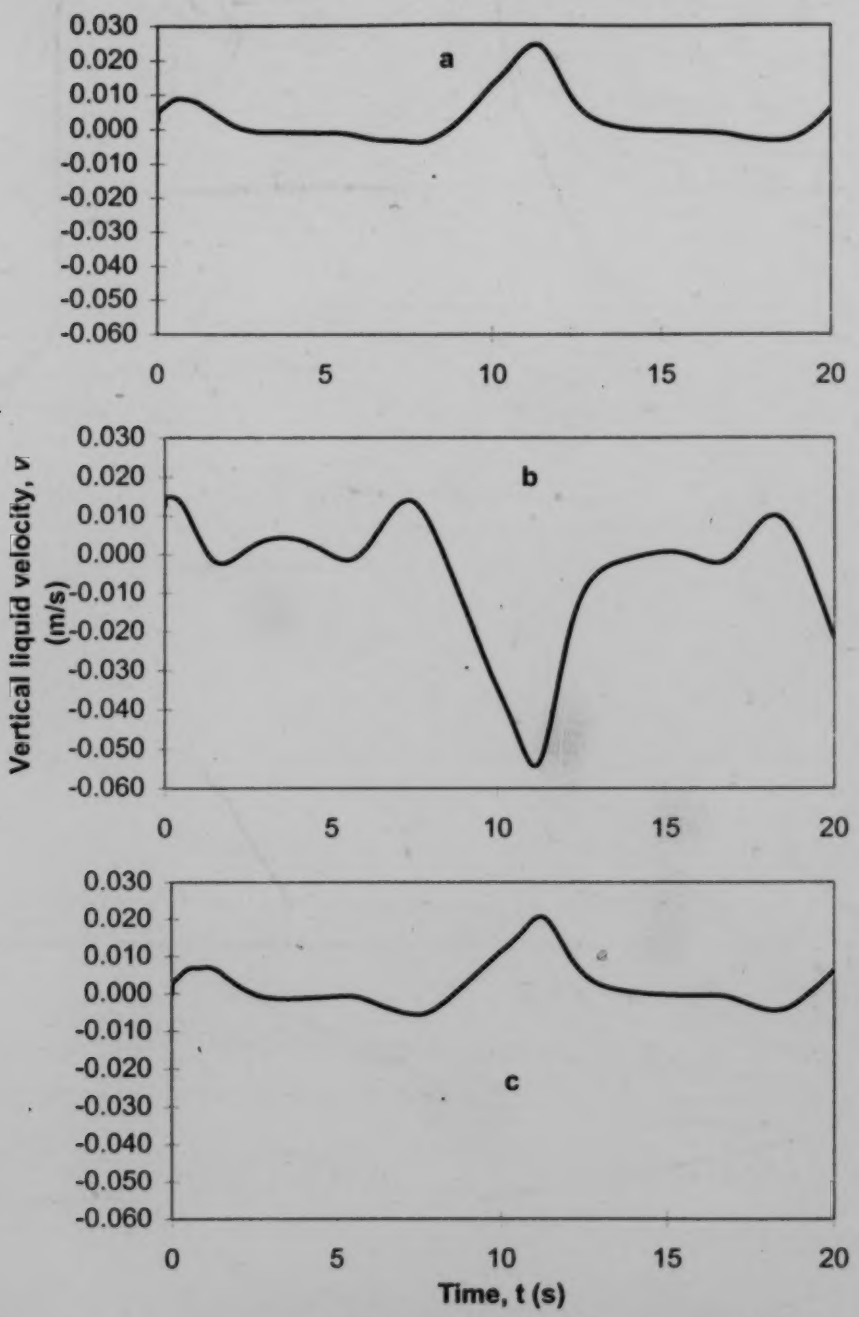


**Figure 4.17. Local liquid velocity 11.25 cm from the bottom of the column. a) top-left (tl), b) top-center (tc), c) top-right (tr) $U_g$ = 2.20 cm/s.**

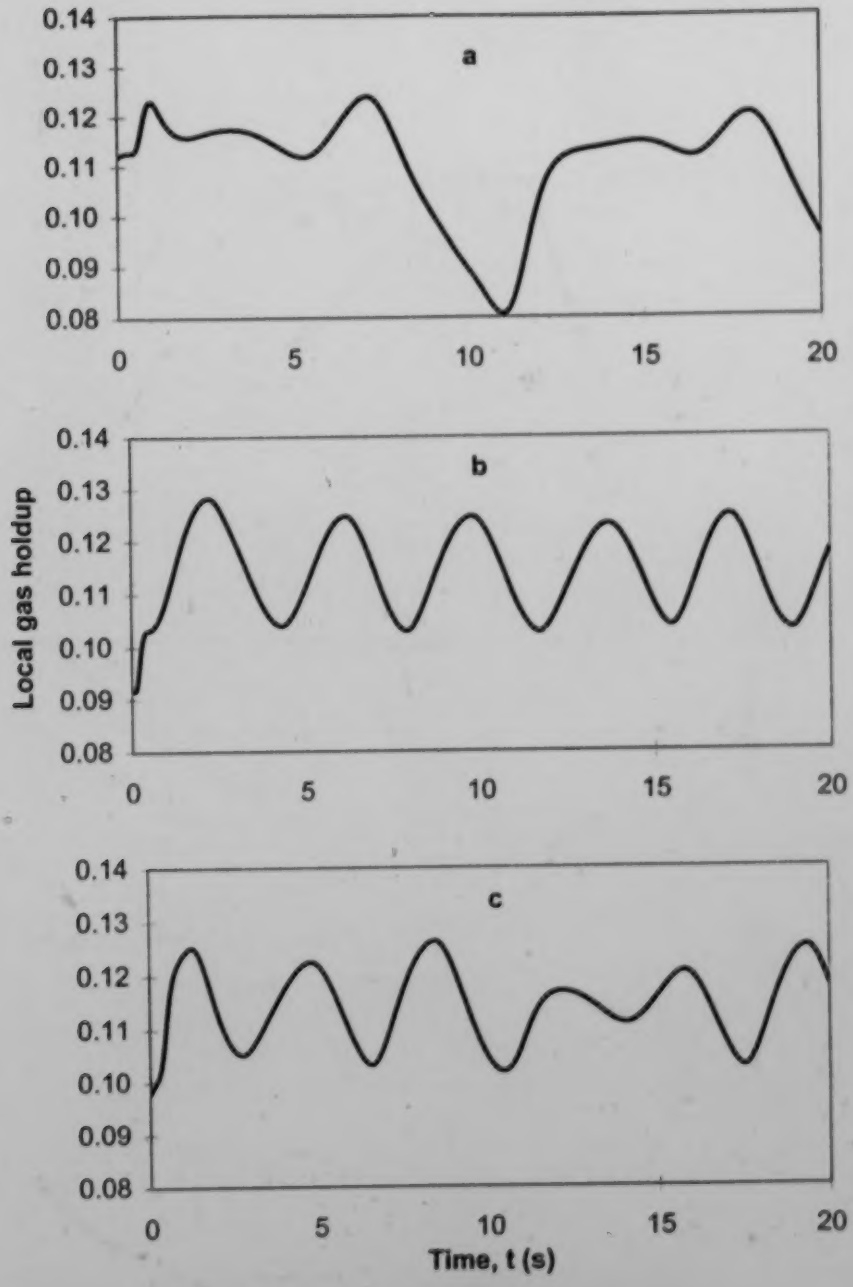


**Figure 4.18. Local gas holdup in horizontal center of column.**
**a) bottom-center (bc), b) center-center (cc),**
**c) top-center (tc). $U_g$ = 2.20 cm/s.**

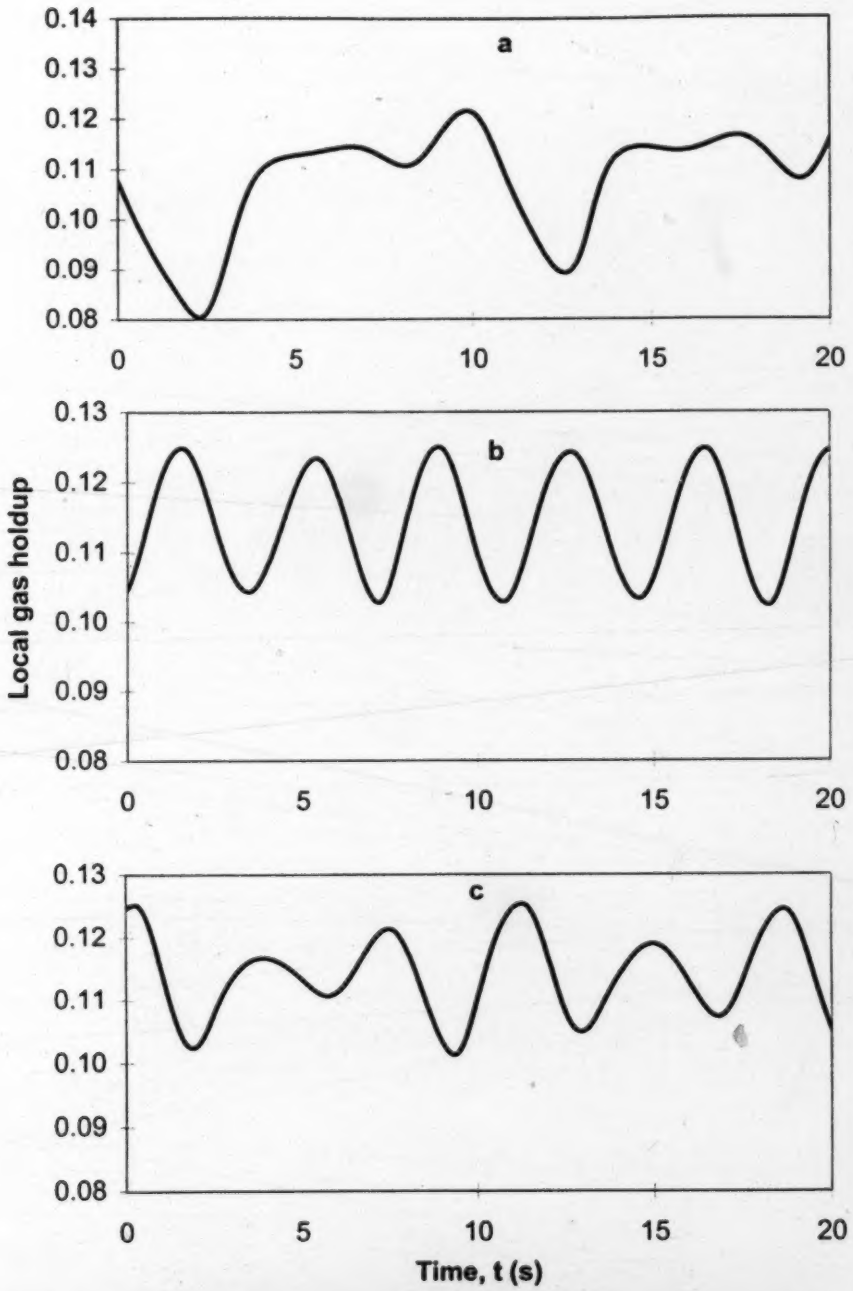


**Figure 4.19. Local gas holdup in horizontal center of column (Hybrid differencing scheme). a) bottom-center (bc), b) center-center (cc), c) top-center (tc). $U_g$ = 2.20 cm/s.**

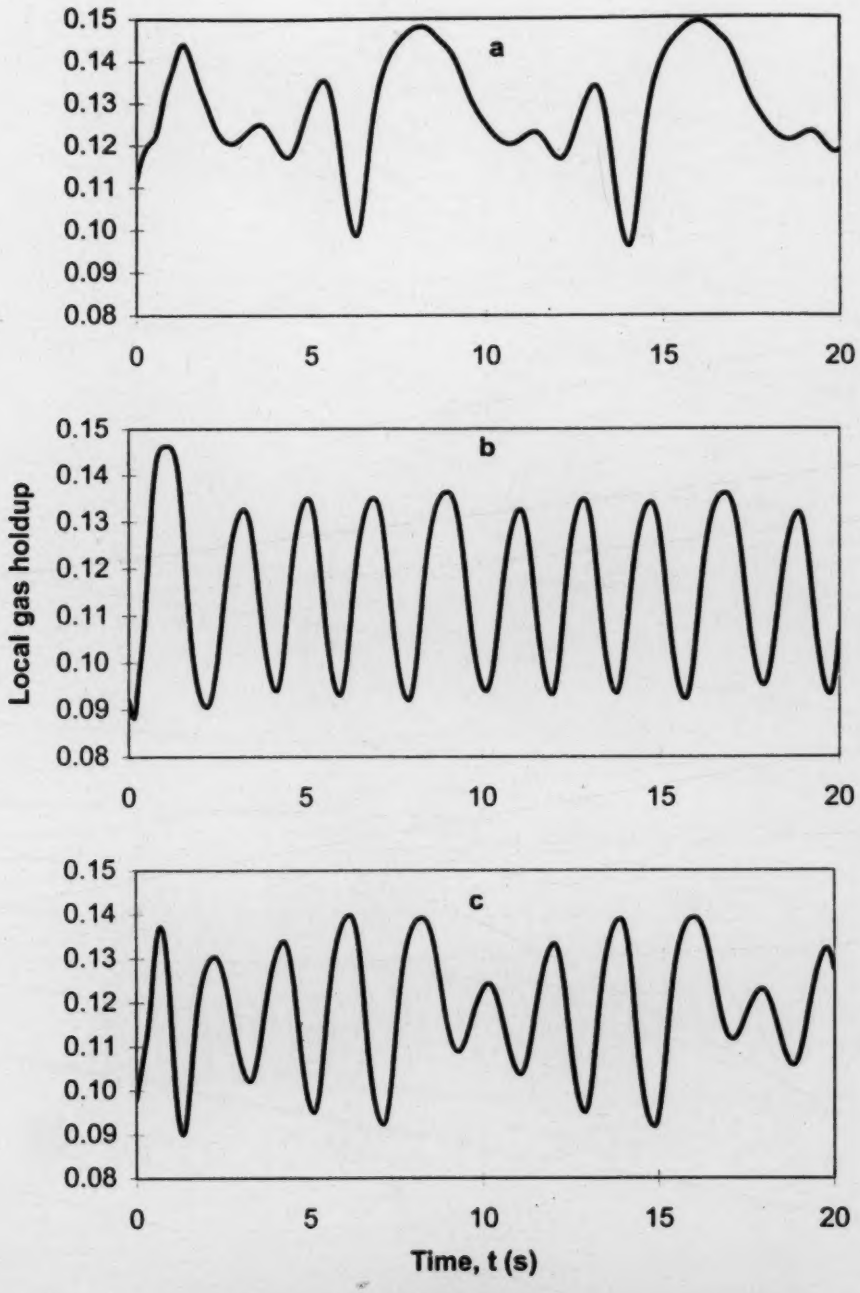


**Figure 4.20. Local gas holdup in horizontal center of column (Crank-Nicolson time discritization). a) bottom-center (bc), b) center-center (cc), c) top-center (tc). $U_g$ = 2.20 cm/s.**

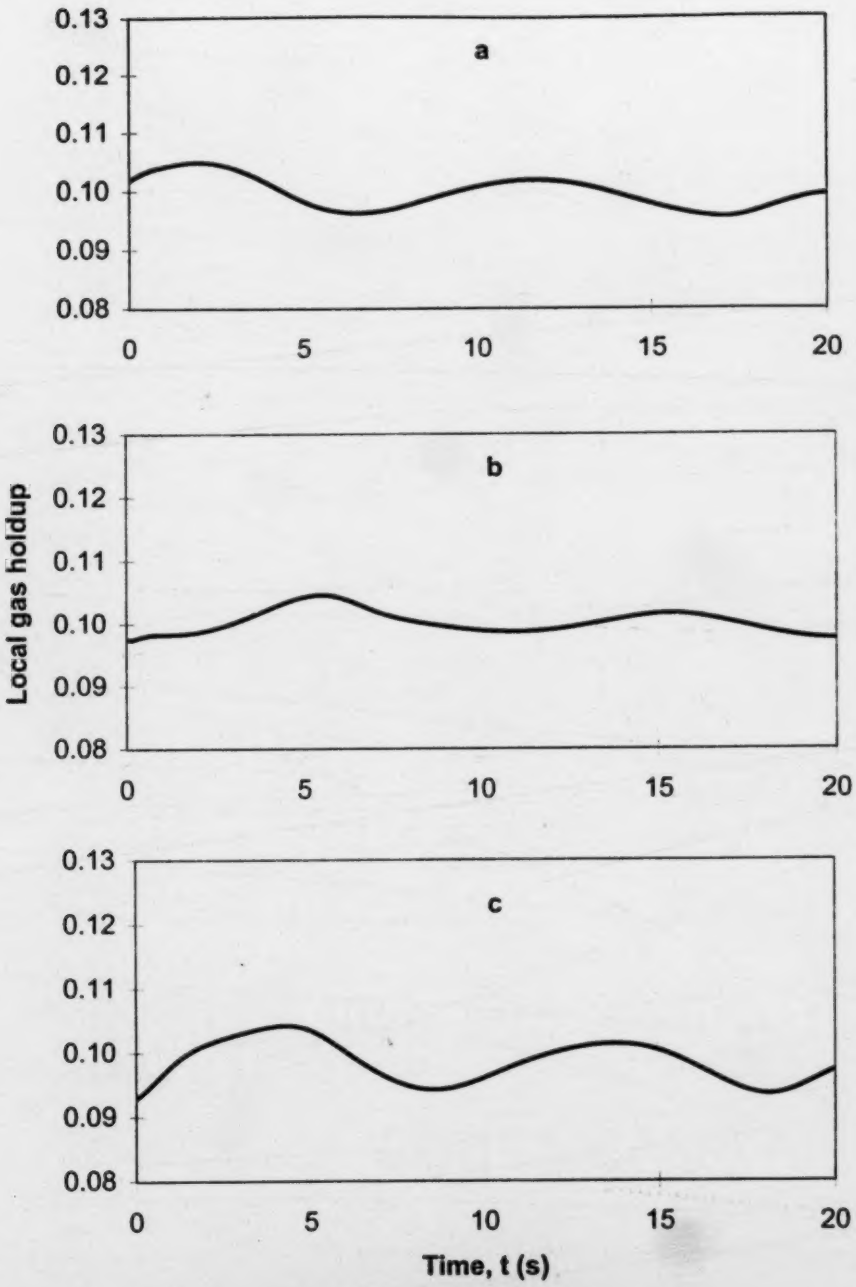


**Figure 4.21. Local gas holdup in horizontal center of column (added mass included in code). a) bottom-center (bc), b) center-center (cc), c) top-center (tc). $U_g$ = 2.20 cm/s.**

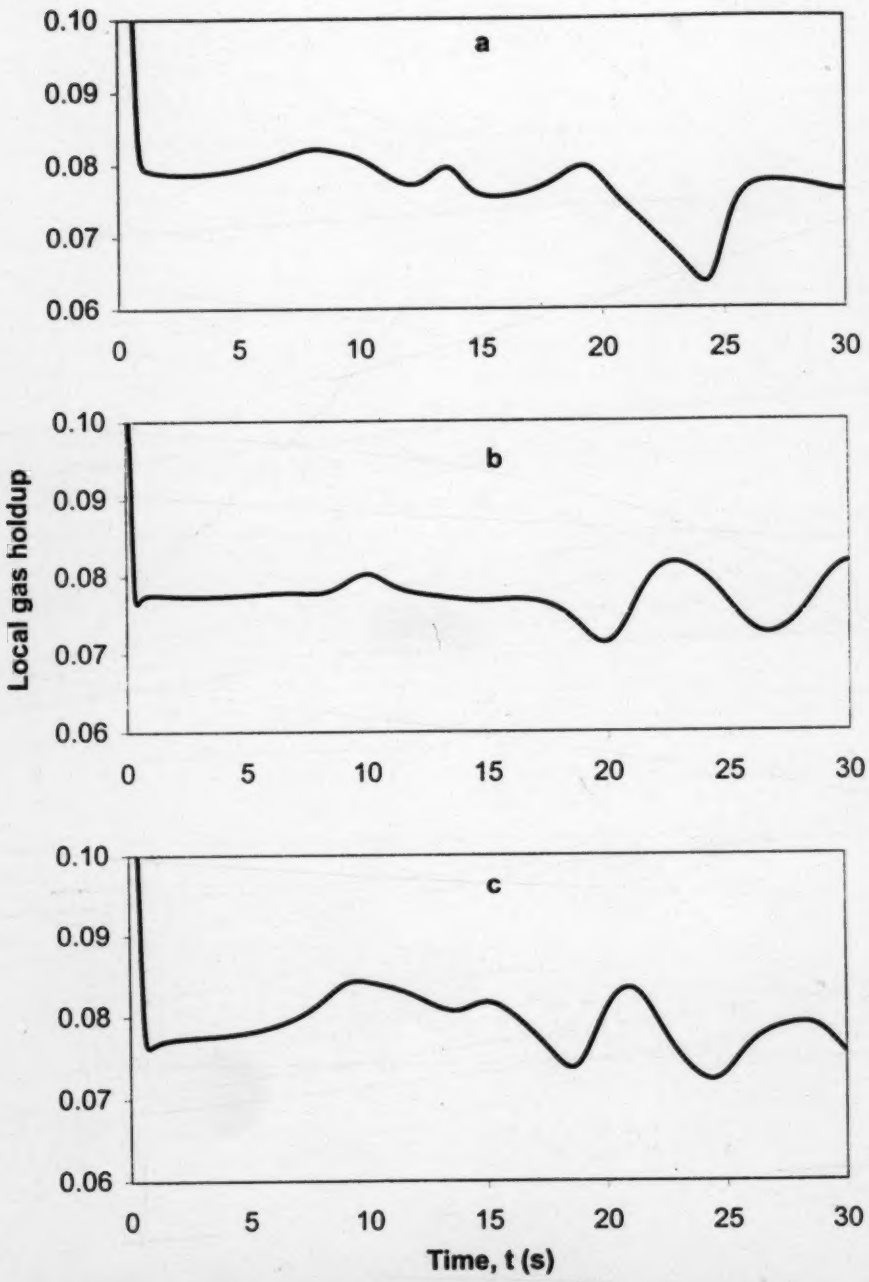


**Figure 4.22. Local gas holdup in horizontal center of column (20x60 grid, 0.01 s time step). a) bottom-center (bc), b) center-center (cc), c) top-center (tc). $U_g$ = 1.53 cm/s.**

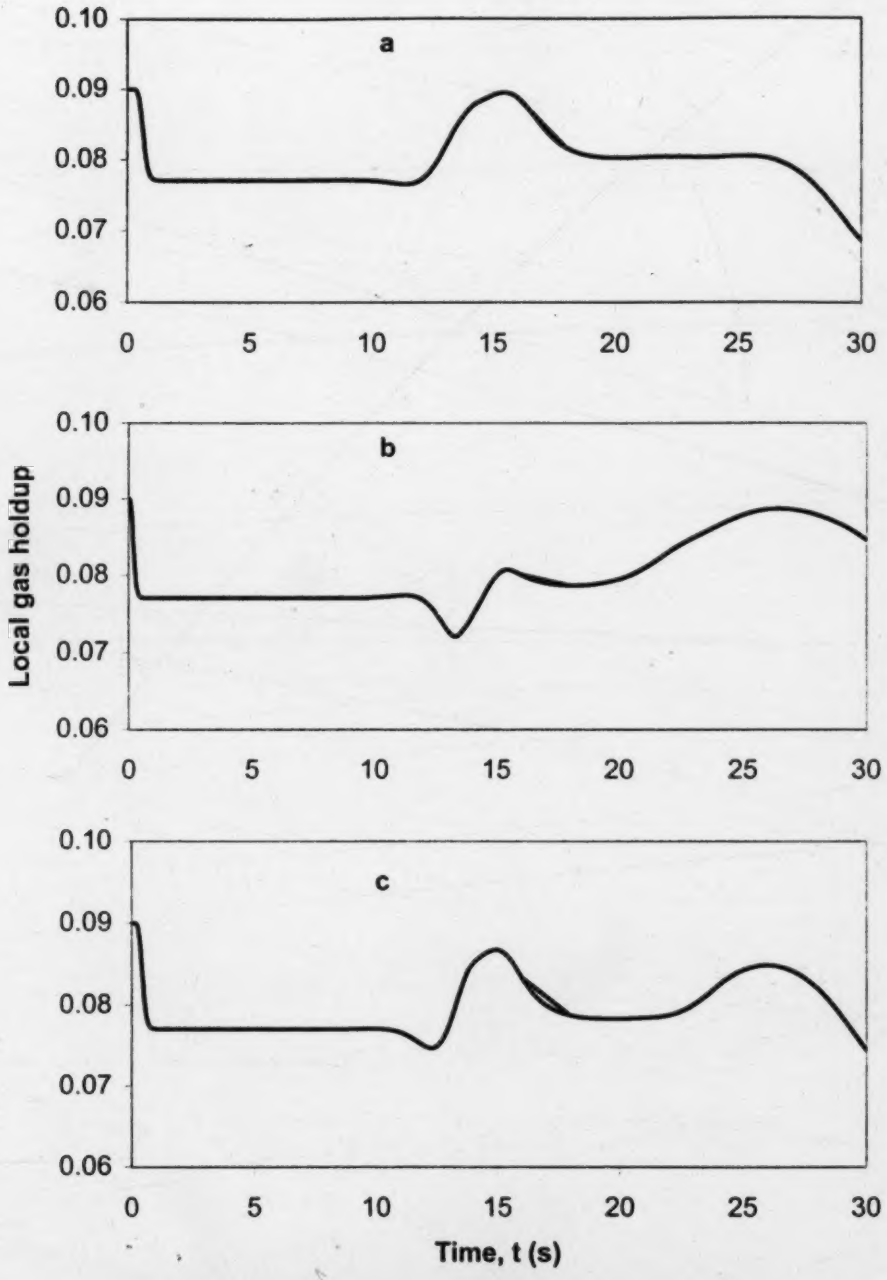


**Figure 4.23. Local gas holdup in horizontal center of column (10x30 grid, 0.01 s time step). a) bottom-center (bc), b) center-center (cc), c) top-center (tc). $U_g$ = 1.53 cm/s.**

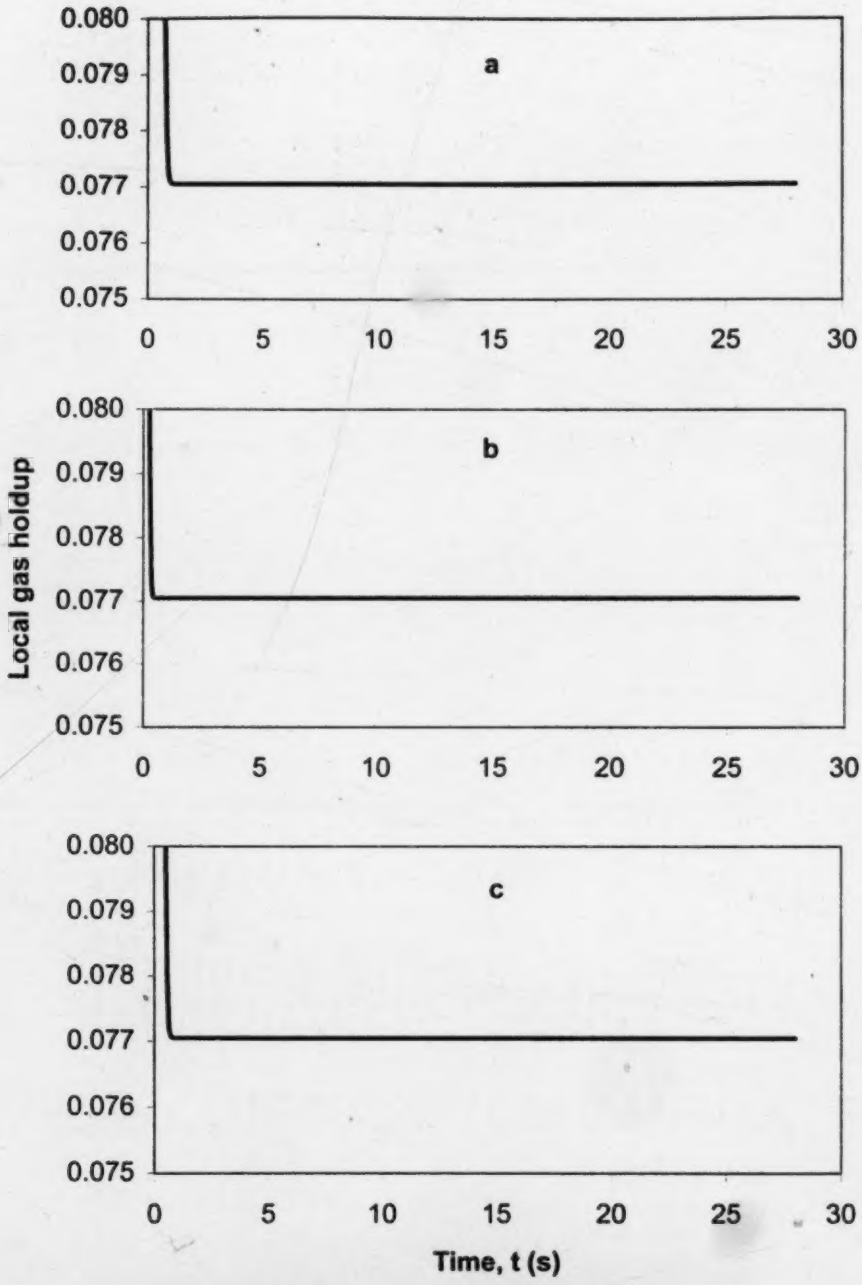


**Figure 4.24. Local gas holdup in horizontal center of column (40x120 grid, 0.01 s time step). a) bottom-center (bc), b) center-center (cc), c) top-center (tc). $U_g$ = 1.53 cm/s.**

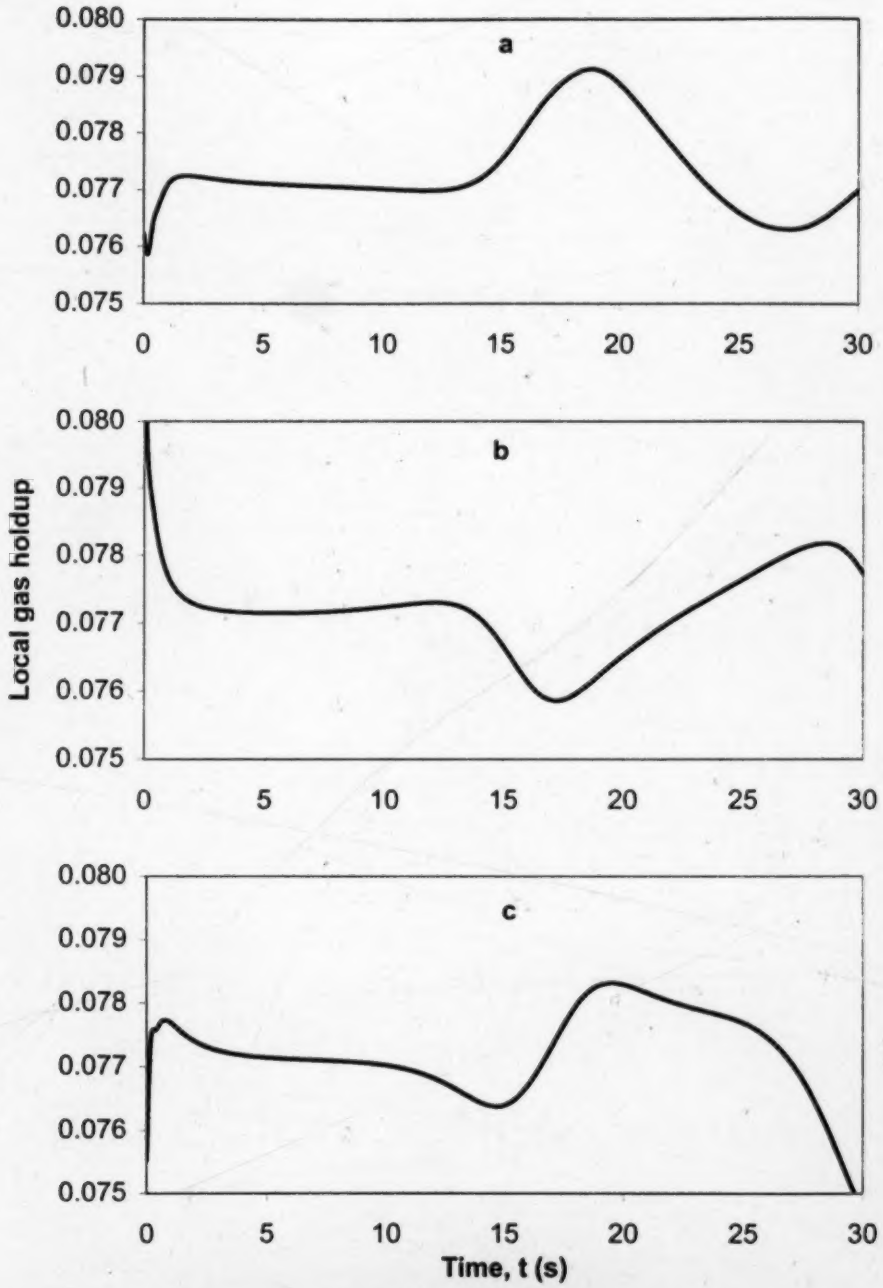


**Figure 4.25. Local gas holdup in horizontal center of column (20x60 grid, 0.02 s time step). a) bottom-center (bc), b) center-center (cc), c) top-center (tc). $U_g$ = 1.53 cm/s.**

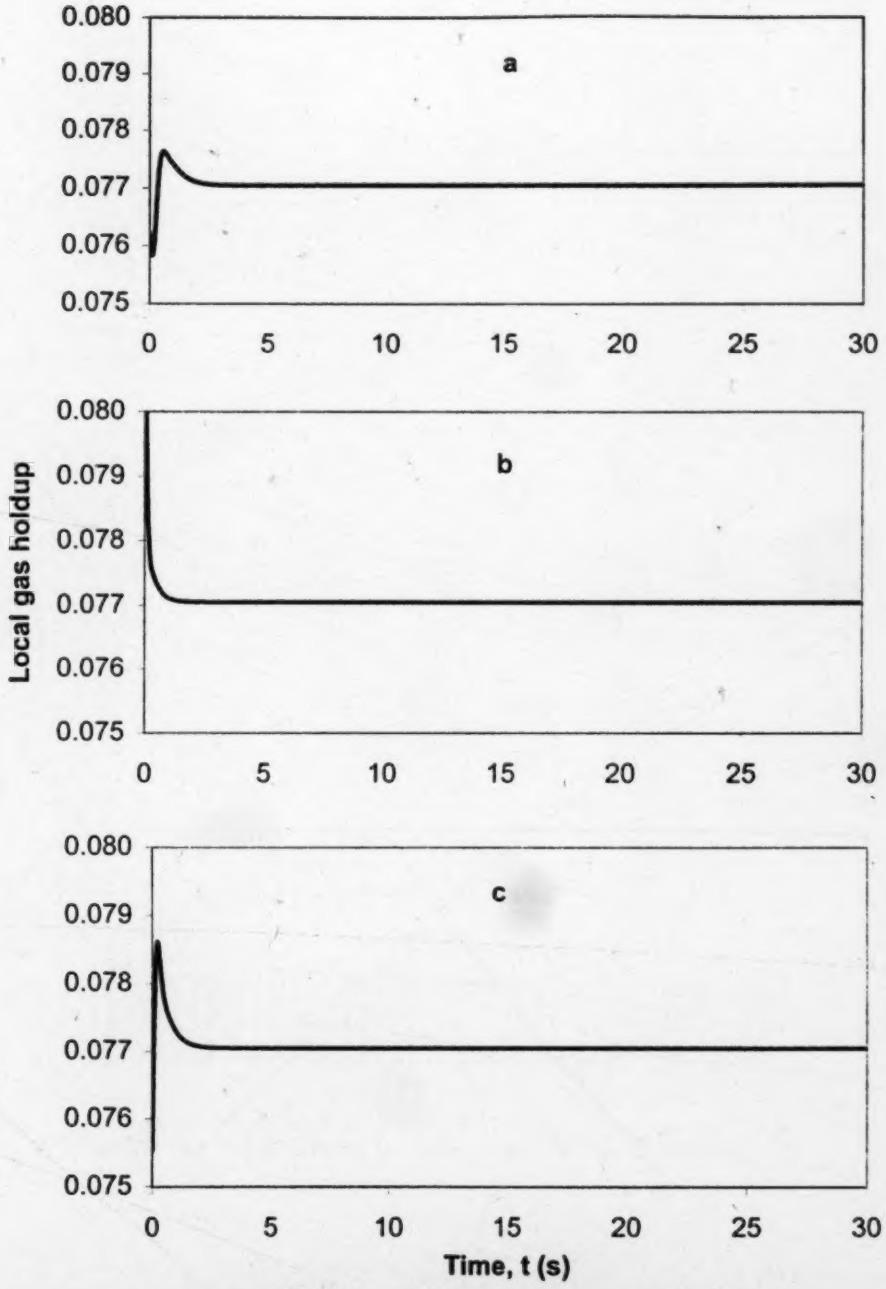


**Figure 4.26. Local gas holdup in horizontal center of column (20x60 grid, 0.05 s time step). a) bottom-center (bc), b) center-center (cc), c) top-center (tc). $U_g$ = 1.53 cm/s.**

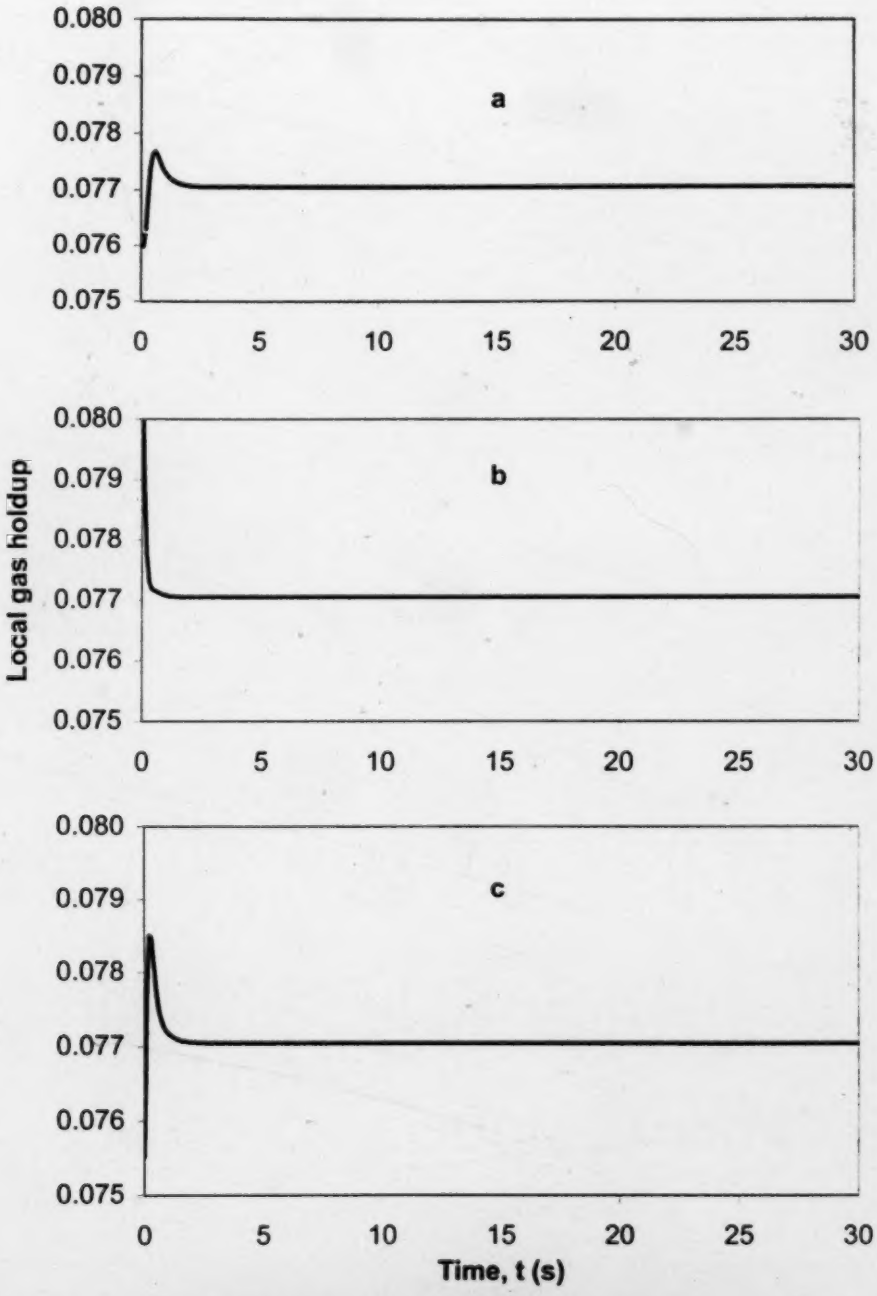


**Figure 4.27. Local gas holdup in horizontal center of column (20x60 grid, 0.10 s time step). a) bottom-center (bc), b) center-center (cc), c) top-center (tc). $U_g$ = 1.53 cm/s.**

# Chapter 5. Discussion

In this chapter, an in depth discussion of the numerical results is presented. Where possible, comparisons will be made to experimental results and empirical models. It includes discussions on the steady state behavior, dynamic macro behavior and the dynamic micro behavior.

## 5.1 Steady state

Before any confidence can be placed in any model, the model must be able to accurately predict the basic macro quantities in the system. In this case, the numerical model should be able to accurately predict the average gas holdup in the bubble column for a constant inlet gas flow rate. For the purpose of this study, only flows in the homogeneous bubble regime are considered because the bubbles in the column are all of relatively the same size (see Figures 3.2 to 3.4).

An important consideration when dealing with gas-liquid flows, such as the bubble column, is the model used to account for the drag force between the phases. Not only does the interaction between the phases need to be accounted for but so too must the interaction between the bubbles and between the bubbles and the walls. The model that was found to incorporate this the best, was the Ishii-Zuber model. However, this model does not take into consideration the wall effects. To incorporate this into the model it was assumed that the $C_D$ value calculated from the Ishii-Zuber drag model could be multiplied by a constant. Figures 4.2 to 4.4 illustrate that for the air-water, air-methanol and air-cyclohexane systems a constant of 1.2 can be used to accurately account for the wall effects. Since this is the same for all three systems and over three different flow rates it was concluded that a

constant was valid and did in fact account for the wall effects. It is expected that this constant will be different for each system and go to a value of unity for columns with large diameters.

The next test is to make sure the average holdup in the column is not a function of time for a set flow rate. At a set flow rate the experimental results conclude that the average gas holdup slightly fluctuates but remains relatively constant (deviations are much smaller than the calculated error in the experimentally measured holdup values). Figures 4.5 to 4.7 show that the simulated bubble column does in fact have steady holdup values. The values slightly fluctuate (< 1%) with time just as is observed experimentally.

Since the numerical average holdup values can be considered constant, the next consideration must be how well they agree with the experimental values. Figure 4.8 shows that for the air-water system, at the flow rates studied, the simulated holdups are all within error of the experimental values. Figures 4.9 and 4.10 show the same agreement for the air-methanol and air-cyclohexane systems. The best agreement is observed in the air-water system with the difference between the experimental and numerical values being less than 5.3 % for all five flow rates examined (Table 4.3). The maximum error for the air-methanol system is 6.7 % (Table 4.4) and for the air-cyclohexane system it is 21 % (Table 4.5). The rather large error for the air-cyclohexane system is observed only at the lowest flow rate with the rest of the values being within 7.9 % of each other. The large discrepancy at the low flow rate could possibly be accounted for if the flow rate was not set exactly at 0.377 cm/s when the experimental results where obtained. At such a low

flow rate a small error in the flow rate could create the large difference observed. Even with the large error though, the numerical and experimental values do agree within error. Therefore, it can be concluded for the pure liquid systems the numerical model used does accurately predict the steady state average gas holdup in the bubble column accurately.

The numerical model was also tested for the methanol-water systems. For theses runs nothing in the model was changed from the pure liquid system runs and the results are shown in Figure 4.11. For methanol mass fractions of 0.1, 0.3, 0.5 and 0.7 the predicted holdup is larger than the experimentally determined value and outside of the error. For a mole fraction of 0.9 the numerical value is lower (and again outside error) than the experimental value. A possible reason for this discrepancy could be accounted for in the drag model used. For the methanol-water mixture systems the bubble diameters are much smaller than those in the pure component systems (Figures 3.8 and 3.9). The bubble diameters are the smallest for low concentrations of methanol in water. As the concentration is increased, the bubble diameters increase as well (Figures 3.5 to 3.7 and 3.9). With smaller diameters the flow regime is likely not the distorted particle regime but instead would be the undistorted particle regime. Qualitatively, however, the simulated holdup does follow the same pattern as observed experimentally. The highest holdups occur with just a small amount of methanol in water and as the concentration increases the holdup decreases.

## 5.2 Bubble column dynamics

Since the steady state simulation results agree within error of the experimental results, the next step in validating the code is to check the dynamics. It is again necessary to compare the dynamic results for the simulated bubble column with the results obtained from experimental observations. First, the macro quantities of the bubble column must compare (such as average gas holdup). If these comparisons are valid then it is possible and reasonable to discuss the micro dynamic quantities in the bubble column (such as local liquid velocities and local gas holdups).

### 5.2.1 Dynamics of average holdup

To test the macro dynamics of the bubble column a step change experiment was conducted. In this experiment, the flow rate of the air was increased instantaneously and the average gas holdup in the column was recorded over time. For the air-water system Figure 4.12 shows the results. From this figure it is evident that the simulated holdup in the bubble column agrees very well with the experimentally measured holdup. There is a difference between the numerical and experimental findings of only 0.3 s for the holdup to go from the initial steady state value to the final one. Therefore, for the air-water system, it can be concluded that the macro dynamics in the column are indeed predicted accurately and confidence can be gained in the model. For the air-methanol system the results are again vary similar. Figure 4.13 shows the agreement between the numerical and experimental results. In this case, it takes 1.4 s to complete the numerical step change as compared to 1.5 s experimentally. Again, this agreement is quite good with the only

problem being the steady state holdups at the final flow rate do not agree within experimental error. This does not, however, include the error in the flow rate itself and if a slightly lower flow rate was used for the simulation the results would agree within error. For the final system, air-cyclohexane, the results can be observed in Figure 4.14. Again the numerical and simulated holdup values are very similar and the time needed to complete the step change quite similar. For this case as well, if the error in flow rate is included in the simulated bubble column the steady state results would be within error of each other. Liquid can leave, and enter, through the top of the simulated column but bed expansion has not been included in the simulations. Experimentally, the initial liquid height of the liquid in the column (at the low flow rate) was just over 15 cm for all three systems. As the step change in flow rate is introduced, and the volume fraction of the gas phase increases, the absolute height of the gas-liquid interface increases. Numerically, the height used is constant at 15 cm. Thus, it is expected that the experimental step change take slightly longer to go from one steady state to another, as the total volume of the liquid is larger. Since the experimental height was close to 15 cm this effect should be negligible. Since for all three systems the average gas holdup can be predicted for a dynamic process more confidence can be placed in the code and the next step examined.

### 5.2.2 Spatial variations

In this section, only numerical results are discussed. Experimental results for local, instantaneous velocities and gas holdups were not obtained for comparison. It is difficult to measure these quantities on such a small scale and at such small time intervals. Therefore, all conclusions made do not necessarily agree with what is actually happening experimentally.

Figures 4.15 to 4.17 show the vertical component of the local liquid velocity in the simulated bubble column. The liquid velocities at the bottom and center (Figures 4.15 and 4.16) of the column oscillate, but are bounded. The velocity at the center of the column is higher than the velocity at the walls. The velocities at the left side of the column are not the same as those of the right side. Both curves have the same shapes but the velocities at the left side of the column tend to stay closer to zero while those at the right almost always have a larger magnitude in their peak heights. This asymmetry has been observed in experimental bubble columns (Hills, 1974) and is not necessarily a numerical artifact. The derivative of the velocity with respect to time has a different sign (positive or negative) at the center of the column than at walls. At the top of the column the velocities behave differently than they do in the center or at the bottom. At the top of the column (Figure 4.17) the average wavelength (time between peaks) is almost 5 s (Table 4.5), as compared to 3.7 s at the bottom and middle. As well as the wavelengths being different so too is the rate at which the peak heights change. At the bottom and middle of the column the peak heights change in value, however, the changes are small. At the top of the column, the peak heights are noticeably different from each other. The derivative of the

velocities at the top of the column follows the same pattern as what is observed at the bottom and middle. When the velocity at the center of the column is increasing the velocities at the walls are decreasing (and vise versa). These parameters seem to be behaving in a chaotic, but bounded manner. Before any confidence can be placed in these predictions, they need to be compared to experimental data as was done for the average gas holdup. However, from experimental observation, it is unlikely that oscillations would have a wavelength as large as 3.7 s. As seen in the step change results, it only takes about 1.5 s for a bubble to travel the length of the column. Therefore, it is unlikely that the velocities and holdups oscillate with a wavelength of 3.7 s. It would be expected that the wavelength should be less than 1.5 s.

Figure 4.18 shows the local gas holdup at the bottom, middle and top of the bubble column (all at the horizontal center of the column). The average wavelength for the local gas holdup is similar to the wavelength of the liquid velocities at the bottom and center of the column (3.7 s, Table 4.6). As the liquid velocity is fluctuating, so is the gas holdup. It is expected that they should have similar wavelengths since they are dependent on each other. It is the gas holdup, or the rising of a bubble through the liquid, that creates movement in the liquid. As was observed for the velocities, the peak heights of the holdups are not a constant value, but change slightly with time. In general, it can be observed that the curve of the holdup at the middle of the column is similar to the one at the bottom of the column only shifted by about 2 seconds. This would indicate that fluctuations occurring at the bottom of the column do not disappear, but are carried up the column. Again, it

is imperative that these results be compared to experimental values before any confidence can be placed in them.

**5.3 Numerical tests**

The effects of changing discritizing schemes, the interphase transfer term, time steps and the grid size will be discussed in this section. These tests are done to verify the validity of the simulation results.

With a superficial gas flow rate of 2.20 cm/s the simulation of the bubble column was run using the first order Hybrid regime instead of the CCCT regime. This made virtually no difference to the results. The average gas holdup was lower by only 0.002 (1.8%). In comparing Figures 4.18 (CCCT) and 4.19 (Hybrid) it can be observed that the figures are almost identical. The average wavelengths and peak heights are the same in both cases. This suggests that the discritization scheme does not have an effect in this system and the lower order Hybrid scheme could be used with the same accuracy as the CCCT scheme.

When the Crank Nicolson scheme was used (instead of backwards differencing) to discritize the time steps the simulation results were changed. Although the average gas holdup in the column did not change, it did fluctuate much more than when the backwards differencing scheme was used. The dynamics in the column were also changed. In Figure 4.20, it can be seen that the wavelength is only 2 s. This is about half the value of the wavelength observed when backwards differencing was used. Without having experimental data for comparison it is not know which method is correct (if any), however, since the overall holdup fluctuates

with the Crank Nicolson scheme it is expected that the backwards differencing scheme is more accurate.

When added mass force was included in the interphase transfer term in the momentum equations the average gas holdup in the column decreased by 15% compared to the holdup calculated without the added mass term. The dynamic behavior is also much different, as the added mass term seems to dampen out the dynamics. The wavelength is 9.7 s with added mass and 3.7 s without. In addition, the range of the peak heights (minimums and maximums) is much smaller when the added mass term is included. Including the added mass force in the interphase transfer term does not seem to be important. In fact, it leads to a lower average gas holdup and dampened out dynamics.

Grid and time tests were performed for the air-water system with a superficial gas flow rate of 1.53 cm/s. As shown in Table 4.5 the average gas holdup in the column is unaffected by the different grids and time steps examined. The grid was both doubled and halved (while keeping the time step the same) and the average gas holdup only changed by 1%. This indicates that the code is stable on a macro basis and the grid chosen is appropriate. The same is observed for different time steps. The time step was increased by factors of 2, 5 and 10 with very little effect on the overall holdup. Again, on a macro basis, the time step of 0.1 s is appropriate and can be used with confidence. The local gas holdup in the column is affected, however, by the grid and time step chosen. Similar results are observed for the simulations run with 20x60 and 10x30 grids. The fluctuations are on the same scale as each other as shown on Table 4.5. When the grid is increased to double the

original (40x120) the fluctuations completely disappear and the local holdup is constant with the same value as the average holdup. This is observed at the bottom, center and top of the column. Similar results occur for larger time steps. When the time step is increased to 0.02 s there is still some fluctuation in the local holdup, but it is much smaller than what is observed from the case where the time step is 0.01 s. A possible explanation for this is that numerical diffusion varies with $\Delta t$ when backwards differencing is used. When the grid is doubled, the time step would need to be reduced to get rid of numerical diffusion. This causes the dynamics to be dampened out as the time step is increased. When the time steps are increased to 0.05 and 0.1 s the local holdup is again constant, with a value the same as the average gas holdup. With large time steps, numerical diffusion dampens out all oscillations. Therefore, it is important to chose the correct time steps if local, instantaneous values (such as local gas holdup and local liquid velocity) are required. If only macro quantities (such as average gas holdup) are required then larger time steps can be used.

## Chapter 6. Conclusions and recommendations.

The objective of this study was to validate the CFX-F3D code for multiphase flow in a bubble column. In order to do this the simulation results must be comparable, quantitatively, to experimental results. For this purpose a two dimension bubble column (3.5 cm wide and 1.0cm deep, with a liquid height greater than 15 cm) was studied. Both simulation and experimental data was collected for various systems (air-water, air-methanol, air-cyclohexane and air-water/methanol mixtures) at various flow rates (superficial gas velocities ranged from 0.377 cm/s to 2.20 cm/s). Only the homogeneous, bubble flow regime was studied. The simulations were run using the CFX-F3D code by AEA Technologies.

The average gas holdup in the bubble column was predicted accurately by the numerical model. For the pure component systems, the experimental and numerical holdups were within error for all flow rates examined. For the air-water/methanol mixture systems, the average holdups did not agree. This was mainly because the wrong drag correlation was used. Qualitatively, the gas holdups as a function of methanol concentration did agree with each other. The highest average gas holdups where observed when the mass fraction of methanol in water was 0.3.

Since the steady state holdups were predicted accurately, the code was also tested to see if the dynamics of a gas flow rate step change could be predicted. For the air-water, air-methanol and air-cyclohexane systems the average gas holdup was observed for a step increase in the air flow rate. In all three cases the time for the numerically predicted holdup to reach the second steady state was in good

agreement with the experimental time. To this end, the CFD code was validated as the numerical results matched the experimental ones.

The dynamic behavior of the liquid velocity and gas holdup was also examined. Since there was no experimental data for comparison the results obtained are not necessarily accurate. Further work needs to be done in the experimental area to get local values on a very small time scale (0.01 s) and for a fine mesh. The numerical results predicted the velocity and holdup profiles to be oscillatory, although the peak heights changed with time.

Other areas that need further attention are the exploration of different bubble columns and the numerical boundary condition at the top of the bubble column. Bubble columns with a liquid circulation (co- and counter-current) could be examined. In addition, a three phase bubble column could be studied. With the results obtained from this study it would be worthwhile to examine the effects in larger bubble columns as well. In larger columns the side walls would not play a major role in the drag correlation. The boundary condition at the top of the column could be tested. It would be more advantageous if the liquid-gas interface could be modeled. This would allow for the examination of bed expansion/contractions at different gas flow rates.

## Nomenclature

| | | |
|---|---|---|
| $A$ | constant from empirical holdup correlation | |
| $A_x$ | constant used to calculate grid locations | |
| $B$ | buoyancy force | $N \cdot m^{-3}$ |
| $B_x$ | constant used to calculate grid locations | |
| $C$ | constants | |
| $C_D$ | drag coefficient | |
| $C_x$ | constant used to calculate grid locations | |
| $C_{\alpha\beta}$ | interphase transfer term | $kg \cdot m^{-3}s^{-1}$ |
| $D$ | diameter | m |
| $D_x$ | constant used to calculate grid locations | |
| $E$ | energy input rate | $W \cdot m^{-2}$ |
| **F** | force on a bubble | N |
| $G$ | production due to body force | $N \cdot m^{-2}s^{-1}$ |
| $h$ | height | m |
| $H$ | height | m |
| $k$ | turbulent kinetic energy | $m^2s^{-2}$ |
| $K$ | consistency index | $Pa \cdot s^n$ |
| $k^*$ | wall correction factor for $C_D$ | |
| $m$ | mass of a bubble | kg |
| $N$ | constant | |
| $n$ | flow behavior index | |
| $N_\mu$ | viscosity number | |

| | | |
|---|---|---|
| $P$ | pressure | MPa |
| $P^*$ | shear production | $N \cdot m^{-2}s^{-1}$ |
| $r$ | bubble radius | m |
| $S$ | energy dissipation rate at the gas-liquid interface | $W \cdot m^{-2}$ |
| $t$ | time | s |
| $\mathbf{U}$ | velocity vector | $m \cdot s^{-1}$ |
| $U_g$ | superficial gas velocity | $m \cdot s^{-1}$ |
| $U_{trans}$ | superficial gas velocity at transition between homogeneous and heterogeneous flow | $m \cdot s^{-1}$ |
| $\mathbf{v}$ | velocity of a bubble | $m \cdot s^{-1}$ |
| $v_\infty$ | single bubble rise velocity | $m \cdot s^{-1}$ |
| $W$ | energy dissipation rate due to the liquid motion | $W \cdot m^{-2}$ |
| $\mathbf{x}$ | position of a bubble | m |
| $X(l)$ | location of horizontal grid lines | cm |

Greek letters

| | | |
|---|---|---|
| $\alpha$ | used in CCCT discritization scheme | |
| $\beta$ | constant in RNG $k$-$\varepsilon$ model | |
| $\varepsilon$ | turbulent dissipation rate | $m^2s^{-3}$ |
| $\phi$ | variable being discritized | |
| $\gamma$ | function of $r^*$ | |
| $\eta$ | function in RNG $k$-$\varepsilon$ model | |
| $\eta_o$ | constant in RNG $k$-$\varepsilon$ model | |
| $\mu$ | viscosity | $kg \cdot m^{-1}s^{-1}$ |

| | | |
|---|---|---|
| $\mu_{eff}$ | effective viscosity | $kg \cdot m^{-1}s^{-1}$ |
| $\rho$ | density | $kg \cdot m^{-3}$ |
| $\sigma$ | surface tension | $N \cdot m^{-1}$ |
| $\psi$ | volume fraction (holdup) | |

subscripts

| | |
|---|---|
| f | final |
| i | initial |
| g | gas |
| l | liquid |
| p | particle or bubble |
| c | continuous phase |
| d | dispersed phase |
| turb | turbulent (used to denote turbulent viscosity) |
| atm | atmospheric |
| e | east |
| w | west |
| n | north |
| s | south |
| x | denotes constants used to generate numerical grid |
| 1 | denotes constants used in $k$-$\varepsilon$ model |
| 1RNG | denotes constants used in $k$-$\varepsilon$ model |
| 2 | denotes constants used in $k$-$\varepsilon$ model |

| | |
|---|---|
| 3 | denotes constants used in $k$-$\varepsilon$ model |
| 4 | denotes constants used in $k$-$\varepsilon$ model |
| P | pressure gradient |
| D | drag |
| VM | virtual mass |
| L | lift |
| G | gravity |

## References

AEA Technolgy, "CFX-4.1: User Manual: Solver" (1997).

Alderton, J. H. and N. S. Wilkes, *Some Applications of New Finite Difference Schemes for Fluid Flow Problems*, AERE-R 13234 (1988).

Asai, S., amd Yoshizawa, H., "Individual Longitudinal Dispersion Coefficients of Two Immiscible Liquids in Bubble Columns," *Ind. Eng. Chem. Res.*, **31**, 587 (1992).

Becker, S., A. Sokolichin, and G. Eigenberger, "Gas-Liquid Flow in Bubble Columns and Loop Reactors: Part II. Comparison of Detailed Experiments and Flow Simulations," *Chem. Eng. Sci.*, **49** (24B), 5747 (1995).

Bisio, A., and R. L. Kabel, *Scaleup of Chemical Precesses*, p. 217 – 251, John Wiley & Sons, Inc., United States of America (1985).

Chang, J.S., and G.D. Harvel, "Determination of Gas-Liquid Bubble Column Instantaneous Interficial Area and Void Fraction by a Real-Time Neutron Radiography Method," *Chem. Eng. Sci.*, **47** (13/14), 3639 (1992).

Chen, R. C., J. Reece, and L.-S. Fan, "Flow Structure in a Three-Dimensional Bubble Column and Three-Phase Fluidized Bed," *AIChE J.*, **40** (7), 1093 (1994).

Chen, Z., C. Zheng, and Y. Feng, "Modeling of Three-Phase Fluidized Beds Based on Local Bubble Characteristics Measurements," *Chem. Eng. Sci.*, **50** (2), 231 (1995).

Deckwer, W.-D., and A. Schumpe, "Improved Tools For Bubble Column Reactor Design and Scale-Up," *Chem. Eng. Sci.*, **48**, 889 (1993).

Delnoij, E., F. A. Lammers, J. A. M. Kuipers, and W. P. M. van Swaaij, "Dynamic Simulation of Dispersed Gas-Liquid Two-Phase flow using a discrete bubble model," *Chem. Eng. Sci.*, **52** (9), 1429 (1997).

Devanathan, N., M. P. Dudukovic, and A. Lapin, "Chaotic Flow in Bubble Column Reactors," *Chem. Eng. Sci.*, **50** (16), 2661 (1995).

Fletcher, C. A. J., *Computation Techniques for Fluid Dynamics Volume II*, Springer-Verlag Berlin Heidelberg (1988).

Garcia-Calvo, E., P. Leton, and M. A. Arranz, "Theoretical Prediction of Gas Holdup in Bubble Columns with Newtonian and Non-Newtonian Liquids," *Chem. Eng. Comm.*, **143**, 117 (1996).

Garcia-Calvo, E., and P. Leton, "Prediction of Fluid Dynamics and Liquid Mixing in Bubble Columns," *Chem. Eng. Sci.*, **49** (21), 3643 (1994).

Geary, N.W., and R.G. Rice, "Circulation and Scale up in Bubble Columns," *AIChE J.*, **38**, 76 (1992).

Gharat, S. D., and J. B. Joshi, "Transport Phenomena in Bubble Column Reactors I: Flow Pattern," *Chem. Eng. J.*, **48**, 141 (1992).

Grienberger, J., and H. Hofmann, "Investigation and Modelling of Bubble Columns," *Chem. Eng. Sci.*, **47** (9-11), 2215 (1992).

Hammer, H., H. Schrag, K. Hektor, K. Schonau, W. Kusters, A. Soemarno, U. Sahabi, and W. Napp, "New Subfunctions on Hydrodynamics, Heat and Mass Transfer for Gas/Liquid and Gas/Solid Chemical and Biochemical Reactors," *Front. Chem. Reac. Eng.*, 464 (1984).

Herbrechtsmeier, P., Schafer, H. , and Steiner, R., "Influence of Operating Parameters on Interfacial Area in Downflow Bubble Columns," *Ger. Chem. Eng.*, **8**, 57 (1985).

Hikita, H., S. Asai, K. Tanigawa, K. Segawa, and M. Kitao, "Gas Hold-up in Bubble Columns," *Chem. Eng. J.*, **20**, 59 (1980).

Hillmer, G., L. Weismantel, and H. Hofmann, "Investigations and Modelling of Slurry Bubble Columns," *Chem. Eng. Sci.*, **49** (6), 837 (1994).

Hills, J.H., "Radial Non-Uniformity of Velocity and Voidage in a Bubble Column," *Trans. Int. Chem. Eng.*, **52**, 1 (1974).

Holman, J.P., *Experimental Methods for Engineers*, McGraw Hill, 3rd Edition (1988).

Hubertus, C., J. Hoefsloot, and R. Krishna, " Influence of Gas Density on the Stability of Homogeneous Flow in Bubble Columns," *Ind. Eng. Chem. Res.*, **32**, 747 (1993).

Hyndman, C.L., and C. Guy, "Gas Phase Hydrodynamics in Bubble Columns," *Trans. Int. Chem. Eng.*, **73** (A), 302 (1995).

Hyndman, C.L., and C. Guy, "Gas Phase Flow in Bubble Columns: A Convective Phenomenon," *Can. J. Chem. Eng.*, **73**, 426 (1995).

Idogawa, K., K. Ikeda, F. Fukuda, and S. Morooka, "Effect of Gas and Liquid Properties on the Behavior of Bubbles in a Bubble Column Under High Pressure," *Kag. Kog. Ronb.*, **11**, 432 (1985).

Idogawa, K., K. Ikeda, F. Fukuda, and S. Morooka, "Effect of Gas and Liquid Properties on the Behavior of Bubbles in a Bubble Column Under High Pressure," *Int. Chem. Eng.*, **27**, 93 (1987).

Ishii, M., and N. Zuber, "Drag Coefficient and Relative Velocity in Bubbly, Droplet or Particulate Flows," *AIChE J.*, **25** (5), 843 (1979).

Koide, K., S. Morooka, K. Ueyama, A. Matsuura, F. Yamashita, S. Iwamoto, Y. Kato, H. Inoue, M. Shigeta, S. Suzuki, and T. Akehata, "Behavior of Bubbles in Large Scale Bubble Columns," *J. Chem. Eng. Japan.*, **12** (2), 98 (1979).

Koide, K., A. Takazawa, M. Komura, and H. Matsunaga, "Gas Holdup and Volumetric Liquid-Phase Mass Transfer Coefficient in Solid-Suspended Bubble Columns," J. Chem. Eng. Japan., **17** (5), 459 (1984).

Koide, K., "Design Parameters of Bubble Column Reactors With and Without Solid Suspensions," *J. Chem. Eng. Japan.*, **29** (5), 745 (1996).

Krishna, R., J. W. A. de Swart, D. E. Hennephof, J. Ellenberger, and H. C. J. Hoefsloot, "Influence of Increased Gas Density on Hydrodynamics of Bubble-Column Reactors," *AIChE J.*, **40** (1), 112 (1994).

Krishna, R., and J. Ellenberger, "A Unified Approach to the Scale-Up of 'Fluidized' Multiphase Reactors," *Trans IChemE*, **73** (A), 217 (1995).

Krishna, R., J. Ellenberger, and S. T. Sie, "Reactor Development for Conversion of Natural Gas to Liquid Fuels: A Scale-Up Strategy Relying on Hydrodynamic Analogies," *Chem. Eng. Sci.*, **51** (10), 2041 (1996).

Krishna, R., P. M. Wilkinson, and L. L. van Dierendonck, "A Model for Gas Holdup in Bubble Columns Incorporating the Influence of Gas Density on Flow Regime Transitions," *Chem. Eng. Sci.*, **46** (10), 2491 (1991).

Lapin, A., and A. Lubbert, "Numerical Simulation of the Dynamics of Two-Phase Gas-Liquid Flows in Bubble Columns," *Chem. Eng. Sci.*, **49** (21), 3661 (1994).

Lin, T.-J., J. Reese, T. Hong, and L. –S. Fan, "Quantitative Analysis and Computation of Two-Dimensional Bubble Columns," *AIChE J.*, **42** (2), 301 (1996).

Lin, T.-J., K. Tsuchiya, and L.-S. Fan, "Bubble Flow Characteristics in Bubble Columns at Elevated Pressure and Temperature," *AIChE J.*, **44** (3), 545 (1998).

Luo, H., and H.F. Svendsen, "Turbulent Circulation in Bubble Columns from Eddy Viscosity Distributions of Single Phase Pipe Flow," *Can. J. Chem. Eng.*, **69**, 1389 (1991).

Menzel T., T. Weide, O. Staudacher, and U. Onken, *Industrial Engineering Chemistry Research*, **29**, 988 (1990).

Miyauchi, T., and C.-N. Shyu; "Flow of Fluid in Gas-Bubble Columns," *Kagaku Kogaku*, **34**, 958 (1970).

Molerus, O., and M. Kurtin, "Hydrodynamics of Bubble Columns in the Uniform Bubbling Regime," *Chem. Eng. Sci.*, **40** (4), 647 (1985).

Molerus, O., "Dependance of the Drag on Particles Concentration - A Basic Model and its Practical Application -," *Chem. Eng. Sci.*, **42** (4), 689 (1987).

Patankar, S. V., *Numerical Heat Transfer and Fluid Flow*, New York: McGraw-Hill (1980).

Perry, R. H., D. W. Green, and J. O. Maloney, *Perry's Chemical Engineers' Handbook*, 6th Ed., New York: McGraw-Hill (1984)

Que, F., *Dynamic Simulation of Gas-Liquid Mixing in a 2-D Bubble Column*, PhD Thesis, UMIST, Manchester (1991).

Ranade, V.V., " TPFLOW: A Code for Simulating Three Dimensional Two Phase Flows," *NCL Internal Report* (1991).

Ranade, V. V., "Flow in Bubble Columns: Some Numerical Experiments," *Chem. Eng. Sci.*, **47** (8), 1857 (1992).

Reese, J., and L.-S. Fan, "Transient Flow Structure in the Entrance Region of a Bubble Column Using Particle Image Velocimetry," *Chem. Eng. Sci.*, **49** (24B), 5623 (1994).

Reilly, I. G., D. S. Scott, T. de Bruijn, A. Jain, and J. Diskorz, "Correlation of Gas Holdup in Turbulent Coalescing Bubble Columns," *Can. J. Chem. Eng.*, **64**, 705 (1986).

Richardson, J. F., and W. N. Zaki, "Sedimentation and Fluidization: Part I," *Trans. Inst. Chem. Eng.*, **32**, 35 (1954).

Rietema, K., and S.P.P. Ottengraf, " Laminar Liquid Circulation and Bubble Street Formation in a Gas-Liquid System," *Trans. Int. Chem. Eng.*, **48**, T54 (1970).

Salinas-Rodriguez, E., R.F. Rodriguez, A. Soria, and N. Aquino, "Volume Fraction Autocorrelation Functions in a Two-Phase Bubble Column," Int. J. Multiphase Flow, 24 (1), 93 (1998).

Schwarz, M. P., and W. J. Turner, "Applicability of the Standard $k$-$\varepsilon$ Turbulence Model to Gas-Stirred Baths," *Appl. Math. Modelling*, **12**, 273 (1988).

Shen, G., and J.A. Finch, "Bubble Swarm Velocity in a Column," *Chem. Eng. Sci.*, **51** (14), 3665 (1996).

Sokolichin, A., G. Eigenberger, A. Lapin, and A. Lubbert, "Dynamic Numerical Simulation of Gas-Liquid Two-Phase Flows – Euler/Euler versus Euler/Lagrange", *Chem. Eng. Sci.*, **52** (4), 611 (1997).

Sokolichin, A., and G. Eigenberger; "Gas-Liquid Flow in Bubble Columns and Loop Reactors: Part 1. Detailed Modelling and Numerical Simulation," *Chem. Eng. Sci.*, **49**, 5735 (1994).

Soong, Y., I.K. Gamwo, A.G. Blackwell, F.W. Harke, R.R. Schehl, and M.F. Zarochak, "Ultrasonic Characterizations of Gas Holdup in Bubble Column Reactors," *Chem. Eng. Comm.*, **158**, 181 (1997).

Svendsen, H. F., H. A. Jakobsen, and R. Torvik, "Local Flow Structures in Internal Loop and Bubble Column Reactors," *Chem. Eng. Sci.*, **47** (13/14), 3297 (1992).

Torvik, R., and H. F. Svendsen, "Modelling of Slurry Reactors. A Fundamental Approach," *Chem. Eng. Sci.*, **45** (8), 2325 (1990).

Tsuchiya, K., and O. Nakanishi, "Gas Holdup Behavior in a Tall Bubble Column with Perforated Plate Distributors," *Chem. Eng. Sci.*, **47** (13/14), 3347 (1992).

Tzeng, J.-W., R. C. Chen, and L.-S. Fan, "Visualization of Flow Characteristics in a 2-D Bubble Column and Three-Phase Fluidized Bed," *AIChE J.*, **39** (5), 733 (1993).

Ueyama, K., and T. Miyauchi, "Properties of Recirculating Turbulent Two Phase Flow in Gas Bubble Columns," *AIChE J.*, **25** (2), 258 (1979).

Wallis, G. B., *One-dimensional Two-Phase Flow*, New York: McGraw-Hill (1969).

Webb, C., F. Que, and P. R. Senior, "Dynamic Simulation of Gas- Liquid Dispersion behavior in a 2-D Bubble Column using a Graphics Mini-Supercomputer," Chem. Eng. Sci., **47** (13/14), 3305 (1992).

Weiss, R. G., N. R. Foster, and K. N. Clark, "The Effect of Liquid Viscosity on Holdup in a Vertical Pipe," *Can. J. Chem. Eng.*, **63**, 173 (1985).

Wilkinson, P. M., A. P. Spek, and L. L. van Dierendonck, "Design Parameters Estimation for Scale-Up of High-Pressure Bubble Columns," *AIChE J.*, **38** (4), 544 (1992).

Yang, Y. B., N. Devanathan, and M. P. Dudukovic; "Liquid Backmixing in Bubble Columns," *Chem. Eng. Sci.*, **47**, 2859 (1992).

Zhu, J.W., and S.C. Saxena, "Prediction of Gas Phase Holdup in a Bubble Column," Chem. Eng. Comm. **161**, 149 (1997).

Zhu, J.W., V.H. Trivedi, and S.C. Saxena, "Gas-Phase Holdup in a Slurry-Bubble Column," Chem. Eng. Comm., **157**, 53 (1997).

## Appendix A. Sample CFX-F3D code.

This code was used to simulate the air-water system with a superficial air velocity of 0.815cm/s. The CCCT method is used to discritized the equations. The time step used is 0.01 s and the grid is a 20 x 60 grid. The key characteristics are in bold.

```
/*************************************************************/
/* 2-D Bubble column simulation in a rectangular domain      */
/*************************************************************/
>>CFXF3D
  >>OPTIONS
    TWO DIMENSIONS
    BODY FITTED GRID
    NUMBER OF PHASES 2
    TRANSIENT FLOW
    TURBULENT FLOW
    INCOMPRESSIBLE FLOW
    BUOYANT FLOW
  >>USER FORTRAN
    USRIPT
    USRGRD
    USRBCS
    USRTRN
>>MODEL TOPOLOGY
  >>CREATE BLOCK
    BLOCK NAME 'BLOCK-NUMBER-1'
    BLOCK DIMENSIONS 20  60  1
  >>CREATE PATCH
    PATCH NAME 'GAS-INLET'
    PATCH TYPE 'INLET'
    BLOCK NAME 'BLOCK-NUMBER-1'
    LOW J
  >>CREATE PATCH
    PATCH NAME 'GAS-OUTLET'
    PATCH TYPE 'PRESSURE BOUNDARY'
    BLOCK NAME 'BLOCK-NUMBER-1'
    PATCH GROUP NUMBER 1
    HIGH J
>>MODEL DATA
  >>TITLE
    PROBLEM TITLE 'Bubble column'
  /*>>AMBIENT VARIABLES
    PHASE NAME 'PHASE1'
    VOLUME FRACTION 0.91
    END
  >>AMBIENT VARIABLES
    PHASE NAME 'PHASE2'
    VOLUME FRACTION 0.09
    END*/
  >>SET INITIAL GUESS
    >>INPUT FROM FILE
      READ DUMP FILE
```

```
  >>WALL TREATMENTS
    PHASE NAME 'PHASE1'
    NO SLIP
  >>WALL TREATMENTS
    PHASE NAME 'PHASE2'
    SLIP
  >>PHYSICAL PROPERTIES
    >>BUOYANCY PARAMETERS
      GRAVITY VECTOR 0.0 -9.8 0.0
      BUOYANCY REFERENCE DENSITY 998.0
    >>FLUID PARAMETERS
      PHASE NAME 'PHASE1'      /* continuous */
      VISCOSITY 1.0E-3
      DENSITY 998.0
    >>FLUID PARAMETERS
      PHASE NAME 'PHASE2'     /* dispersed */
      VISCOSITY 1.8E-5
      DENSITY 1.222E+0
    >>TURBULENCE PARAMETERS
      >>TURBULENCE CONSTANTS
        INITIAL EDDY VISCOSITY ITERATIONS 100
      >>TURBULENCE MODEL
        PHASE NAME 'PHASE1'
        TURBULENCE MODEL 'RNG K-EPSILON'
        PHASE NAME 'PHASE2'
        TURBULENCE MODEL 'LAMINAR'
    >>MULTIPHASE PARAMETERS
      >>MULTIPHASE MODELS
        >>MOMENTUM
          INTER PHASE TRANSFER
          SINCE
          IPSAC
        >>PHASE DESCRIPTION
          PHASE NAME 'PHASE1'
          LIQUID
          CONTINUOUS
        >>PHASE DESCRIPTION
          PHASE NAME 'PHASE2'
          GAS
          DISPERSE
          MEAN DIAMETER 3.0E-3
    >>TRANSIENT PARAMETERS
      >>FIXED TIME STEPPING
        TIME STEPS 200*0.01
        BACKWARD DIFFERENCE
  >>DIFFERENCING SCHEME
    ALL EQUATIONS 'CCCT'
>>SOLVER DATA
  >>PROGRAM CONTROL
    MAXIMUM NUMBER OF ITERATIONS 200
    MINIMUM NUMBER OF ITERATIONS 20
    OUTPUT MONITOR BLOCK 'BLOCK-NUMBER-1'
    OUTPUT MONITOR POINT 10 34 1
    MASS SOURCE TOLERANCE 1.0E-09
  >>UNDER RELAXATION FACTORS
    ALL PHASES
    U VELOCITY 0.4
```

```
    V VELOCITY 0.4
    PRESSURE 0.5
    VOLUME FRACTION 0.4
/*  >>SWEEPS INFORMATION
    >>MINIMUM NUMBER
      PRESSURE 3
      VFRAC 3
    >>MAXIMUM NUMBER
      PRESSURE 30
      VFRAC 30
  >>REDUCTION FACTORS
    PRESSURE 0.01
    VFRAC 0.01        */
  >>EQUATION SOLVERS
    U VELOCITY 'AMG'
    V VELOCITY 'AMG'
    VOLUME FRACTION 'AMG'
    PRESSURE 'AMG'
  /*>>ALGEBRAIC MULTIGRID PARAMETERS
    CONNECTIVITY TOLERANCE 1.0E-08
    SINGULARITY TOLERANCE 0.1*/
>>CREATE GRID
>>MODEL BOUNDARY CONDITIONS
  >>SET VARIABLES
    PATCH NAME 'GAS-INLET'
    PHASE NAME 'PHASE2'
    U VELOCITY  0.0
    V VELOCITY  0.0163
    END
>>OUTPUT OPTIONS
  >>PRINT OPTIONS
    >>WHAT
      NO GEOMETRIC INFORMATION
>>STOP
```

## Appendix B. Fortran user routine USRGRD (grid generation)

This appendix gives an example of the Fortran code used to generate the numerical grid. The actual code used to generate the grid is shown in bold.

```
SUBROUTINE
USRGRD(U,V,W,P,VFRAC,DEN,VIS,TE,ED,RS,T,H,RF,SCAL,XP,
     +
YP,ZP,VOL,AREA,VPOR,ARPOR,WFACT,XCOLD,YCOLD,
     +
ZCOLD,XC,YC,ZC,IPT,IBLK,IPVERT,IPNODN,IPFACN,
     +                  IPNODF,IPNODB,IPFACB,WORK,IWORK,CWORK)
C
C***************************************************************
*********
C
C   USER SUBROUTINE TO ALLOW USERS TO GENERATE A GRID FOR CFX-
F3D
C
C   >>> IMPORTANT
<<<
C   >>>
<<<
C   >>> USERS MAY ONLY ADD OR ALTER PARTS OF THE SUBROUTINE
WITHIN  <<<
C   >>> THE DESIGNATED USER AREAS
<<<
C
C***************************************************************
*********
C
C   THIS SUBROUTINE IS CALLED BY THE FOLLOWING SUBROUTINES
C      CREATE  CUSR
C
C***************************************************************
*********
C   CREATED
C      27/04/90  ADB
C   MODIFIED
C      05/08/91  IRH  NEW STRUCTURE
C      09/09/91  IRH  CORRECT EXAMPLE
C      01/10/91  DSC  REDUCE COMMENT LINE GOING OVER 72
COLUMNS.
C      29/11/91  PHA  UPDATE CALLED BY COMMENT, ADD RF
ARGUMENT,
C                     CHANGE LAST DIMENSION OF RS TO 6 AND
IVERS TO 2
C      03/06/92  PHA  ADD PRECISION FLAG AND CHANGE IVERS TO 3
C      03/07/92  DSC  CORRECT COMMON MLTGRD.
C      23/11/93  CSH  EXPLICITLY DIMENSION IPVERT ETC.
C      03/02/94  PHA  CHANGE FLOW3D TO CFDS-FLOW3D
C      03/03/94  FHW  CORRECTION OF SPELLING MISTAKE
```

```
C      22/08/94  NSW  MOVE 'IF(IUSED.EQ.0) RETURN' OUT OF USER
AREA
C      19/12/94  NSW  CHANGE FOR CFX-F3D
C
C*************************************************************
*********
C
C   SUBROUTINE ARGUMENTS
C
C     U       - U COMPONENT OF VELOCITY
C     V       - V COMPONENT OF VELOCITY
C     W       - W COMPONENT OF VELOCITY
C     P       - PRESSURE
C     VFRAC   - VOLUME FRACTION
C     DEN     - DENSITY OF FLUID
C     VIS     - VISCOSITY OF FLUID
C     TE      - TURBULENT KINETIC ENERGY
C     ED      - EPSILON
C     RS      - REYNOLD STRESSES
C     T       - TEMPERATURE
C     H       - ENTHALPY
C     RF      - REYNOLD FLUXES
C     SCAL    - SCALARS (THE FIRST 'NCONC' OF THESE ARE MASS
FRACTIONS)
C     XP      - X COORDINATES OF CELL CENTRES
C     YP      - Y COORDINATES OF CELL CENTRES
C     ZP      - Z COORDINATES OF CELL CENTRES
C     VOL     - VOLUME OF CELLS
C     AREA    - AREA OF CELLS
C     VPOR    - POROUS VOLUME
C     ARPOR   - POROUS AREA
C     WFACT   - WEIGHT FACTORS
C   * XC      - X COORDINATES OF CELL VERTICES
C   * YC      - Y COORDINATES OF CELL VERTICES
C   * ZC      - Z COORDINATES OF CELL VERTICES
C     XCOLD   - X COORDINATES OF CELL VERTICES AT START OF TIME
STEP
C     YCOLD   - Y COORDINATES OF CELL VERTICES AT START OF TIME
STEP
C     ZCOLD   - Z COORDINATES OF CELL VERTICES AT START OF TIME
STEP
C
C     IPT     - 1D POINTER ARRAY
C     IBLK    - BLOCK SIZE INFORMATION
C     IPVERT  - POINTER FROM CELL CENTERS TO 8 NEIGHBOURING
VERTICES
C     IPNODN  - POINTER FROM CELL CENTERS TO 6 NEIGHBOURING
CELLS
C     IPFACN  - POINTER FROM CELL CENTERS TO 6 NEIGHBOURING
FACES
C     IPNODF  - POINTER FROM CELL FACES TO 2 NEIGHBOURING CELL
CENTERS
C     IPNODB  - POINTER FROM BOUNDARY CENTERS TO CELL CENTERS
C     IPFACB  - POINTER FROM BOUNDARY CENTERS TO BOUNDARY
FACESS
C
C     WORK    - REAL WORKSPACE ARRAY
```

```
C     IWORK  - INTEGER WORKSPACE ARRAY
C     CWORK  - CHARACTER WORKSPACE ARRAY
C
C   SUBROUTINE ARGUMENTS PRECEDED WITH A '*' ARE ARGUMENTS
THAT MUST
C   BE SET  BY THE USER IN THIS ROUTINE.
C
C   NOTE THAT OTHER DATA MAY BE OBTAINED FROM CFX-F3D USING
THE
C   ROUTINE GETADD, FOR FURTHER DETAILS SEE THE VERSION 4
C   USER MANUAL.
C
C*****************************************************************
*********
C
      DOUBLE PRECISION U
      DOUBLE PRECISION V
      DOUBLE PRECISION W
      DOUBLE PRECISION P
      DOUBLE PRECISION VFRAC
      DOUBLE PRECISION DEN
      DOUBLE PRECISION VIS
      DOUBLE PRECISION TE
      DOUBLE PRECISION ED
      DOUBLE PRECISION RS
      DOUBLE PRECISION T
      DOUBLE PRECISION H
      DOUBLE PRECISION RF
      DOUBLE PRECISION SCAL
      DOUBLE PRECISION XP
      DOUBLE PRECISION YP
      DOUBLE PRECISION ZP
      DOUBLE PRECISION VOL
      DOUBLE PRECISION AREA
      DOUBLE PRECISION VPOR
      DOUBLE PRECISION ARPOR
      DOUBLE PRECISION WFACT
      DOUBLE PRECISION XCOLD
      DOUBLE PRECISION YCOLD
      DOUBLE PRECISION ZCOLD
      DOUBLE PRECISION XC
      DOUBLE PRECISION YC
      DOUBLE PRECISION ZC
      DOUBLE PRECISION WORK
      DOUBLE PRECISION SMALL
      DOUBLE PRECISION SORMAX
      DOUBLE PRECISION DTUSR
      DOUBLE PRECISION TIME
      DOUBLE PRECISION DT
      DOUBLE PRECISION DTINVF
      DOUBLE PRECISION TPARM
      LOGICAL
LDEN,LVIS,LTURB,LTEMP,LBUOY,LSCAL,LCOMP,LRECT,LCYN,LAXIS,
     +        LPOROS,LTRANS
C
      CHARACTER*(*) CWORK
C
```

```
C+++++++++++++++++ USER AREA 1
++++++++++++++++++++++++++++++++++++++
C---- AREA FOR USERS EXPLICITLY DECLARED VARIABLES
      DOUBLE PRECISION XX
C
C+++++++++++++++++ END OF USER AREA 1
++++++++++++++++++++++++++++++++
C
      COMMON /ALL/NBLOCK,NCELL,NBDRY,NNODE,NFACE,NVERT,NDIM,
     +
/ALLWRK/NRWS,NIWS,NCWS,IWRFRE,IWIFRE,IWCFRE,/ADDIMS/NPHASE,
     +
NSCAL,NVAR,NPROP,NDVAR,NDPROP,NDXNN,NDGEOM,NDCOEF,NILIST,
     +
NRLIST,NTOPOL,/CHKUSR/IVERS,IUCALL,IUSED,/CONC/NCONC,
     +
/DEVICE/NREAD,NWRITE,NRDISK,NWDISK,/IDUM/ILEN,JLEN,
     +
/LOGIC/LDEN,LVIS,LTURB,LTEMP,LBUOY,LSCAL,LCOMP,LRECT,LCYN,
     +       LAXIS,LPOROS,LTRANS,/MLTGRD/MLEVEL,NLEVEL,ILEVEL,
     +
/SGLDBL/IFLGPR,ICHKPR,/SPARM/SMALL,SORMAX,NITER,INDPRI,
     +
MAXIT,NODREF,NODMON,/TIMUSR/DTUSR,/TRANSI/NSTEP,KSTEP,MF,
     +       INCORE,/TRANSR/TIME,DT,DTINVF,TPARM
C
C+++++++++++++++++ USER AREA 2
++++++++++++++++++++++++++++++++++++++
C---- AREA FOR USERS TO DECLARE THEIR OWN COMMON BLOCKS
C     THESE SHOULD START WITH THE CHARACTERS 'UC' TO ENSURE
C     NO CONFLICT WITH NON-USER COMMON BLOCKS
C
C+++++++++++++++++ END OF USER AREA 2
++++++++++++++++++++++++++++++++
C
      DIMENSION
U(NNODE,NPHASE),V(NNODE,NPHASE),W(NNODE,NPHASE),
     +
P(NNODE,NPHASE),VFRAC(NNODE,NPHASE),DEN(NNODE,NPHASE),
     +
VIS(NNODE,NPHASE),TE(NNODE,NPHASE),ED(NNODE,NPHASE),
     +
RS(NNODE,NPHASE,6),T(NNODE,NPHASE),H(NNODE,NPHASE),
     +          RF(NNODE,NPHASE,4),SCAL(NNODE,NPHASE,NSCAL)
      DIMENSION
XP(NNODE),YP(NNODE),ZP(NNODE),XC(NVERT),YC(NVERT),
     +
ZC(NVERT),XCOLD(NVERT),YCOLD(NVERT),ZCOLD(NVERT),
     +
VOL(NCELL),AREA(NFACE,3),VPOR(NCELL),ARPOR(NFACE,3),
     +
WFACT(NFACE),IPT(*),IBLK(5,NBLOCK),IPVERT(NCELL,8),
     +
IPNODN(NCELL,6),IPFACN(NCELL,6),IPNODF(NFACE,4),
     +
IPNODB(NBDRY,4),IPFACB(NBDRY),IWORK(*),WORK(*),CWORK(*)
C
```

```
C+++++++++++++++++ USER AREA 3
++++++++++++++++++++++++++++++++++++++++
C---- AREA FOR USERS TO DIMENSION THEIR ARRAYS
      DIMENSION XX(100)
C
C---- AREA FOR USERS TO DEFINE DATA STATEMENTS
C
C+++++++++++++++++ END OF USER AREA 3
++++++++++++++++++++++++++++++++
C
C---- STATEMENT FUNCTION FOR ADDRESSING
      IP(I,J,K) = IPT((K-1)*ILEN*JLEN+ (J-1)*ILEN+I)
C
C---- VERSION NUMBER OF USER ROUTINE AND PRECISION FLAG
C
      IVERS = 3
      ICHKPR = 2
C
C+++++++++++++++++ USER AREA 4
++++++++++++++++++++++++++++++++++++++++
C---- TO USE THIS USER ROUTINE FIRST SET IUSED=1
C
      IUSED = 1
C
C+++++++++++++++++ END OF USER AREA 4
++++++++++++++++++++++++++++++++
C
      IF (IUSED.EQ.0) RETURN
C
C---- FRONTEND CHECKING OF USER ROUTINE
      IF (IUCALL.EQ.0) RETURN
C
C+++++++++++++++++ USER AREA 5
++++++++++++++++++++++++++++++++++++++++
C
C---- EXAMPLE: DEFINE INITIAL GRID
C
C-- USE IPREC TO FIND ADDRESSES
C      CALL IPREC('BLOCK-NUMBER-
1','BLOCK','VERTICES',IPT,ILEN,JLEN,
C     +           KLEN,CWORK,IWORK)
C
C-- LOOP OVER BLOCK
C      DO 100 K=1,KLEN
C        DO 120 J=1,JLEN
C           DO 130 I=1,ILEN
C-- USE STATEMENT FUNCTION IP TO GET ADDRESSES
C           INODE = IP(I,J,K)
C-- DEFINE LOCATION OF GRID VERTICES
C           XC(INODE)=FLOAT(I-1)/FLOAT(ILEN-1)
C           YC(INODE)=FLOAT(J-1)/FLOAT(JLEN-1)
C           ZC(INODE)=FLOAT(K-1)/FLOAT(KLEN-1)
C 130       CONTINUE
C 120    CONTINUE
C 100  CONTINUE
C
C---- END OF EXAMPLE
```

```
C
C-- USE IPREC TO FIND ADDRESSES
       CALL IPREC('BLOCK-NUMBER-
1','BLOCK','VERTICES',IPT,ILEN,JLEN,
     +            KLEN,CWORK,IWORK)
      BETA = 1.05D0
      ONE  = 1.0D0
      TWO  = 2.0D0
      XMAX = 0.035
      TMP1 = (BETA + ONE)/(BETA - ONE)
      DO 90 I = 1, ILEN
        TMP2 = 2 * FLOAT(I-1)/FLOAT(ILEN-1) - ONE
        TMP3 = TMP1 ** TMP2
        TMP4 = ((ONE + BETA) * TMP3 + (ONE - BETA))/
     $           (TWO*(ONE+TMP3))
        XX(I) = (TWO * TMP4 - ONE)*XMAX/TWO
 90     CONTINUE
      write(6,*) 'XX',  (XX(I),I=1,ILEN)
      YMAX = 0.150
      ZMAX = 0.01
C
C-- LOOP OVER BLOCK
       DO 100 K=1,KLEN
         DO 120 J=1,JLEN
            DO 130 I=1,ILEN
C-- USE STATEMENT FUNCTION IP TO GET ADDRESSES
            INODE = IP(I,J,K)
C-- DEFINE LOCATION OF GRID VERTICES
            XC(INODE)=XX(I)
            YC(INODE)=YMAX* (FLOAT(J-1)/FLOAT(JLEN-1))
            ZC(INODE)=ZMAX* (FLOAT(K-1)/FLOAT(KLEN-1))
  130       CONTINUE
  120    CONTINUE
  100  CONTINUE
C
C---- END OF EXAMPLE
C
C
C+++++++++++++++++ END OF USER AREA 5
++++++++++++++++++++++++++++++++
C
      RETURN
C
      END
```

## Appendix C. Fortran user routine USRBCS (boundary conditions)

This appendix gives an example of the Fortran code used to set the boundary conditions for the top surface of the bubble column. The actual code used to set the boundary conditions is shown in bold.

```
SUBROUTINE USRBCS(VARBCS,VARAMB,A,B,C,ACND,BCND,CCND,IWGVEL,
     +
NDVWAL,FLOUT,NLABEL,NSTART,NEND,NCST,NCEN,U,V,W,
     +
P,VFRAC,DEN,VIS,TE,ED,RS,T,H,RF,SCAL,XP,YP,ZP,
     +
VOL,AREA,VPOR,ARPOR,WFACT,IPT,IBLK,IPVERT,
     +
IPNODN,IPFACN,IPNODF,IPNODB,IPFACB,WORK,IWORK,
     +                    CWORK)
C
C***************************************************************
**********
C
C  USER ROUTINE TO SET REALS AT BOUNDARIES.
C
C   >>> IMPORTANT
<<<
C   >>>
<<<
C   >>> USERS MAY ONLY ADD OR ALTER PARTS OF THE SUBROUTINE
WITHIN  <<<
C   >>> THE DESIGNATED USER AREAS
<<<
C
C***************************************************************
**********
C
C  THIS SUBROUTINE IS CALLED BY THE FOLLOWING SUBROUTINE
C    CUSR  SRLIST
C
C***************************************************************
**********
C   CREATED
C      30/11/88 ADB
C   MODIFIED
C      08/09/90 ADB  RESTRUCTURED FOR USER-FRIENDLINESS.
C      10/08/91 IRH  FURTHER RESTRUCTURING ADD ACND BCND CCND
C      22/09/91 IRH  CHANGE ICALL TO IUCALL + ADD /SPARM/
C      10/03/92 PHA  UPDATE CALLED BY COMMENT, ADD RF
ARGUMENT,
C                    CHANGE LAST DIMENSION OF RS TO 6 AND
IVERS TO 2
C      03/06/92 PHA  ADD PRECISION FLAG AND CHANGE IVERS TO 3
C      30/06/92 NSW  INCLUDE FLAG FOR CALLING BY ITERATION
C                    INSERT EXTRA COMMENTS
C      03/08/92 NSW  MODIFY DIMENSION STATEMENTS FOR VAX
```

```
C      21/12/92 CSH  INCREASE IVERS TO 4
C      02/08/93 NSW  INCORRECT AND MISLEADING COMMENT REMOVED
C      05/11/93 NSW  INDICATE USE OF FLOUT IN MULTIPHASE FLOWS
C      23/11/93 CSH  EXPLICITLY DIMENSION IPVERT ETC.
C      01/02/94 NSW  SET VARIABLE POINTERS IN WALL EXAMPLE.
C                    CHANGE FLOW3D TO CFDS-FLOW3D.
C                    MODIFY MULTIPHASE MASS FLOW BOUNDARY
TREATMENT.
C      03/03/94 FHW  CORRECTION OF SPELLING MISTAKE
C      02/07/94 BAS  SLIDING GRIDS - ADD NEW ARGUMENT IWGVEL
C                    TO ALLOW VARIANTS OF TRANSIENT-GRID WALL
BC
C                    CHANGE VERSION NUMBER TO 5
C      09/08/94 NSW  CORRECT SPELLING
C                    MOVE 'IF(IUSED.EQ.0) RETURN' OUT OF USER
AREA
C      19/12/94 NSW  CHANGE FOR CFX-F3D
C      02/02/95 NSW  CHANGE COMMON /IMFBMP/
C
C*************************************************************
**********
C
C   SUBROUTINE ARGUMENTS
C
C     VARBCS - REAL BOUNDARY CONDITIONS
C     VARAMB - AMBIENT VALUE OF VARIABLES
C     A      - COEFFICIENT IN WALL BOUNDARY CONDITION
C     B      - COEFFICIENT IN WALL BOUNDARY CONDITION
C     C      - COEFFICIENT IN WALL BOUNDARY CONDITION
C     ACND   - COEFFICIENT IN CONDUCTING WALL BOUNDARY
CONDITION
C     BCND   - COEFFICIENT IN CONDUCTING WALL BOUNDARY
CONDITION
C     CCND   - COEFFICIENT IN CONDUCTING WALL BOUNDARY
CONDITION
C     IWGVEL - USAGE OF INPUT VELOCITIES (0 = AS IS,1 = ADD
GRID MOTION)
C     NDVWAL - FIRST DIMENSION OF ARRAY IWGVEL
C     FLOUT  - MASS FLOW/FRACTIONAL MASS FLOW
C     NLABEL - NUMBER OF DISTINCT OUTLETS
C     NSTART - ARRAY POINTER
C     NEND   - ARRAY POINTER
C     NCST   - ARRAY POINTER
C     NCEN   - ARRAY POINTER
C     U      - U COMPONENT OF VELOCITY
C     V      - V COMPONENT OF VELOCITY
C     W      - W COMPONENT OF VELOCITY
C     P      - PRESSURE
C     VFRAC  - VOLUME FRACTION
C     DEN    - DENSITY OF FLUID
C     VIS    - VISCOSITY OF FLUID
C     TE     - TURBULENT KINETIC ENERGY
C     ED     - EPSILON
C     RS     - REYNOLD STRESSES
C     T      - TEMPERATURE
C     H      - ENTHALPY
C     RF     - REYNOLD FLUXES
```

```
C     SCAL   - SCALARS (THE FIRST 'NCONC' OF THESE ARE MASS
FRACTIONS)
C     XP     - X COORDINATES OF CELL CENTRES
C     YP     - Y COORDINATES OF CELL CENTRES
C     ZP     - Z COORDINATES OF CELL CENTRES
C     VOL    - VOLUME OF CELLS
C     AREA   - AREA OF CELLS
C     VPOR   - POROUS VOLUME
C     ARPOR  - POROUS AREA
C     WFACT  - WEIGHT FACTORS
C
C     IPT    - 1D POINTER ARRAY
C     IBLK   - BLOCK SIZE INFORMATION
C     IPVERT - POINTER FROM CELL CENTERS TO 8 NEIGHBOURING
VERTICES
C     IPNODN - POINTER FROM CELL CENTERS TO 6 NEIGHBOURING
CELLS
C     IPFACN - POINTER FROM CELL CENTERS TO 6 NEIGHBOURING
FACES
C     IPNODF - POINTER FROM CELL FACES TO 2 NEIGHBOURING CELL
CENTERS
C     IPNODB - POINTER FROM BOUNDARY CENTERS TO CELL CENTERS
C     IPFACB - POINTER TO NODES FROM BOUNDARY FACES
C
C     WORK   - REAL WORKSPACE ARRAY
C     IWORK  - INTEGER WORKSPACE ARRAY
C     CWORK  - CHARACTER WORKSPACE ARRAY
C
C   SUBROUTINE ARGUMENTS PRECEDED WITH A '*' ARE ARGUMENTS
THAT MUST
C   BE SET  BY THE USER IN THIS ROUTINE.
C
C   NOTE THAT OTHER DATA MAY BE OBTAINED FROM CFX-F3D USING
THE
C   ROUTINE GETADD, FOR FURTHER DETAILS SEE THE VERSION 4
C   USER MANUAL.
C
C*************************************************************
**********
      DOUBLE PRECISION VARBCS
      DOUBLE PRECISION VARAMB
      DOUBLE PRECISION A
      DOUBLE PRECISION B
      DOUBLE PRECISION C
      DOUBLE PRECISION ACND
      DOUBLE PRECISION BCND
      DOUBLE PRECISION CCND
      DOUBLE PRECISION FLOUT
      DOUBLE PRECISION U
      DOUBLE PRECISION V
      DOUBLE PRECISION W
      DOUBLE PRECISION P
      DOUBLE PRECISION VFRAC
      DOUBLE PRECISION DEN
      DOUBLE PRECISION VIS
      DOUBLE PRECISION TE
      DOUBLE PRECISION ED
```

```
      DOUBLE PRECISION RS
      DOUBLE PRECISION T
      DOUBLE PRECISION H
      DOUBLE PRECISION RF
      DOUBLE PRECISION SCAL
      DOUBLE PRECISION XP
      DOUBLE PRECISION YP
      DOUBLE PRECISION ZP
      DOUBLE PRECISION VOL
      DOUBLE PRECISION AREA
      DOUBLE PRECISION VPOR
      DOUBLE PRECISION ARPOR
      DOUBLE PRECISION WFACT
      DOUBLE PRECISION WORK
      DOUBLE PRECISION SMALL
      DOUBLE PRECISION SORMAX
      DOUBLE PRECISION TIME
      DOUBLE PRECISION DT
      DOUBLE PRECISION DTINVF
      DOUBLE PRECISION TPARM
      LOGICAL
LDEN,LVIS,LTURB,LTEMP,LBUOY,LSCAL,LCOMP,LRECT,LCYN,LAXIS,
     +        LPOROS,LTRANS
C
      CHARACTER*(*) CWORK
C
C+++++++++++++++++ USER AREA 1
++++++++++++++++++++++++++++++++++++++++
C---- AREA FOR USERS EXPLICITLY DECLARED VARIABLES
C
C+++++++++++++++++ END OF USER AREA 1
++++++++++++++++++++++++++++++++
C
      COMMON /ALL/NBLOCK,NCELL,NBDRY,NNODE,NFACE,NVERT,NDIM,
     +
/ALLWRK/NRWS,NIWS,NCWS,IWRFRE,IWIFRE,IWCFRE,/ADDIMS/NPHASE,
     +
NSCAL,NVAR,NPROP,NDVAR,NDPROP,NDXNN,NDGEOM,NDCOEF,NILIST,
     +
NRLIST,NTOPOL,/BCSOUT/IFLOUT,/CHKUSR/IVERS,IUCALL,IUSED,
     +
/DEVICE/NREAD,NWRITE,NRDISK,NWDISK,/IDUM/ILEN,JLEN,
     +
/IMFBMP/IMFBMP,JMFBMP,/LOGIC/LDEN,LVIS,LTURB,LTEMP,LBUOY,
     +
LSCAL,LCOMP,LRECT,LCYN,LAXIS,LPOROS,LTRANS,/MLTGRD/MLEVEL,
     +
NLEVEL,ILEVEL,/SGLDBL/IFLGPR,ICHKPR,/SPARM/SMALL,SORMAX,
     +
NITER,INDPRI,MAXIT,NODREF,NODMON,/TRANSI/NSTEP,KSTEP,MF,
     +
INCORE,/TRANSR/TIME,DT,DTINVF,TPARM,/UBCSFL/IUBCSF
C
C+++++++++++++++++ USER AREA 2
++++++++++++++++++++++++++++++++++++++++
C---- AREA FOR USERS TO DECLARE THEIR OWN COMMON BLOCKS
C     THESE SHOULD START WITH THE CHARACTERS 'UC' TO ENSURE
```

```
C     NO CONFLICT WITH NON-USER COMMON BLOCKS
C
C+++++++++++++++++ END OF USER AREA 2
+++++++++++++++++++++++++++++++++
C
      DIMENSION
VARBCS(NVAR,NPHASE,NCELL+1:NNODE),VARAMB(NVAR,NPHASE),
     +
A(4+NSCAL,NPHASE,NSTART:*),B(4+NSCAL,NPHASE,NSTART:*),
     +
C(4+NSCAL,NPHASE,NSTART:*),FLOUT(*),ACND(NCST:*),
     +
BCND(NCST:*),CCND(NCST:*),IWGVEL(NDVWAL,NPHASE)
C
      DIMENSION
U(NNODE,NPHASE),V(NNODE,NPHASE),W(NNODE,NPHASE),
     +
P(NNODE,NPHASE),VFRAC(NNODE,NPHASE),DEN(NNODE,NPHASE),
     +
VIS(NNODE,NPHASE),TE(NNODE,NPHASE),ED(NNODE,NPHASE),
     +
RS(NNODE,NPHASE,6),T(NNODE,NPHASE),H(NNODE,NPHASE),
     +           RF(NNODE,NPHASE,4),SCAL(NNODE,NPHASE,NSCAL)
C
      DIMENSION
XP(NNODE),YP(NNODE),ZP(NNODE),VOL(NCELL),AREA(NFACE,3),
     +
VPOR(NCELL),ARPOR(NFACE,3),WFACT(NFACE),IPT(*),
     +
IBLK(5,NBLOCK),IPVERT(NCELL,8),IPNODN(NCELL,6),
     +
IPFACN(NCELL,6),IPNODF(NFACE,4),IPNODB(NBDRY,4),
     +           IPFACB(NBDRY),IWORK(*),WORK(*),CWORK(*)
C
C+++++++++++++++++ USER AREA 3
++++++++++++++++++++++++++++++++++++++++
C---- AREA FOR USERS TO DIMENSION THEIR ARRAYS
C
C---- AREA FOR USERS TO DEFINE DATA STATEMENTS
C
C+++++++++++++++++ END OF USER AREA 3
+++++++++++++++++++++++++++++++++
C
C---- STATEMENT FUNCTION FOR ADDRESSING
      IP(I,J,K) = IPT((K-1)*ILEN*JLEN+ (J-1)*ILEN+I)
C
C----VERSION NUMBER OF USER ROUTINE AND PRECISION FLAG
C
      IVERS = 5
      ICHKPR = 2
C
C+++++++++++++++++ USER AREA 4
++++++++++++++++++++++++++++++++++++++++
C---- TO USE THIS USER ROUTINE FIRST SET IUSED=1
C     AND SET IUBCSF FLAG:
C     BOUNDARY CONDITIONS NOT CHANGING
IUBCSF=0
```

```
C     BOUNDARY CONDITIONS CHANGING WITH ITERATION
IUBCSF=1
C     BOUNDARY CONDITIONS CHANGING WITH TIME
IUBCSF=2
C     BOUNDARY CONDITIONS CHANGING WITH TIME AND ITERATION
IUBCSF=3
C
      IUBCSF = 3
      IUSED = 1
C
C+++++++++++++++++ END OF USER AREA 4
++++++++++++++++++++++++++++++++
C
      IF (IUSED.EQ.0) RETURN
C
C---- FRONTEND CHECKING OF USER ROUTINE
      IF (IUCALL.EQ.0) RETURN
C
C+++++++++++++++++ USER AREA 5
++++++++++++++++++++++++++++++++++++++
C
C---- AREA FOR SETTING VALUES AT INLETS, PRESSURE BOUNDARIES
C     AND OUTLETS. (NOTE THAT THE MASS FLOW AT OUTLETS IS
C     SPECIFIED IN USER AREA 7)
C
C     IF USING A REYNOLDS STRESS OR FLUX MODEL, NOTE THAT AT
INLETS
C     IT IS IMPORTANT THAT THE USER SETS ALL COMPONENTS OF THE
C     REYNOLDS STRESS AND FLUX AND THE TURBULENT KINETIC
ENERGY
C     AS WELL AS THE ENERGY DISSIPATION RATE.
C
C     SET THE VALUES IN VARBCS(NVAR,NPHASE,ILEN,JLEN,KLEN)
C
C---- EXAMPLE: SETTING A LINEAR T PROFILE ON INLET PATCH
'ENTRANCE'
C               LEAVE OTHER VARIABLES AS SET IN COMMAND
LANGUAGE
C
C--  INTERROGATE GETVAR FOR VARIABLE NUMBERS.
C
C     CALL GETVAR('USRBCS','T     ',IT)
C
C  SET IPHS = 1 FOR SINGLE PHASE FLOW.
C
C     IPHS = 1
C
C  USE IPREC TO FIND ADDRESSES
C
C     CALL
IPREC('ENTRANCE','PATCH','CENTRES',IPT,ILEN,JLEN,KLEN,
C    +            CWORK,IWORK)
C
C     XMAX=2.0
C     XMIN=1.0
C     TMAX=300.0
C     TMIN=250.0
```

```
C  LOOP OVER PATCH
C     DO 103 K = 1, KLEN
C        DO 102 J = 1, JLEN
C           DO 101 I = 1, ILEN
C  USE STATEMENT FUNCTION IP TO GET ADDRESSES
C           INODE = IP(I,J,K)
C  SET VARBCS
C           F=(XP(INODE)-XMIN)/(XMAX-XMIN)
C           VARBCS(IT,IPHS,INODE) = (1.0-F)*TMAX + F*TMIN
C 101       CONTINUE
C 102    CONTINUE
C 103  CONTINUE
C
C----END OF EXAMPLE
C
C+++++++++++++++++ END OF USER AREA 5
+++++++++++++++++++++++++++++++++
C
C+++++++++++++++++ USER AREA 6
++++++++++++++++++++++++++++++++++++++++
C
C---- AREA FOR SETTING VALUES AT WALLS
C
C     USE A(2+NSCAL,NPHASE,ILEN,JLEN,KLEN)
C     WHERE NSCAL = NO. OF SCALARS, AND NPHASE = NO. OF
PHASES.
C
C     THE CONVENTION FOR VARIABLE NUMBERS IS DIFFERENT IN THIS
ROUTINE
C     FROM THAT IN THE REST OF THE PROGRAM. IT IS:
C
C     IU = 1, IV = 2 , IW = 3, IT = 4, IS = 5
C
C---- EXAMPLE: SETTING FREE SLIP BOUNDARY CONDITIONS AT ALL
WALLS
C              AND SETTING T=300.0 AND SCALAR1 AND SCALAR2
=0.0
C              ON WALL1. SET T=400.0 ON CONDUCTING SOLID
BOUNDARY WALL2
C
C-- SET POINTERS
C
      IU = 1
      IV = 2
C     IW = 3
C     IT = 4
C     IS = 5
      CALL GETVAR('USRBCS','VFRAC     ',IVFRAC)
C
C-- SET IPHS = 1 FOR SINGLE PHASE FLOW.
C
C     IPHS = 1
C
C  USE IPALL TO FIND 1D ADDRESSES OF A GROUP OF PATCH CENTRES
C
C     CALL
IPALL('*','WALL','PATCH','CENTRES',IPT,NPT,CWORK,IWORK)
```

```
C
C  LOOP OVER GROUP OF PATCHES
C     DO 200 I=1,NPT
C  USE ARRAY IPT TO GET ADDRESS
C       INODE=IPT(I)
C       A(IU,IPHS,INODE) = 0.0
C       B(IU,IPHS,INODE) = 1.0
C       C(IU,IPHS,INODE) = 0.0
C
C       A(IV,IPHS,INODE) = 0.0
C       B(IV,IPHS,INODE) = 1.0
C       C(IV,IPHS,INODE) = 0.0
C
C       A(IW,IPHS,INODE) = 0.0
C       B(IW,IPHS,INODE) = 1.0
C       C(IW,IPHS,INODE) = 0.0
C 200   CONTINUE
C
C  USE IPREC TO FIND ADDRESSES OF SINGLE PATCH
C
C     CALL IPREC('WALL1','PATCH','CENTRES',IPT,ILEN,JLEN,KLEN,
C    +           CWORK,IWORK)
C  LOOP OVER PATCH
C         DO 203 K = 1, KLEN
C            DO 202 J = 1, JLEN
C               DO 201 I = 1, ILEN
C  USE STATEMENT FUNCTION IP TO GET ADDRESSES
C               INODE = IP(I,J,K)
C
C               A(IT,IPHS,INODE) = 1.0
C               B(IT,IPHS,INODE) = 0.0
C               C(IT,IPHS,INODE) = 300.0
C
C               A(IS,IPHS,INODE) = 1.0
C               B(IS,IPHS,INODE) = 0.0
C               C(IS,IPHS,INODE) = 0.0
C
C               A(IS+1,IPHS,INODE) = 1.0
C               B(IS+1,IPHS,INODE) = 0.0
C               C(IS+1,IPHS,INODE) = 0.0
C
C 201           CONTINUE
C 202        CONTINUE
C 203    CONTINUE
C
C  USE IPALL TO FIND 1D ADDRESSES OF A GROUP OF PATCH CENTRES
C
C     CALL
IPALL('WALL2','*','PATCH','CENTRES',IPT,NPT,CWORK,IWORK)
C
C  LOOP OVER GROUP OF PATCHES
C     DO 300 I=1,NPT
C  USE ARRAY IPT TO GET ADDRESS
C       INODE=IPT(I)
C       ACND(INODE) = 1.0
C       BCND(INODE) = 0.0
C       CCND(INODE) = 400.0
```

```
C 300   CONTINUE
C
C----END OF EXAMPLE
C
C
      RISEVL = 0.00815D0
      GASFRC = 0.0468D0

      CALL IPREC('GAS-
OUTLET','PATCH','CENTRES',IPT,ILEN,JLEN,KLEN,
     +           CWORK,IWORK)
C  LOOP OVER PATCH
          DO 303 K = 1, KLEN
             DO 302 J = 1, JLEN
                DO 301 I = 1, ILEN
C
C  USE STATEMENT FUNCTION IP TO GET ADDRESSES
                INODE = IP(I,J,K)
                IBDRY = INODE-NCELL
                INODE1 = IPNODB(IBDRY,1)

                 A(IU,1,INODE) = 0.0
                 B(IU,1,INODE) = 1.0
                 C(IU,1,INODE) = 0.0

                 A(IV,1,INODE) = 0.0
                 B(IV,1,INODE) = 1.0
                 C(IV,1,INODE) = 0.0

                 A(IU,2,INODE) = 0.0
                 B(IU,2,INODE) = 1.0
                 C(IU,2,INODE) = 0.0

                 A(IV,2,INODE) = 1.0
                 B(IV,2,INODE) = 0.0
                 C(IV,2,INODE) = RISEVL/GASFRC
C
C  SET VARBCS
                VARBCS(IVFRAC,1,INODE) = VFRAC(INODE1,1)
                TERM = 1.0 - VARBCS(IVFRAC,1,INODE)
              VARBCS(IVFRAC,2,INODE)=TERM

  301            CONTINUE
  302          CONTINUE
  303      CONTINUE
C+++++++++++++++++ END OF USER AREA 6
++++++++++++++++++++++++++++++++++
C
C
C+++++++++++++++++ USER AREA 7
++++++++++++++++++++++++++++++++++++++++
C
C----- DEFINE FLOW AT OUTLETS (MASS FLOW BOUNDARIES)
C      (TO TEMPERATURES AND SCALARS AT MASS FLOW BOUNDARIES
USE
C       USER AREA 5)
C
```

```
C     SET PARAMETER IFLOUT:
C     IFLOUT = 1  ==> MASS FLOW SPECIFIED AT LABELLED OUTLETS.
C     IFLOUT = 2  ==> FRACTIONAL MASS FLOW SPECIFIED AT
LABELLED OUTLETS
C     IFLOUT = 2
C
C     SET OUTLET FLOW RATES:
C     FLOUT(LABEL) = MASS FLOW OUT OF OUTLETS LABELLED LABEL
(IFLOUT=1).
C     FLOUT(LABEL) = FRACTIONAL MASS FLOW OUT OF OUTLETS
LABELLED LABEL
C                    (IFLOUT=2).
C     FOR MULTIPHASE FLOWS IT IS NECESSARY TO SET
C     EITHER
C                    FLOUT(LABEL) = TOTAL MASS FLOW
C                    IFLOUT = 1
C                    IMFBMP = 0
C     OR
C                    FLOUT(LABEL + (IPHASE-1)*NLABEL) FOR EACH
PHASE
C                    IFLOUT = 1 OR 2
C                    IMFBMP = 1
C
C---- EXAMPLE: EQUIDISTRIBUTION OF FRACTIONAL MASS FLOW
AMONGST OUTLETS
C
C     IFLOUT=2
C     FRAC = 1.0 / MAX( 1.0, FLOAT(NLABEL) )
C     DO 300 ILABEL = 1, NLABEL
C        FLOUT(ILABEL) = FRAC
C300  CONTINUE
C
C----END OF EXAMPLE
C
C+++++++++++++++++ END OF USER AREA 7
+++++++++++++++++++++++++++++++++
C
      RETURN
C
      END
```

## Appendix D. Fortran user routine USRIPT (drag correlation)

This appendix gives an example of the Fortran code used to compute the interphase transfer term (based on the drag force). The actual code used to calculate the interphase transfer is shown in bold.

```
SUBROUTINE
USRIPT(IEQN,CNAME,CALIAS,PHI,CAB,U,V,W,P,VFRAC,DEN,VIS,
     +
TE,ED,RS,T,H,RF,SCAL,XP,YP,ZP,VOL,AREA,VPOR,
     +
ARPOR,WFACT,IPT,IBLK,IPVERT,IPNODN,IPFACN,
     +                    IPNODF,IPNODB,IPFACB,WORK,IWORK,CWORK)
C
C***************************************************************
**********
C
C   THIS SUBROUTINE COMPUTES INTERPHASE EXCHANGE COEFFICIENTS.
C
C   >>> IMPORTANT
<<<
C   >>>
<<<
C   >>> USERS MAY ONLY ADD OR ALTER PARTS OF THE SUBROUTINE
WITHIN  <<<
C   >>> THE DESIGNATED USER AREAS
<<<
C
C***************************************************************
**********
C
C   THIS SUBROUTINE IS CALLED BY THE FOLLOWING SUBROUTINE
C      CUSR  INPEXC
C
C***************************************************************
**********
C   CREATED
C     01/05/91 ADB  BASED ON ROUTINE IPMOMT FROM MPHASE 1.3.
C   MODIFIED
C     05/08/91 IRH  NEW STRUCTURE
C     05/09/91 IRH  CHANGE ICALL TO IUCALL
C     27/11/91 ADB  REMOVE COMMENTING OUT OF EXAMPLES
C     28/01/92 PHA  UPDATE CALLED BY COMMENT, ADD RF ARGUMENT,
C                   CHANGE LAST DIMENSION OF RS TO 6 AND IVERS
TO 2
C     03/06/92 PHA  ADD PRECISION FLAG AND CHANGE IVERS TO 3
C     01/07/92 NSW  VAX CORRECTIONS
C     23/11/93 CSH  EXPLICITLY DIMENSION IPVERT ETC.
C     03/02/94 PHA  CHANGE FLOW3D TO CFDS-FLOW3D
C     23/03/94 FHW  EXAMPLES COMMENTED OUT
C     09/08/94 NSW  CORRECT SPELLING
C                   MOVE 'IF(IUSED.EQ.0) RETURN' OUT OF USER
AREA
```

```
C                    INCLUDE COMMENT ON SLIP VELOCITY
C     19/12/94 NSW  CHANGE FOR CFX-F3D
C
C*************************************************************
**********
C
C   SUBROUTINE ARGUMENTS
C
C     IEQN   - EQUATION NUMBER
C     CNAME  - EQUATION NAME
C     CALIAS - ALIAS OF EQUATION NAME
C     PHI    - VARIABLE CNAME
C  *  CAB    - INTERPHASE EXCHANGE COEFFICIENT
C     U      - U COMPONENT OF VELOCITY
C     V      - V COMPONENT OF VELOCITY
C     W      - W COMPONENT OF VELOCITY
C     P      - PRESSURE
C     VFRAC  - VOLUME FRACTION
C     DEN    - DENSITY OF FLUID
C     VIS    - VISCOSITY OF FLUID
C     TE     - TURBULENT KINETIC ENERGY
C     ED     - EPSILON
C     RS     - REYNOLD STRESSES
C     T      - TEMPERATURE
C     H      - ENTHALPY
C     RF     - REYNOLD FLUXES
C     SCAL   - SCALARS (THE FIRST 'NCONC' OF THESE ARE MASS
FRACTIONS)
C     XP     - X COORDINATES OF CELL CENTRES
C     YP     - Y COORDINATES OF CELL CENTRES
C     ZP     - Z COORDINATES OF CELL CENTRES
C     VOL    - VOLUME OF CELLS
C     AREA   - AREA OF CELLS
C     VPOR   - POROUS VOLUME
C     ARPOR  - POROUS AREA
C     WFACT  - WEIGHT FACTORS
C
C     IPT    - 1D POINTER ARRAY
C     IBLK   - BLOCK SIZE INFORMATION
C     IPVERT - POINTER FROM CELL CENTERS TO 8 NEIGHBOURING
VERTICES
C     IPNODN - POINTER FROM CELL CENTERS TO 6 NEIGHBOURING
CELLS
C     IPFACN - POINTER FROM CELL CENTERS TO 6 NEIGHBOURING
FACES
C     IPNODF - POINTER FROM CELL FACES TO 2 NEIGHBOURING CELL
CENTERS
C     IPNODB - POINTER FROM BOUNDARY CENTERS TO CELL CENTERS
C     IPFACB - POINTER FROM BOUNDARY CENTERS TO BOUNDARY
FACESS
C
C     WORK   - REAL WORKSPACE ARRAY
C     IWORK  - INTEGER WORKSPACE ARRAY
C     CWORK  - CHARACTER WORKSPACE ARRAY
C
C   SUBROUTINE ARGUMENTS PRECEDED WITH A '*' ARE ARGUMENTS
THAT MUST
```

```
C   BE SET  BY THE USER IN THIS ROUTINE.
C
C   NOTE THAT OTHER DATA MAY BE OBTAINED FROM CFX-F3D USING
THE
C   ROUTINE GETADD, FOR FURTHER DETAILS SEE THE VERSION 4
C   USER MANUAL.
C
C*************************************************************
**********
C
      DOUBLE PRECISION PHI
      DOUBLE PRECISION CAB
      DOUBLE PRECISION U
      DOUBLE PRECISION V
      DOUBLE PRECISION W
      DOUBLE PRECISION P
      DOUBLE PRECISION VFRAC
      DOUBLE PRECISION DEN
      DOUBLE PRECISION VIS
      DOUBLE PRECISION TE
      DOUBLE PRECISION ED
      DOUBLE PRECISION RS
      DOUBLE PRECISION T
      DOUBLE PRECISION H
      DOUBLE PRECISION RF
      DOUBLE PRECISION SCAL
      DOUBLE PRECISION XP
      DOUBLE PRECISION YP
      DOUBLE PRECISION ZP
      DOUBLE PRECISION VOL
      DOUBLE PRECISION AREA
      DOUBLE PRECISION VPOR
      DOUBLE PRECISION ARPOR
      DOUBLE PRECISION WFACT
      DOUBLE PRECISION WORK
      LOGICAL
LDEN,LVIS,LTURB,LTEMP,LBUOY,LSCAL,LCOMP,LRECT,LCYN,LAXIS,
     +        LPOROS,LTRANS
C
      CHARACTER*(*) CWORK
      CHARACTER CNAME*6,CALIAS*24
C
C+++++++++++++++++ USER AREA 1
++++++++++++++++++++++++++++++++++++++++
C---- AREA FOR USERS EXPLICITLY DECLARED VARIABLES
C
C+++++++++++++++++ END OF USER AREA 1
++++++++++++++++++++++++++++++++
C
      COMMON /ALL/NBLOCK,NCELL,NBDRY,NNODE,NFACE,NVERT,NDIM,
     +
/ADDIMS/NPHASE,NSCAL,NVAR,NPROP,NDVAR,NDPROP,NDXNN,NDGEOM,
     +
NDCOEF,NILIST,NRLIST,NTOPOL,/ADDMPH/NAB,NCOMPT,NCOMB,
     +
NSCUSR,/CHKUSR/IVERS,IUCALL,IUSED,/DEVICE/NREAD,NWRITE,
```

```
     +
NRDISK,NWDISK,/IDUM/ILEN,JLEN,/LOGIC/LDEN,LVIS,LTURB,LTEMP,
     +       LBUOY,LSCAL,LCOMP,LRECT,LCYN,LAXIS,LPOROS,LTRANS,
     +
/MLTGRD/MLEVEL,NLEVEL,ILEVEL,/SGLDBL/IFLGPR,ICHKPR
C
C+++++++++++++++++ USER AREA 2
++++++++++++++++++++++++++++++++++++++++
C---- AREA FOR USERS TO DECLARE THEIR OWN COMMON BLOCKS
C     THESE SHOULD START WITH THE CHARACTERS 'UC' TO ENSURE
C     NO CONFLICT WITH NON-USER COMMON BLOCKS
C
C+++++++++++++++++ END OF USER AREA 2
++++++++++++++++++++++++++++++++++
C
      DIMENSION
PHI(NNODE),CAB(NCELL,*),U(NNODE,NPHASE),V(NNODE,NPHASE),
     +
W(NNODE,NPHASE),P(NNODE,NPHASE),VFRAC(NNODE,NPHASE),
     +
DEN(NNODE,NPHASE),VIS(NNODE,NPHASE),TE(NNODE,NPHASE),
     +
ED(NNODE,NPHASE),RS(NNODE,NPHASE,6),T(NNODE,NPHASE),
     +           H(NNODE,NPHASE),RF(NNODE,NPHASE,4),
     +           SCAL(NNODE,NPHASE,NSCAL)
      DIMENSION
XP(NNODE),YP(NNODE),ZP(NNODE),VOL(NCELL),AREA(NFACE,3),
     +
VPOR(NCELL),ARPOR(NFACE,3),WFACT(NFACE),IPT(*),
     +
IBLK(5,NBLOCK),IPVERT(NCELL,8),IPNODN(NCELL,6),
     +
IPFACN(NCELL,6),IPNODF(NFACE,4),IPNODB(NBDRY,4),
     +           IPFACB(NBDRY),IWORK(*),WORK(*),CWORK(*)
C
C+++++++++++++++++ USER AREA 3
++++++++++++++++++++++++++++++++++++++++
C---- AREA FOR USERS TO DIMENSION THEIR ARRAYS
C
C---- AREA FOR USERS TO DEFINE DATA STATEMENTS
C
C+++++++++++++++++ END OF USER AREA 3
++++++++++++++++++++++++++++++++++
C
C---- STATEMENT FUNCTION FOR ADDRESSING
      IP(I,J,K) = IPT((K-1)*ILEN*JLEN+ (J-1)*ILEN+I)
C
C----VERSION NUMBER OF USER ROUTINE AND PRECISION FLAG
C
      IVERS = 3
      ICHKPR = 2
C
C+++++++++++++++++ USER AREA 4
++++++++++++++++++++++++++++++++++++++++
C---- TO USE THIS USER ROUTINE FIRST SET IUSED=1
C
      IUSED = 1
```

```
C
C+++++++++++++++++ END OF USER AREA 4
++++++++++++++++++++++++++++++++++
C
      IF (IUSED.EQ.0) RETURN
C
C---- FRONTEND CHECKING OF USER ROUTINE
      IF (IUCALL.EQ.0) RETURN
C
C+++++++++++++++++ USER AREA 5
++++++++++++++++++++++++++++++++++++++++
C
C   N.B: CAB(NCELL,NAB) IS THE INTERPHASE EXCHANGE COEFFICIENT
SUCH
C   THAT INTERPHASE EXCHANGE BETWEEN PHASE A AND B IS
CALCULATED AS:
C
C         F(AB) = CAB(INODE,AB)*(PHI(A)-PHI(B))
C
C   WHERE F(AB) IS INTERPHASE FRICTION IN MOMENTUM EQUATION
C         F(AB) IS INTERPHASE HEAT TRANSFER IN ENERGY EQUATION
ETC.
C
C   SINCE C(AB) = C(BA) AND C(AA) = 0, STORAGE SPACE FOR
C(BA), C(AA)
C   IS NOT PROVIDED. HENCE THE DIMENSION NAB IS GIVEN BY:
C
C         NAB =  NPHASE*(NPHASE-1) / 2.
C
C   THE ORDERING OF NAB IS AS FOLLOWS:
C
C   2-PHASE FLOW: NSHEAR    1
C                   (AB)   12
C   3-PHASE FLOW: NSHEAR    1   2   3
C                   (AB)   12  13  23
C   4-PHASE FLOW: NSHEAR    1   2   3   4   5   6
C                   (AB)   12  13  14  23  24  34      ETC.
C
C
C*****************************************************************
**********
C
C----SET EXAMPLE HERE
C
C      EXAMPLE 1   ==>  PARTICLE MODEL
C      EXAMPLE 2   ==>  MIXTURE MODEL
C      EXAMPLE 3   ==>  STRATIFIED MODEL
C
C----NOTE THAT IN ALL THE EXAMPLES, A SIMPLE FORMULA FOR SLIP
IS USED
C    WHICH IS STRICTLY ONLY APPROPRIATE FOR UNIDIRECTIONAL
FLOW
C    SEE MANUAL FOR DETAILS
C
C----USE IPALL TO FIND 1D ADDRESSES OF ALL CELL CENTRES
C
```

```
      CALL IPALL
('*','*','BLOCK','CENTRES',IPT,NPT,CWORK,IWORK)
C
C----EXAMPLE 1: PARTICLE MODEL.
C
C----INTER-PHASE MOMENTUM TRANSFER:
C----CAB    = 0.75*CD*VF(B)*RHO(A)*SLIP*VOL/DP
C----CD     = DRAG COEFF.  ; DP = PARTICLE DIAMETER.
C----(A) CONTINUOUS PHASE ; (B) DISPERSED PHASE.
C
C----INTER-PHASE HEAT TRANSFER:
C----CAB    = HINP*AINP*(T(A)-T(B))
C----HINP   = INTERPHASE HEAT TRANSFER COEFF =  6*CH /DP
C----AINP   = INTERFACIAL AREA = 6*VF / DP
C----(A) CONTINUOUS PHASE ; (B) DISPERSED PHASE.
C
C     IA  = 1
C     IB  = 2
C     IAB = 1
C     CD = 0.44
C     DP = 1.0E-5
C     CF = 0.75*CD / DP
C
C     CH = 1.0E-3
C     HINP = 6*CH / DP
C
C     IF (CNAME(1:2).EQ.'U ') THEN
C
C----LOOP OVER ALL INTERIOR CELLS
C        DO 110 I = 1,NPT
C----USE ARRAY IPT TO GET ADDRESS
C           INODE=IPT(I)
C           SLIP  = ABS( U(INODE,IA) - U(INODE,IB) )
C           CAB(INODE,IAB) = CF*
C    +
VFRAC(INODE,IB)*DEN(INODE,IA)*SLIP*VPOR(INODE)
C 110    CONTINUE
C
C     ELSE IF (CNAME(1:2).EQ.'V ') THEN
C
C        DO 120 I = 1,NPT
C           INODE=IPT(I)
C           SLIP  = ABS( V(INODE,IA) - V(INODE,IB) )
C           CAB(INODE,IAB) = CF*
C    +          VFRAC(INODE,IB)*DEN(INODE,IA)*SLIP*VPOR(INODE)
C 120    CONTINUE
C
C     ELSE IF (CNAME(1:2).EQ.'W ') THEN
C
C        DO 130 I = 1,NPT
C           INODE=IPT(I)
C           SLIP  = ABS( W(INODE,IA) - W(INODE,IB) )
C           CAB(INODE,IAB) = CF*
C    +          VFRAC(INODE,IB)*DEN(INODE,IA)*SLIP*VPOR(INODE)
C 130    CONTINUE
C
C     ELSE IF (CNAME(1:2).EQ.'H ') THEN
```

```
C
C        DO 140 I = 1,NPT
C           INODE=IPT(I)
C           CAB(INODE,IAB) = HINP*VFRAC(INODE,IB)*VPOR(INODE)
C 140    CONTINUE
C
C     ENDIF
C
C----END OF EXAMPLE 1
C
C----EXAMPLE 2: MIXTURE MODEL.
C
C----CAB = CD*RHOM*AI*SLIP
C----CD  = DRAG COEFF. ;       DP = INTERFACE LENGTH SCALE
C----RHOM  = MIXTURE DENSITY  = VF(1)*DEN(1) + VF(2)*DEN(2)
C----AI    = INTERFACIAL AREA = VF(1)*VF(2)*VOL/DP
C
C----SLIP  = RELATIVE VELOCITY ;
C
C    IA  = 1
C    IB  = 2
C    IAB = 1
C    CD = 0.44
C    DP = 1.0E-2
C
C    DPINV = 1.0 / DP
C
C    IF (CNAME(1:2).EQ.'U ') THEN
C
C       DO 210 I = 1,NPT
C          INODE=IPT(I)
C          SLIP  = ABS( U(INODE,IA) - U(INODE,IB) )
C          RHOM = VFRAC(INODE,IA)*DEN(INODE,IA)
C    +          + VFRAC(INODE,IB)*DEN(INODE,IB)
C          AI    = VFRAC(INODE,IA)*VFRAC(INODE,IB)
C    +           *VPOR(INODE)*DPINV
C          CAB(INODE,IAB) = CD*RHOM*AI*SLIP
C 210   CONTINUE
C
C     ELSE IF (CNAME(1:2).EQ.'V ') THEN
C
C        DO 220 I = 1,NPT
C           INODE=IPT(I)
C           SLIP  = ABS( V(INODE,IA) - V(INODE,IB) )
C           RHOM = VFRAC(INODE,IA)*DEN(INODE,IA)
C    +          + VFRAC(INODE,IB)*DEN(INODE,IB)
C           AI    = VFRAC(INODE,IA)*VFRAC(INODE,IB)
C    +           *VPOR(INODE)*DPINV
C           CAB(INODE,IAB) = CD*RHOM*AI*SLIP
C 220    CONTINUE
C
C     ELSE IF (CNAME(1:2).EQ.'W ') THEN
C
C        DO 230 I = 1,NPT
C           INODE=IPT(I)
C           SLIP  = ABS( W(INODE,IA) - W(INODE,IB) )
C           RHOM = VFRAC(INODE,IA)*DEN(INODE,IA)
```

```
C     +            + VFRAC(INODE,IB)*DEN(INODE,IB)
C             AI    = VFRAC(INODE,IA)*VFRAC(INODE,IB)
C     +              *VPOR(INODE)*DPINV
C             CAB(INODE,IAB) = CD*RHOM*AI*SLIP
C 230     CONTINUE
C
C           ENDIF
C
C----END OF EXAMPLE 2
C
C----EXAMPLE 3: STRATIFIED MODEL (LAMINAR STRATIFIED FLOWS).
C
C----CAB = 0.5*CF*RHOM*AI*SLIP
C----CF     = DRAG COEFF.       = C/RE
C----RE     = REYNOLDS NO.      = RHOM*SLIP*H/VISM
C----RHOM   = MIXTURE DENSITY   = VF(1)*DEN(1) + VF(2)*DEN(2)
C
C----HENCE:
C
C----CAB = CD*VISM*AI
C----CD  = 0.5*C/HT ;  HT = LENGTH SCALE;  DP = INTERFACE
LENGTH SCALE
C----AI     = INTERFACIAL AREA = VF(1)*VF(2)*VOL/DP
C----VISM   = MIXTURE VISCOSITY= VF(1)*VIS(1) + VF(2)*VIS(2)
C
C     IA  = 1
C     IB  = 2
C     IAB = 1
C     C  = 24
C     HT  = 1.0
C     DP = 1.0E-2
C
C     DPINV = 1.0 / DP
C     CD    = 0.5*C / HT
C
C     IF (CNAME(1:2).EQ.'U ' .OR. CNAME(1:2).EQ.'V '
C     +                       .OR. CNAME(1:3).EQ.'W ') THEN
C
C        DO 310 I = 1,NPT
C           INODE=IPT(I)
C           VISM = VFRAC(INODE,IA)*VIS(INODE,IA)
C     +          + VFRAC(INODE,IB)*VIS(INODE,IB)
C           AI    = VFRAC(INODE,IA)*VFRAC(INODE,IB)
C     +            *VPOR(INODE)*DPINV
C           CAB(INODE,IAB) = CD*VISM*AI
C 310    CONTINUE
C
C     ENDIF
C
C----END OF EXAMPLE 3
C
      IA  = 1
      IB  = 2
      IAB = 1
      SL = 1.0E-12
C     CD = 0.44
C     Particle diameter
```

```
      DP = 0.003
C     Container width
      WD = 0.035
C     Container thickness
      TK = 0.01
C     CF = 0.75*CD / DP
C
C     CH = 1.0E-3
C     HINP = 6*CH / DP
C
      IF (CNAME(1:2).EQ.'U ') THEN
C
C----LOOP OVER ALL INTERIOR CELLS
        DO 110 I = 1,NPT
C----USE ARRAY IPT TO GET ADDRESS
          INODE = IPT(I)
         USLIP = ABS(U(INODE,IA)-U(INODE,IB))
          VSLIP = ABS(V(INODE,IA)-V(INODE,IB))
          WSLIP = ABS(W(INODE,IA)-W(INODE,IB))
          SLIP = SQRT(USLIP**2+VSLIP**2+WSLIP**2)
          IF(SLIP.EQ.0)THEN
            SLIP = 1.0D-12
          ENDIF
          VFB=VFRAC(INODE,IB)
          IF(VFB.LT.0.0001)VFRAC(INODE,IB)=1.0E-20
          BRE = (DEN(INODE,IA)*SLIP*DP)/VIS(INODE,IA)
C      Standard drag curve
C           CD = (24.0/BRE)+(5.48/(BRE**0.573))+0.36
C      Standard drag curve (Clift, Grace and Zaki)
C       WA = ALOG10(BRE)
C       IF(BRE.LE.0.01)CD = (3.0/16.0)+(24.0/BRE)
C       IF(BRE.GT.0.01)THEN
C       IF(BRE.LE.20)CD = (24/BRE)*(1.0+0.1315*(BRE**(0.82-
0.05*WA)))
C          IF(BRE.GT.20)CD =
(24/BRE)*(1.0+0.1935*(BRE**0.6305))
C       ENDIF
C      Richardson and Zaki
C           IF(BRE.LE.0.2)AN = 4.65+((19.5*DP)/TK)
C           IF(BRE.GT.0.2)THEN
C            IF(BRE.LE.1)AN = (4.35+(17.5*DP)/TK)*(BRE**(-
0.03))
C            IF(BRE.GT.1)THEN
C             IF(BRE.LE.200)AN = (4.45+(18.0*DP)/TK)*(BRE**(-
0.1))
C             IF(BRE.GT.200)AN = 4.45*(BRE**(-0.1))
C            ENDIF
C           ENDIF
C           CD = (CD*(1.0-VFRAC(INODE,IB)))/(((1.0-
VFRAC(INODE,IB))**AN)).
C
C     ZUBER AND ISHII
          CD
=1.2*2./3.*DP*((9.81*DEN(INODE,IA)/0.07275)**(0.5))*
     +          ((1-VFB)**(-0.5))
          CF = 0.75*CD/DP
          CAB(INODE,IAB) = CF*
```

```
     +
VFRAC(INODE,IB)*DEN(INODE,IA)*SLIP*VPOR(INODE)
 110     CONTINUE
C
      ELSE IF (CNAME(1:2).EQ.'V ') THEN
C
        DO 120 I = 1,NPT
           INODE=IPT(I)
         USLIP = ABS(U(INODE,IA)-U(INODE,IB))
           VSLIP = ABS(V(INODE,IA)-V(INODE,IB))
           WSLIP = ABS(W(INODE,IA)-W(INODE,IB))
           SLIP = SQRT(USLIP**2+VSLIP**2+WSLIP**2)
           IF(SLIP.EQ.0)THEN
             SLIP = 1.0E-12
           ENDIF
           VFB=VFRAC(INODE,IB)
           IF(VFB.LT.0.0001)VFRAC(INODE,IB)=1.0E-20
             BRE = (DEN(INODE,IA)*SLIP*DP)/VIS(INODE,IA)
C        Standard drag curve
C             CD = (24.0/BRE)+(5.48/(BRE**0.573))+0.36
C        Standard drag curve (Clift, Grace and Weber)
C         WA = ALOG10(BRE)
C         IF(BRE.LE.0.01)CD = (3.0/16.0)+(24.0/BRE)
C         IF(BRE.GT.0.01)THEN
C        IF(BRE.LE.20)CD = (24.0/BRE)*(1.0+0.1315*(BRE**(0.82-
0.05*WA)))
C          IF(BRE.GT.20)CD =
(24.0/BRE)*(1.0+0.1935*(BRE**0.6305))
C         ENDIF
C        Richardson and Zaki
C          IF(BRE.LE.0.2)AN = 4.65+((19.5*DP)/TK)
C           IF(BRE.GT.0.2)THEN
C             IF(BRE.LE.1)AN = (4.35+(17.5*DP)/TK)*(BRE**(-
0.03))
C             IF(BRE.GT.1)THEN
C              IF(BRE.LT.200)AN = (4.45+(18.0*DP)/TK)*(BRE**(-
0.1))
C              IF(BRE.GT.200)AN = 4.45*(BRE**(-0.1))
C             ENDIF
C           ENDIF
C              CD = (CD*(1.0-VFRAC(INODE,IB)))/((1.0-
VFRAC(INODE,IB))**AN))
C
C     ZUBER AND ISHII

CD=1.2*2./3.*DP*((9.81*DEN(INODE,IA)/0.07275)**(0.5))*
     +          ((1-VFB)**(-0.5))
           CF = 0.75*CD/DP
           CAB(INODE,IAB) = CF*
     +          VFRAC(INODE,IB)*DEN(INODE,IA)*SLIP*VPOR(INODE)
 120     CONTINUE
C
      ELSE IF (CNAME(1:2).EQ.'W ') THEN
C
        DO 130 I = 1,NPT
           INODE=IPT(I)
         USLIP = ABS(U(INODE,IA)-U(INODE,IB))
```

```
            VSLIP = ABS(V(INODE,IA)-V(INODE,IB))
            WSLIP = ABS(W(INODE,IA)-W(INODE,IB))
            SLIP = SQRT(USLIP**2+VSLIP**2+WSLIP**2)
            IF(SLIP.EQ.0)THEN
              SLIP = 1.0E-12
            ENDIF
            VFB=VFRAC(INODE,IB)
            IF(VFB.LT.0.0001)VFRAC(INODE,IB)=1.0E-20
              BRE = (DEN(INODE,IA)*SLIP*DP)/VIS(INODE,IA)
C       Standard drag curve
C            CD = (24.0/BRE)+(5.48/(BRE**0.573))+0.36
C       Standard drag curve (Clift, Grace and Weber)
C        WA = ALOG10(BRE)
C        IF(BRE.LE.0.01)CD = (3.0/16.0)+(24/BRE)
C        IF(BRE.GT.0.01)THEN
C       IF(BRE.LE.20)CD = (24.0/BRE)*(1.0+0.1315*(BRE**(0.82-
0.05*WA)))
C         IF(BRE.GT.20)CD =
(24.0/BRE)*(1.0+0.1935*(BRE**0.6305))
C        ENDIF
C       Richardson and Zaki
C         IF(BRE.LE.0.2)AN = 4.65+((19.5*DP)/TK)
C         IF(BRE.GT.0.2)THEN
C          IF(BRE.LE.1)AN = (4.35+(17.5*DP)/TK)*(BRE**(-0.03))
C          IF(BRE.GT.1)THEN
C           IF(BRE.LE.200)AN = (4.45+(18.0*DP)/TK)*(BRE**(-
0.1))
C           IF(BRE.GT.200)AN = 4.45*(BRE**(-0.1))
C          ENDIF
C         ENDIF
C            CD = (CD*(1.0-VFRAC(INODE,IB)))/((1.0-
VFRAC(INODE,IB))**AN)
C
C     ZUBER AND ISHII

CD=1.2*2./3.*DP*((9.81*DEN(INODE,IA)/0.07275)**(0.5))*
     +           ((1-VFB)**(-0.5))
            CF = 0.75*CD/DP
            CAB(INODE,IAB) = CF*
     +           VFRAC(INODE,IB)*DEN(INODE,IA)*SLIP*VPOR(INODE)
 130     CONTINUE
        ENDIF
C
C+++++++++++++++++ END OF USER AREA 5
++++++++++++++++++++++++++++++++++
C
      RETURN
C
      END
```

## Appendix E. Fortran user routine USRTRN (dynamic results)

This appendix gives an example of the Fortran code used to get the local liquid velocity and local gas holdup values at different locations in the column. The actual code used to extract these results is shown in bold.

```
SUBROUTINE
USRTRN(U,V,W,P,VFRAC,DEN,VIS,TE,ED,RS,T,H,RF,SCAL,XP,
     +
YP,ZP,VOL,AREA,VPOR,ARPOR,WFACT,CONV,IPT,IBLK,
     +
IPVERT,IPNODN,IPFACN,IPNODF,IPNODB,IPFACB,WORK,
     +                    IWORK,CWORK)
C
C*************************************************************
*********
C
C   USER SUBROUTINE TO ALLOW USERS TO MODIFY OR MONITOR THE
SOLUTION AT
C   THE END OF EACH TIME STEP
C   THIS SUBROUTINE IS CALLED BEFORE THE START OF THE RUN AS
WELL AS AT
C   THE END OF EACH TIME STEP
C
C   >>> IMPORTANT
<<<
C   >>>
<<<
C   >>> USERS MAY ONLY ADD OR ALTER PARTS OF THE SUBROUTINE
WITHIN  <<<
C   >>> THE DESIGNATED USER AREAS
<<<
C
C*************************************************************
*********
C
C   THIS SUBROUTINE IS CALLED BY THE FOLLOWING SUBROUTINES
C      CUSR  TRNMOD
C
C*************************************************************
**********
C   CREATED
C      27/04/90  ADB
C   MODIFIED
C      05/08/91  IRH  NEW STRUCTURE
C      01/10/91  DSC  REDUCE COMMENT LINE GOING OVER COLUMN
72.
C      29/11/91  PHA  UPDATE CALLED BY COMMENT, ADD RF
ARGUMENT,
C                     CHANGE LAST DIMENSION OF RS TO 6 AND
IVERS TO 2
C      05/06/92  PHA  ADD PRECISION FLAG AND CHANGE IVERS TO 3
C      03/07/92  DSC  CORRECT COMMON MLTGRD.
```

```
C      23/11/93  CSH  EXPLICITLY DIMENSION IPVERT ETC.
C      03/02/94  PHA  CHANGE FLOW3D TO CFDS-FLOW3D
C      22/08/94  NSW  MOVE 'IF(IUSED.EQ.0) RETURN' OUT OF USER
AREA
C      19/12/94  NSW  CHANGE FOR CFX-F3D
C
C*************************************************************
**********
C
C   SUBROUTINE ARGUMENTS
C
C     U       - U COMPONENT OF VELOCITY
C     V       - V COMPONENT OF VELOCITY
C     W       - W COMPONENT OF VELOCITY
C     P       - PRESSURE
C     VFRAC   - VOLUME FRACTION
C     DEN     - DENSITY OF FLUID
C     VIS     - VISCOSITY OF FLUID
C     TE      - TURBULENT KINETIC ENERGY
C     ED      - EPSILON
C     RS      - REYNOLD STRESSES
C     T       - TEMPERATURE
C     H       - ENTHALPY
C     RF      - REYNOLD FLUXES
C     SCAL    - SCALARS (THE FIRST 'NCONC' OF THESE ARE MASS
FRACTIONS)
C     XP      - X COORDINATES OF CELL CENTRES
C     YP      - Y COORDINATES OF CELL CENTRES
C     ZP      - Z COORDINATES OF CELL CENTRES
C     VOL     - VOLUME OF CELLS
C     AREA    - AREA OF CELLS
C     VPOR    - POROUS VOLUME
C     ARPOR   - POROUS AREA
C     WFACT   - WEIGHT FACTORS
C     CONV    - CONVECTION COEFFICIENTS
C
C     IPT     - 1D POINTER ARRAY
C     IBLK    - BLOCK SIZE INFORMATION
C     IPVERT  - POINTER FROM CELL CENTERS TO 8 NEIGHBOURING
VERTICES
C     IPNODN  - POINTER FROM CELL CENTERS TO 6 NEIGHBOURING
CELLS
C     IPFACN  - POINTER FROM CELL CENTERS TO 6 NEIGHBOURING
FACES
C     IPNODF  - POINTER FROM CELL FACES TO 2 NEIGHBOURING CELL
CENTERS
C     IPNODB  - POINTER FROM BOUNDARY CENTERS TO CELL CENTERS
C     IPFACB  - POINTER FROM BOUNDARY CENTERS TO BOUNDARY
FACESS
C
C     WORK    - REAL WORKSPACE ARRAY
C     IWORK   - INTEGER WORKSPACE ARRAY
C     CWORK   - CHARACTER WORKSPACE ARRAY
C
C   SUBROUTINE ARGUMENTS PRECEDED WITH A '*' ARE ARGUMENTS
THAT MUST
C   BE SET  BY THE USER IN THIS ROUTINE.
```

```
C
C   NOTE THAT OTHER DATA MAY BE OBTAINED FROM CFX-F3D USING
THE
C   ROUTINE GETADD, FOR FURTHER DETAILS SEE THE VERSION 4
C   USER MANUAL.
C
C*****************************************************************
*********
C
C
      DOUBLE PRECISION U
      DOUBLE PRECISION V
      DOUBLE PRECISION W
      DOUBLE PRECISION P
      DOUBLE PRECISION VFRAC
      DOUBLE PRECISION DEN
      DOUBLE PRECISION VIS
      DOUBLE PRECISION TE
      DOUBLE PRECISION ED
      DOUBLE PRECISION RS
      DOUBLE PRECISION T
      DOUBLE PRECISION H
      DOUBLE PRECISION RF
      DOUBLE PRECISION SCAL
      DOUBLE PRECISION XP
      DOUBLE PRECISION YP
      DOUBLE PRECISION ZP
      DOUBLE PRECISION VOL
      DOUBLE PRECISION AREA
      DOUBLE PRECISION VPOR
      DOUBLE PRECISION ARPOR
      DOUBLE PRECISION WFACT
      DOUBLE PRECISION CONV
      DOUBLE PRECISION WORK
      DOUBLE PRECISION SMALL
      DOUBLE PRECISION SORMAX
      DOUBLE PRECISION DTUSR
      DOUBLE PRECISION TIME
      DOUBLE PRECISION DT
      DOUBLE PRECISION DTINVF
      DOUBLE PRECISION TPARM
      LOGICAL
LDEN,LVIS,LTURB,LTEMP,LBUOY,LSCAL,LCOMP,LRECT,LCYN,LAXIS,
     +        LPOROS,LTRANS
C
      CHARACTER*(*) CWORK
C
C+++++++++++++++++ USER AREA 1
++++++++++++++++++++++++++++++++++++++++
C---- AREA FOR USERS EXPLICITLY DECLARED VARIABLES
C
C+++++++++++++++++ END OF USER AREA 1
++++++++++++++++++++++++++++++++
C
      COMMON /ALL/NBLOCK,NCELL,NBDRY,NNODE,NFACE,NVERT,NDIM,
     +
/ALLWRK/NRWS,NIWS,NCWS,IWRFRE,IWIFRE,IWCFRE,/ADDIMS/NPHASE,
```

```
     +
NSCAL,NVAR,NPROP,NDVAR,NDPROP,NDXNN,NDGEOM,NDCOEF,NILIST,
     +
NRLIST,NTOPOL,/CHKUSR/IVERS,IUCALL,IUSED,/CONC/NCONC,
     +
/DEVICE/NREAD,NWRITE,NRDISK,NWDISK,/IDUM/ILEN,JLEN,
     +
/LOGIC/LDEN,LVIS,LTURB,LTEMP,LBUOY,LSCAL,LCOMP,LRECT,LCYN,
     +       LAXIS,LPOROS,LTRANS,/MLTGRD/MLEVEL,NLEVEL,ILEVEL,
     +
/SGLDBL/IFLGPR,ICHKPR,/SPARM/SMALL,SORMAX,NITER,INDPRI,
     +
MAXIT,NODREF,NODMON,/TIMUSR/DTUSR,/TRANSI/NSTEP,KSTEP,MF,
     +  /     INCORE,/TRANSR/TIME,DT,DTINVF,TPARM
C
C+++++++++++++++++ USER AREA 2
++++++++++++++++++++++++++++++++++++++++
C---- AREA FOR USERS TO DECLARE THEIR OWN COMMON BLOCKS
C     THESE SHOULD START WITH THE CHARACTERS 'UC' TO ENSURE
C     NO CONFLICT WITH NON-USER COMMON BLOCKS
C
C+++++++++++++++++ END OF USER AREA 2
++++++++++++++++++++++++++++++++++
C
      DIMENSION
U(NNODE,NPHASE),V(NNODE,NPHASE),W(NNODE,NPHASE),
     +
P(NNODE,NPHASE),VFRAC(NNODE,NPHASE),DEN(NNODE,NPHASE),
     +
VIS(NNODE,NPHASE),TE(NNODE,NPHASE),ED(NNODE,NPHASE),
     +
RS(NNODE,NPHASE,6),T(NNODE,NPHASE),H(NNODE,NPHASE),
     +          RF(NNODE,NPHASE,4),SCAL(NNODE,NPHASE,NSCAL)
      DIMENSION
XP(NNODE),YP(NNODE),ZP(NNODE),VOL(NCELL),AREA(NFACE,3),
     +          VPOR(NCELL),ARPOR(NFACE,3),WFACT(NFACE),
     +          CONV(NFACE,NPHASE),IPT(*),IBLK(5,NBLOCK),
     +
IPVERT(NCELL,8),IPNODN(NCELL,6),IPFACN(NCELL,6),
     +
IPNODF(NFACE,4),IPNODB(NBDRY,4),IPFACB(NBDRY),IWORK(*),
     +          WORK(*),CWORK(*)
C
C+++++++++++++++++ USER AREA 3
++++++++++++++++++++++++++++++++++++++++
C---- AREA FOR USERS TO DIMENSION THEIR ARRAYS
C
C---- AREA FOR USERS TO DEFINE DATA STATEMENTS
C
C+++++++++++++++++ END OF USER AREA 3
++++++++++++++++++++++++++++++++++
C
C---- STATEMENT FUNCTION FOR ADDRESSING
      IP(I,J,K) = IPT((K-1)*ILEN*JLEN+ (J-1)*ILEN+I)
C
C----VERSION NUMBER OF USER ROUTINE AND PRECISION FLAG
C
```

```
      IVERS = 3
      ICHKPR = 2
C
C+++++++++++++++++ USER AREA 4
++++++++++++++++++++++++++++++++++++++++
C---- TO USE THIS USER ROUTINE FIRST SET IUSED=1
C
      IUSED = 1
C
C+++++++++++++++++ END OF USER AREA 4
++++++++++++++++++++++++++++++++++
C
      IF (IUSED.EQ.0) RETURN
C
C---- FRONTEND CHECKING OF USER ROUTINE
      IF (IUCALL.EQ.0) RETURN
C
C+++++++++++++++++ USER AREA 5
++++++++++++++++++++++++++++++++++++++++
C
C
C---- EXAMPLE (SET TIME INCREMENT FOR NEXT TIME STEP)
C
C     DTUSR = 0.1
C
C----END OF EXAMPLE
      CALL IPREC('BLOCK-NUMBER-
1','BLOCK','CENTERS',IPT,ILEN,JLEN,KLEN,
     +   CWORK,IWORK)
      INODE1=IP(ILEN/4,JLEN/2,1)
      INODE2=IP(ILEN/2,JLEN/2,1)
      INODE3=IP((ILEN*3)/4,JLEN/2,1)
      INODE4=IP(ILEN/4,JLEN/4,1)
      INODE5=IP(ILEN/2,JLEN/4,1)
      INODE6=IP((3*ILEN)/4,JLEN/4,1)
      INODE7=IP(ILEN/4,(3*JLEN)/4,1)
      INODE8=IP(ILEN/2,(3*JLEN)/4,1)
      INODE9=IP((3*ILEN)/4,(3*JLEN)/4,1)
      WRITE(2,105) TIME, V(INODE1,1), V(INODE2,1),
V(INODE3,1),
     + VFRAC(INODE2,2)
      WRITE(3,105) TIME, V(INODE4,1), V(INODE5,1),
V(INODE6,1),
     + VFRAC(INODE5,2)
      WRITE(4,105) TIME, V(INODE7,1), V(INODE8,1),
V(INODE9,1),
     + VFRAC(INODE8,2)
 105        FORMAT(E11.5,' ',E11.5,' ',E11.5,' ',E11.5,'
',E11.5)
C
C+++++++++++++++++ END OF USER AREA 5
++++++++++++++++++++++++++++++++++
C
      RETURN
C
      END
```